

Universität für Bodenkultur  
Department für Wasser, Atmosphäre und Umwelt  
Institut für Abfallwirtschaft



# **Composting and vermicomposting of biodegradable and non-biodegradable plastics by Eisenia Fetida, Eisenia Andrei and Eisenia Hortensis**

Masterarbeit  
Zur Erlangung des akademischen Grades  
Diplomingenieurin

eingereicht von  
**Antonia Dimas, BA**  
Stud. Kennz.: H 066 427./ Matr. Nr.: 01248428

**Betreuerin:** Univ.Prof. Dipl.-Ing. Dr.nat.techn. Marion Huber-Humer  
**Mitbetreuer:** Mag. Dr. rer.nat. Christian Zafiu

Wien, 04.06.2020

# Danksagung

An dieser Stelle möchte ich mich bei all denjenigen bedanken, die auf unterschiedliche Art zum Gelingen dieser Masterarbeit beigetragen haben.

Mein Dank gebührt Frau Universitätsprofessorin Dipl.-Ing. Dr.nat.techn. Marion Huber-Humer, die meine Masterarbeit betreut und begleitet hat.

Ein besonderer Dank gilt ebenso meinem Mitbetreuer Herrn Mag. Dr. rer.nat. Christian Zafiu, ohne dem dieses Forschungsprojekt nicht zustande gekommen wäre und der meine Masterarbeit von der Konzipierung bis zur Fertigstellung begleitet hat. Des Weiteren möchte ich Herrn Dipl.-Ing. Binner und Herrn Ing. Thomas Ebner ein großes Dankeschön für die tatkräftige Unterstützung bei der Durchführung der Versuche, bei deren Analyse wie auch bei der Auswertung der Ergebnisse aussprechen.

Ich danke auch Herrn Bsc David Witzeneder, Geschäftsführer der Wormsystems GmbH, der mir in Sachen Wurmkompostierung mit Rat und Tat zur Seite stand und die Wurmboxen und Würmer für die Versuche bereitstellte.

Ohne die finanzielle Unterstützung der Kulturabteilung MA7 wären die Versuche zur Wurmkompostierung wie auch die Schwermetallanalyse der Würmer nicht möglich gewesen. Vielen Dank dafür an Frau Heidi Kadensky von der MA7.

Ebenfalls möchte ich mich bei der Wiener Tafel- Verein für sozialen Transfer und bei der MERKUR Warenhandels AG mit Standort Muthgasse 56 - 58 für die Spenden an biogenen Abfällen und für die nicht-bioabbaubaren Knotenbeutel und beim Kompost & Biogas Verband Österreich für die bioabbaubaren „Bio-Kreislauf-Sackerl“, bedanken.

Abschließend gilt ein großer Dank meiner Schwester, Dr. Penelope Dimas, die diese Masterarbeit von Anfang bis zum Ende Korrektur gelesen hat, und meinen Eltern, die mir dieses Studium ermöglicht haben und mir immer zur Seite standen.

## **Eidesstattliche Erklärung**

Ich erkläre eidesstattlich, dass ich die Arbeit selbständig angefertigt habe. Es wurden keine anderen als die angegebenen Hilfsmittel benutzt. Die aus fremden Quellen direkt oder indirekt übernommenen Formulierungen und Gedanken sind als solche kenntlich gemacht. Diese schriftliche Arbeit wurde noch an keiner Stelle vorgelegt.

Diese Arbeit wurde in gleicher oder ähnlicher Form noch bei keiner anderen Prüferin oder bei keinem anderen Prüfer als Prüfungsleistung eingereicht.

Mir ist bekannt, dass Zuwiderhandeln geahndet wird („Verwendung unerlaubter Hilfsmittel“) und weitere rechtliche Schritte nach sich ziehen kann.

Wien, 04.06.2020

## Kurzfassung

Die vorliegende Masterarbeit befasst sich mit dem Abbau von Knotenbeuteln aus Polyethylen niedriger Dichte (LD-PE) oder thermoplastischer Stärke Polybutylenadipat-terephthalat (TPS-PBAT) und deren Einfluss auf die Prozesse der Kompostierung und der Wurmkompostierung über einen Zeitraum von jeweils 120 Tagen. Die LD-PE Knotenbeutel waren nicht für biologische Abbau- oder Kompostierbarkeit zertifiziert. Im Gegensatz dazu trugen die TPS-PBAT Knotenbeutel das Seedling und OK Compost Home Zertifikat und gelten somit als biologisch abbaubar und kompostierbar. Sowohl die Kompostierung wie auch die Wurmkompostierung resultieren in einem nährstoffreichen Kompost beziehungsweise Wurmkompost, der z.B. im Gartenbau und in der Landwirtschaft als Dünger angewendet werden kann. Ein Kompostierungsexperiment und ein Wurmkompostierungsexperiment wurden durchgeführt mit jeweils drei experimentellen Gruppen. Die jeweiligen LD-PE und TPS-PBAT Knotenbeutel wurden in etwa 2- 10 mm Folienstücke geschnitten, um ihre Oberfläche für den mikrobiellen Abbau zu maximieren. In der ersten Gruppe wurde keine Folie, in der zweiten Gruppe wurden LD-PE Folien und in der dritten Gruppe wurden TPS-PBAT Folien hinzugefügt. Eine Nasssiebung der Kompost- und Wurmkompostproben und Analyse mittels abgeschwächter Totalreflexion Infrarotspektroskopie (ATR) zeigten, dass LD-PE Folien in beiden Experimenten erwartungsgemäß nicht abgebaut werden konnten. Hingegen wurden TPS-PBAT Folien zu 99,93 % während der Kompostierung desintegriert und teilweise auch während der Wurmkompostierung abgebaut. Generell hatten die LD-PE und TPS-PBAT Folien unterschiedliche Auswirkungen auf die Kompostqualität. Es bewirkten beide eine Verminderung der Wurmbiomasse im Wurmkompost. Die in dieser Arbeit präsentierten Resultate verdeutlichen die einschränkenden Auswirkungen sowohl von bioabbaubarem als auch von nicht-bioabbaubarem Kunststoff auf Kompostwürmer und die daraus resultierende Hemmung des Nitrifikationszyklus, welche die Qualität des Wurmkompostes negativ beeinflusst.

## Abstract

This master thesis investigates the degradation degree of plastic bags made of either low-density polyethylene (LD-PE) or thermoplastic starch poly(butylene-co-terephthalate) (TPS-PBAT) and their impacts on composting and vermicomposting within 120 days. LD-PE plastic bags were not certified for their biodegradability or compostability. On the contrary, TPS-PBAT plastic bags were labelled with the Seedling and OK compost Home label and are, therefore, considered biodegradable and compostable. Both composting and vermicomposting result in a nutrient-rich compost or vermicompost respectively, which for instance can be further applied to horticulture or agriculture as fertilizer. One composting and one vermicomposting experiment were conducted, each including three experimental groups. The respective LD-PE and TPS-PBAT plastic bags were cut into approximately 2 - 10 mm foil pieces in order to maximize the surface area available for microbial degradation. In the first group no foils were added, in the second group LD-PE foils were added, and in the third group TPS-PBAT foils were added. Wet sieving of the compost and vermicompost samples and analysis by Attenuated total reflection- Fourier transform infrared (ATR-FTIR) spectroscopy showed that LD-PE foils did not degrade in either experiment. In contrast, TPS-PBAT foils disintegrated to 99.93 % during composting and were partially degraded in vermicompost. In general, LD-PE and TPS-PBAT foils had different effects on the compost quality. They caused a decrease in earthworm biomass, highlighting the inhibiting effects of plastic particles on earthworms. The decline in earthworm population provoked a decrease in the nitrification cycle, which negatively impacts the quality of the resulting vermicompost.

# Table of content

1	Introduction .....	1
1.1	Objectives and research questions .....	1
1.2	Structuring .....	2
2	State of the art .....	3
2.1	Composting .....	3
2.1.1	Microbial community .....	4
2.1.2	Hygienisation .....	5
2.1.3	Operating parameters .....	6
2.1.4	Monitoring parameters .....	7
2.1.5	Austrian Compost Ordinance .....	8
2.2	Vermicomposting .....	9
2.2.1	Earthworms .....	9
2.2.1.1	<i>Eisenia Fetida (Savigny 1826) and Eisenia Andrei (Bouché 1972)</i> .....	11
2.2.2	Microbial composition .....	12
2.2.3	Fungal distribution .....	13
2.2.4	Indoor vermicomposting .....	13
2.2.5	Vermicompost and vermicompost tea .....	14
2.2.6	Physico-chemical parameters .....	14
2.2.7	Human pathogens .....	15
2.2.8	Heavy metals .....	15
2.2.9	Greenhouse gas emissions .....	16
2.2.10	Phytosanitary properties .....	16
2.3	Composting versus vermicomposting .....	17
2.4	Plastics .....	18
2.4.1	Biodegradability and compostability .....	18
2.4.2	Classification and composition of biodegradable plastics .....	18
2.4.2.1	<i>Bio-based plastics from renewable resources</i> .....	18
2.4.2.2	<i>Fossil-fuel based plastics</i> .....	19
2.4.3	Microbial and fungal degradation .....	19
2.4.4	Disposal of plastics by earthworms .....	19
2.4.5	Microplastics .....	20
2.4.6	Certification and standardisation .....	21
2.4.7	Testing methods .....	23
2.4.7.1	<i>Visual observations</i> .....	23
2.4.7.2	<i>Mechanical, physical and chemical properties</i> .....	23
2.4.7.3	<i>Respiration test</i> .....	23
2.4.7.4	<i>Gas evolution test</i> .....	23
2.4.7.5	<i>Enzyme assay</i> .....	24
2.4.7.6	<i>Clear-zone technique</i> .....	24
2.4.7.7	<i>Radiolabelling</i> .....	24
2.4.7.8	<i>Laboratory-scale simulated accelerating environments and field trails</i> .....	24
2.5	Fourier transform infrared (FTIR) spectroscopy .....	24
2.5.1	FTIR spectroscopy of compost .....	25
2.5.2	FTIR spectroscopy of low-density polyethylene and thermoplastic starch poly(butylene adipate-co-terephthalate) .....	26
3	Material and methods .....	28
3.1	Experimental set-up .....	28
3.1.1	Input materials .....	28
3.1.1.1	<i>Biogenic waste</i> .....	28
3.1.1.2	<i>Bulking agent</i> .....	29
3.1.1.3	<i>Non-biodegradable plastic bag</i> .....	29

3.1.1.4	<i>Biodegradable plastic bag</i> .....	29
3.1.2	Composting experiment.....	31
3.1.3	Vermicomposting experiment.....	33
3.2	Sampling .....	35
3.2.1	Sample preparation .....	37
3.3	Compost quality.....	37
3.3.1	Water content.....	38
3.3.2	pH and electric conductivity .....	38
3.3.3	Loss on ignition .....	38
3.3.4	Total organic carbon, total nitrogen and C to N ratio .....	38
3.3.5	Respiration activity.....	39
3.3.6	Humic acids .....	39
3.3.7	Nitrate nitrogen .....	40
3.3.8	Ammonium nitrogen.....	41
3.3.9	Kjeldahl nitrogen .....	42
3.3.10	Total Phosphor .....	42
3.3.11	Heavy metal analysis.....	43
3.3.12	Plastic particle analysis .....	43
3.3.13	Attenuated total reflection-Fourier transform infrared (ATR-FTIR) spectroscopy .....	43
4	Results and Discussion.....	44
4.1	Rotting parameters of the composting experiment.....	44
4.2	Rotting parameters of the vermicomposting experiment .....	49
4.3	Plastic particle analysis .....	53
4.4	ATR-FTIR spectroscopy.....	55
4.4.1	Compost.....	55
4.4.2	Vermicompost.....	58
4.4.3	Plastic particles .....	61
4.4.3.1	<i>LD-PE particles</i> .....	61
4.4.3.2	<i>TPS-PBAT particles</i> .....	64
4.5	Earthworm biomass.....	67
4.5.1	Heavy metal content of earthworms .....	69
4.6	Compost quality.....	69
4.6.1	Compost.....	69
4.6.2	Vermicompost.....	75
5	Conclusion and outlook.....	86
	Bibliography .....	89
	Appendix.....	99

# List of figures

Figure 1: Development of the microbial community over time during composting and the associated rise and decline in temperature (Insam & De Beroldi, 2007).....	4
Figure 2: Gut and cast associated processes of earthworms during vermicomposting (Swati & Hait, 2017a) .....	11
Figure 3: Experimental set-up of the compost and vermicompost experiment including three experimental groups; not spiked with foils, spiked with non-biodegradable foils and spiked with biodegradable foils.....	28
Figure 4: Infrared spectrum of the LD-PE bag .....	29
Figure 5: Infrared spectrum of the TPS-PBAT bag .....	30
Figure 6: LD-PE bag (on the left) and TPS-PBAT bag (on the right) .....	31
Figure 7: Schematic drawing of the compost reactors .....	32
Figure 8: Timeline of the composting experiment .....	33
Figure 9: Schematic drawing of the vermicomposters .....	34
Figure 10: Vermicomposters from the company Wormsystems GmbH .....	34
Figure 11: Ruler measuring height of the vermicompost.....	35
Figure 12: Averaged temperature course of C1- Composting without foils, C2- Composting with LD-PE foils and C3- Composting with TPS-PBAT foils.....	44
Figure 13: Averaged temperature course on different levels; Top, Middle, Bottom .....	45
Figure 14: CO <sub>2</sub> concentrations of C1- Composting without foils, C2- Composting with LD-PE foils and C3- Composting with TPS-PBAT foils .....	46
Figure 15: CO <sub>2</sub> concentrations on different levels; Top, Middle, Bottom .....	46
Figure 16: Linear regression model of temperatures and CO <sub>2</sub> concentrations for C1- Composting without foils, C2- Composting with LD-PE foils and C3- Composting with TPS-PBAT foils .....	47
Figure 17: Mass reduction during the composting experiment in C1- Composting without foils, C2- Composting with LD-PE foils and C3- Composting with TPS-PBAT foils .....	48
Figure 18: Condensate that evolved during the composting experiment in C1- Composting without foils, C2- Composting with LD-PE foils and C3- Composting with TPS-PBAT foils.....	48
Figure 19: Timeline of the vermicomposting experiment for V1- Vermicomposting without foils, V2- Vermicomposting with LD-PE foils and V3-Vermicomposting with TPS-PBAT foils .....	49
Figure 20: Input material of the vermicomposting experiment for V1- Vermicomposting without foils, V2- Vermicomposting with LD-PE foils and V3-Vermicomposting with TPS-PBAT foils .....	50
Figure 21: Temperature course of the vermicomposting experiment for V1- Vermicomposting without foils, V2- Vermicomposting with LD-PE foils and V3-Vermicomposting with TPS-PBAT foils.....	50
Figure 22: Degradation of 500 g of biogenic waste within 6 days by vermicomposting.....	51
Figure 23: Mass reduction during the vermicomposting experiment for V1- Vermicomposting without foils, V2- Vermicomposting with LD-PE foils and V3-Vermicomposting with TPS-PBAT foils.....	52
Figure 24: Leachate collection during the vermicomposting experiment for V1- Vermicomposting without foils, V2- Vermicomposting with LD-PE foils and V3-Vermicomposting with TPS-PBAT foils .....	52
Figure 25: LD-PE particles sorted by their particle size; > 6.3 mm, 6.3 – 2 mm, and 2 - 0.63 mm in C2- Composting with LD-PE foils .....	53
Figure 26: LD-PE particles sorted by their particle size; 6.3 – 2 mm and 2 - 0.63 mm in the top layer of V2- Vermicomposting with LD-PE foils.....	54
Figure 27: Number of LD-PE particles/kg dm in C2- Composting with LD-PE foils and in the top layer of V2- Vermicomposting with LD-PE foils at the end of the experiments .....	54



Figure 28: TPS-PBAT particles sorted by their particle size; 6.3 – 2 mm and 2 - 0.63 mm in the top layer (on the left) and bottom layer (on the right) of V3- Vermicomposting with TPS-PBAT foils .....	55
Figure 29: Number of TPS-PBAT particles/kg dm in C3- Composting with TPS-PBAT foils (21 TPS- PBAT particles sized 2 - 0.63 mm) and in the top and bottom layer of V3- Vermicomposting of TPS- PBAT foils at the end of the experiments .....	55
Figure 30: Infrared spectra showing the degradation process of C1- Composting without foils, located at the top level from day 1 - 124 .....	56
Figure 31: Infrared spectra showing the degradation process of C2- Composting with LD-PE foils, located at the top level from day 1 - 124 .....	56
Figure 32: Infrared spectra showing the degradation process of C3- Composting with TPS-PBAT foils, located at the top level from day 1 - 124 .....	57
Figure 33: Comparison between LD-PE bag and final compost on day 124 of C2- Composting with LD-PE foils, located at the top level .....	58
Figure 34: Infrared spectra showing the degradation process of V1- Vermicomposting without foils from input material to the bottom layer .....	58
Figure 35: Infrared spectra showing the degradation process of V2- Vermicomposting with LD-PE foils from input material to the bottom layer .....	59
Figure 36: Infrared spectra showing the degradation process of V3-Vermicomposting with TPS-PBAT foils from input material to the bottom layer .....	60
Figure 37: Comparison of the infrared spectra of the final compost (C1, C2 and C3) and vermicompost (V1, V2 and V3) .....	61
Figure 38: Infrared spectra (on the left) and characteristic wavenumbers selected from the infrared spectra normalized to 2914 cm <sup>-1</sup> (on the right) of manually sorted out LD-PE particles (Number 3, 4, 5, 6, 7) >6.3 mm in C2- Composting with LD-PE foils at the end of the experiment .....	62
Figure 39: Comparison of the infrared spectra of manually sorted out LD-PE particles (Number 3, 15, 18, 20, 21) >6.3 mm which showed impurities and C2-Composting with LD-PE foils at the end of the experiment and the original LD-PE bag .....	62
Figure 40: Infrared spectra (on the left) and characteristic wavenumbers selected from the infrared spectra normalized to 2914 cm <sup>-1</sup> (on the right) of manually sorted out LD-PE particles (Number 8, 16, 20, 25) sized 6.3 - 2 mm in C2- Composting with LD-PE foils at the end of the experiment .....	63
Figure 41: Infrared spectra (on the left) and characteristic wavenumbers selected from the infrared spectra normalized to 2914 cm <sup>-1</sup> (on the right) of manually sorted out LD-PE particles (Number 1, 3, 4, 8, 9) sized 2 - 0.63 mm in C2- Composting with LD-PE foils at the end of the experiment .....	63
Figure 42: Infrared spectra (on the left) and characteristic wavenumbers selected from the infrared spectra normalized to 2914 cm <sup>-1</sup> (on the right) of manually sorted out LD-PE particles (Number 5, 10, 19, 23, 28) sized 6.3 - 2 mm in V2 top layer- Vermicomposting with LD-PE foils at the end of the experiment .....	63
Figure 43: Infrared spectra (on the left) and characteristic wavenumbers selected from the infrared spectra normalized to 2914 cm <sup>-1</sup> (on the right) of manually sorted out LD-PE particles (Number 1, 3, 5, 6, 7) sized 2 - 0.63 mm in V2 top layer- Vermicomposting with LD-PE foils at the end of the experiment .....	64
Figure 44: Infrared spectra (on the left) and characteristic wavenumbers selected from the infrared spectra normalized to 1711 cm <sup>-1</sup> (on the right) of manually sorted out TPS-PBAT particles (Number 1, 2) sized 2 - 0.63 mm in C3- Composting with TPS-PBAT foils at the end of the experiment.....	65
Figure 45: Infrared spectra (on the left) and characteristic wavenumbers selected from the infrared spectra normalized to 1711 cm <sup>-1</sup> (on the right) of manually sorted out TPS-PBAT particles (Number 5, 9, 15, 33, 39) sized 6.3 - 2 mm in V3 top layer- Vermicomposting with TPS-PBAT foils at the end of the experiment .....	65
Figure 46: Infrared spectra (on the left) and characteristic wavenumbers selected from the infrared spectra normalized to 1711 cm <sup>-1</sup> (on the right) of manually sorted out TPS-PBAT particles (Number 11 20, 23, 28, 33, 48) sized 2 - 0.63 mm in V3 top layer- Vermicomposting with TPS-PBAT foils at the end of the experiment .....	66

Figure 47: Infrared spectra (on the left) and characteristic wavenumbers selected from the infrared spectra normalized to $1711\text{ cm}^{-1}$ (on the right) of manually sorted out TPS-PBAT particles (Number 1, 3, 4, 7, 9) sized 2 - 0.63 mm in V3 bottom layer- Vermicomposting with TPS-PBAT foils at the end of the experiment .....	66
Figure 48: Earthworm biomass at the end of the experiment in V1- Vermicomposting without foils, V2- Vermicomposting with LD-PE foils and V3- Vermicomposting with TPS-PBAT foils .....	68
Figure 49: Water content for C1- Composting without foils, C2- Composting with LD-PE foils and C3- Composting with TPS-PBAT foils .....	70
Figure 50: pH for C1- Composting without foils, C2- Composting with LD-PE foils and C3- Composting with TPS-PBAT foils .....	70
Figure 51: Electric conductivity for C1- Composting without foils, C2- Composting with LD-PE foils and C3- Composting with TPS-PBAT foils .....	71
Figure 52: Loss on ignition for C1- Composting without foils, C2- Composting with LD-PE foils and C3- Composting with TPS-PBAT foils .....	72
Figure 53: Total organic carbon for C1- Composting without foils, C2- Composting with LD-PE foils and C3- Composting with TPS-PBAT foils .....	72
Figure 54: Total nitrogen for C1- Composting without foils, C2- Composting with LD-PE foils and C3- Composting with TPS-PBAT foils .....	73
Figure 55: C to N ratio for C1- Composting without foils, C2- Composting with LD-PE foils and C3- Composting with TPS-PBAT foils .....	74
Figure 56: Humic acids for C1- Composting without foils, C2- Composting with LD-PE foils and C3- Composting with TPS-PBAT foils .....	74
Figure 57: Fulvic acids for C1- Composting without foils, C2- Composting with LD-PE foils and C3- Composting with TPS-PBAT foils .....	75
Figure 58: Water content for compost reactors, vermicomposters (T+B) and input material for vermicomposters.....	76
Figure 59: pH for compost reactors, vermicomposters (T+B) and input material for vermicomposters....	77
Figure 60: EC for compost reactors, vermicomposters (T+B) and input material for vermicomposters ...	78
Figure 61: Loss on ignition for compost reactors, vermicomposters (T+B) and input material for vermicomposters.....	78
Figure 62: Total organic carbon for compost reactors, vermicomposters (T+B) and input material for vermicomposters.....	79
Figure 63: Total nitrogen for compost reactors, vermicomposters (T+B) and input material for vermicomposters.....	80
Figure 64: C to N ratio for compost reactors, vermicomposters (T+B) and input material for vermicomposters.....	80
Figure 65: Humic acids for compost reactors, vermicomposters (T+B) and input material for vermicomposters.....	81
Figure 66: Fulvic acids for compost reactors, vermicomposters (T+B) and input material for vermicomposters.....	82
Figure 67: $\text{NH}_4\text{-N}$ for compost reactors, vermicomposters (T+B) and input material for vermicomposters .....	82
Figure 68: $\text{NO}_3\text{-N}$ for compost reactors, vermicomposters (T+B) and input material for vermicomposters .....	83
Figure 69: $\text{RA}_4$ for the input material of the composting experiment.....	84
Figure 70: $\text{RA}_4$ for C1- Composting without foils, C2- Composting with LD-PE foils and C3- Composting with TPS-PBAT foils at the end of the experiment .....	84
Figure 71: $\text{RA}_4$ for the top layer of V1- Vermicomposting without foils, V2- Vermicomposting with LD-PE foils and V3- Vermicomposting with TPS-PBAT foils at the end of the experiment .....	85

Figure 72: RA <sub>4</sub> for the bottom layer of V1- Vermicomposting without foils, V2- Vermicomposting with LD-PE foils and V3- Vermicomposting with TPS-PBAT foils at the end of the experiment .....	85
Figure 73: Calibration curve for photometrical absorbance of NO <sub>3</sub> -N .....	100
Figure 74: Calibration curve for photometrical absorbance of NH <sub>4</sub> -N .....	100
Figure 75: Infrared spectra (on the left) and characteristic wavenumbers selected from the infrared spectra normalized to 2914 cm <sup>-1</sup> (on the right) of manually sorted out LD-PE particles (Number 8, 9, 10, 11, 12) >6.3 mm in C2- Composting with LD-PE foils at the end of the experiment .....	101
Figure 76: Infrared spectra (on the left) and characteristic wavenumbers selected from the infrared spectra normalized to 2914 cm <sup>-1</sup> (on the right) of manually sorted out LD-PE particles (Number 13, 14, 15, 16, 17) >6.3 mm in C2- Composting with LD-PE foils at the end of the experiment .....	101
Figure 77: Infrared spectra (on the left) and characteristic wavenumbers selected from the infrared spectra normalized to 2914 cm <sup>-1</sup> (on the right) of manually sorted out LD-PE particles (Number 18, 19, 20, 21, 22, 23) >6.3 mm in C2- Composting with LD-PE foils at the end of the experiment .....	101
Figure 78: Infrared spectra (on the left) and characteristic wavenumbers selected from the infrared spectra normalized to 2914 cm <sup>-1</sup> (on the right) of manually sorted out LD-PE particles (Number 39, 46, 59, 63) sized 6.3 - 2 mm in V2 top layer- Vermicomposting with LD-PE foils at the end of the experiment .....	102
Figure 79: Infrared spectra (on the left) and characteristic wavenumbers selected from the infrared spectra normalized to 1711 cm <sup>-1</sup> (on the right) of manually sorted out TPS-PBAT particles (Number 52, 61, 67, 72, 86) sized 6.3 - 2 mm in V3 top layer- Vermicomposting with TPS-PBAT foils at the end of the experiment .....	102
Figure 80: Infrared spectra (on the left) and characteristic wavenumbers selected from the infrared spectra normalized to 1711 cm <sup>-1</sup> (on the right) of manually sorted out TPS-PBAT particles (Number 91, 2_7, 2_15, 2_25, 2_33) sized 6.3 - 2 mm in V3 top layer- Vermicomposting with TPS-PBAT foils at the end of the experiment .....	102
Figure 81: Infrared spectra (on the left) and characteristic wavenumbers selected from the infrared spectra normalized to 1711 cm <sup>-1</sup> (on the right) of manually sorted out TPS-PBAT particles (Number 2_48, 2_56, 2_88, 2_98, 3_11) sized 6.3 - 2 mm in V3 top layer- Vermicomposting with TPS-PBAT foils at the end of the experiment .....	103

# List of tables

Table 1: Recommendations for the minimum temperature, time spans, and number of turning events for the hygienisation of compost (Amlinger et al., 2005) .....	6
Table 2: Limiting values for the heavy metal content in quality standard A <sup>+</sup> , A, and B (BGBl. II Nr.292/2001).....	8
Table 3: Additional information about Eisenia Fetida and Eisenia Andrei (Domínguez & Edwards, 2011a) .....	12
Table 4: Comparison of key features between vermicomposting and composting (Amlinger et al., 2005; Domínguez & Edwards, 2011b; R. P. Singh et al., 2011) .....	17
Table 5: Limiting values for heavy metal content in compostable packaging according to EN 13432 .	21
Table 6: Labelling for biodegradable and compostable plastics (TÜV AUSTRIA HOLDING AG, 2020) .....	22
Table 7: Changes in characteristic indicator bands in the infrared spectrum throughout the rotting process (Smidt & Schwanninger, 2005) .....	25
Table 8: Characteristic indicator bands in the infrared spectrum of TPS-PBAT (Barragán et al., 2016; Brandelero et al., 2011; Elfehri Borchani et al., 2015; Kijchavengkul et al., 2008; Yaacob et al., 2016).....	27
Table 9: Composition of the input material of composting without foils .....	32
Table 10: Composition of the input material of composting with LD-PE foils.....	32
Table 11: Composition of the input material of composting with TPS-PBAT foils.....	33
Table 12: Samples taken from the composting experiment and their consecutive analyses .....	35
Table 13: Samples taken from the vermicomposting experiment and their consecutive analyses.....	36
Table 14: Heavy metal content of earthworms at the start and at the end of the experiment in the three vermicomposters (V1, V2 and V3).....	69
Table 15: Parameters assessed for leachate 1 and 2.....	75
Table 16: Compost parameters of C1- Composting without foils.....	103
Table 17: Compost parameters of C2- Composting with LD-PE foils .....	103
Table 18: Compost parameters of C3 Composting with TPS-PBAT foils .....	104
Table 19: Compost parameters of compost and vermicompost (T+B) at the end of the experiment ..	104
Table 20: Compost parameters of the Input material of compost (C) and vermicompost (V).....	105

## List of abbreviations

a.u.	Arbitrary unit
ATR-FTIR	Attenuated total reflection-Fourier transform infrared
C	Carbon
C/N	Carbon to nitrogen ratio
Ca	Calcium
Cd	Cadmium
CH <sub>4</sub>	Methane
CO <sub>2</sub>	Carbon dioxide
Cr	Chrome
Cu	Copper
CuSO <sub>4</sub>	Copper sulphate
dm	Dry matter
EC	Electric conductivity
etc.	Et cetera
FA	Fulvic acids
Fe	Iron
FTIR	Fourier transform infrared
HA	Humic acids
H <sub>3</sub> BO <sub>3</sub>	Boric acid
HCl	Chloric acid
Hg	Mercury
H <sub>2</sub> O	Water
H <sub>2</sub> SO <sub>4</sub>	Sulfuric acid
i.e.	Id est
K	Potassium
LD-PE	Low-density polyethylene
LOI	Loss on ignition
Mg	Magnesium
N	Nitrogen
NaOH	Sodium hydroxide
NH <sub>3</sub>	Ammonia
NH <sub>4</sub>	Ammonium
NH <sub>4</sub> -N	Ammonium nitrogen
Ni	Nickel
NO <sub>3</sub>	Nitrate
NO <sub>3</sub> -N	Nitrate nitrogen
NO <sub>x</sub>	Nitrogen oxides
N <sub>2</sub> O	Nitrous oxide
O <sub>2</sub>	Oxygen
OD	Optical density
odm	Organic dry mass
P	Phosphor
Pb	Lead

PET	Polyethylene terephthalate
PP	Polypropylene
RA <sub>4</sub>	Respiration activity with a test period of 4 days
TC	Total carbon
TIC	Total inorganic carbon
TKN	Total Kjeldahl nitrogen
TN	Total nitrogen
TOC	Total organic carbon
TP	Total Phosphor
TPS-PBAT	Thermoplastic starch poly(butylene adipate-co-terephthalate)
Vol.	Volume
WC	Water content
wm	Wet matter
Zn	Zinc

# 1 Introduction

In recent years, the disposal of biogenic waste has become a big environmental issue. Quantities collected as biogenic waste exceed the capacity of nature to degrade it properly. In small quantities it could be applied as fertilizer on agricultural soils, such as manure. However, high application rates could cause overfertilization, accumulation and concentration of heavy metals, increases in soil alkalinity, salt accumulation in dry conditions, increased anaerobiosis and anoxic decomposition pathways, spreading of human pathogens, and ground water pollution (Domínguez & Edwards, 2011b).

These problems can be avoided by properly treating biogenic wastes in the first place. The aerobic biodegradation of biogenic wastes is an efficient means to stabilize its nutrient-pool and to reduce environmental risks. There are two methods that have proven suitable to achieve this goal; either aerobic decomposition of biogenic waste referenced as composting, which maintain heat at high levels, or employing specific earthworms which fragment, aerate and turn the input material. The end product in both cases is a stabilized and nutrient-rich compost or vermicompost (Domínguez & Edwards, 2011b).

Vienna counts 1.84 million inhabitants as of 2016 and this adds up to a population density of 4,400 per km<sup>2</sup>. 2016 the municipal local waste management company MA 48 collected 1,024,000 tons of solid waste without taking industrial waste streams into account. Furthermore, 64,000 tons of biogenic waste were separately collected at household level in waste bins (2015/16). However, 518,500 tons of residual waste contained 191,105 tons of biogenic waste. This accounts for 36.9 % of the whole residual waste stream. As a result of it, the recovery rate only accounts for 32 % in total for biogenic waste. The recovery rate for biogenic kitchen waste is even lower, it accounts for only 8 % (2015/16). The biogenic waste collected in the residual waste stream is incinerated. In consequence, many nutrients for agricultural usage are lost during the incineration process (Domínguez & Edwards, 2011b; Egle et al., 2017).

Impurities within the biogenic waste stream are 3.6 % (2015). These impurities are divided into secondary raw materials and residual waste. In consequence, the latter are treated in an incineration plant (Egle et al., 2017). Biodegradable plastic bags and non-biodegradable plastic bags belong to the residual waste stream as they are not fitted for composting. They are seen as impurities. Hence, they are sorted out before treatment and are incinerated (Magistratsabteilung 48, 2019). The aim of this work is to assess the degradation degree of non-biodegradable and biodegradable plastics during composting and vermicomposting. The latter is a method that can be applied indoors on a household level and represents an alternative to industrial composting.

## 1.1 Objectives and research questions

A considerable amount of biogenic waste is incinerated in Vienna and many nutrients are lost in the course. This could be changed by increasing its recovery rate. Yet, waste separation in bigger cities is harder to improve than on the countryside, because households are more anonymous (Egle et al., 2017). This master thesis covers the topic of vermicomposting which could be implemented on a household and industrial level. On a household level it provides the possibility to dispose biogenic waste indoors, and harvest its vermicompost, thereby increasing the recovery rate of nutrients from

biogenic waste in the urban environment and reducing the total biogenic waste in the residual waste stream.

With vermicomposting on an industrial level, impurities in biogenic waste must be considered. These consist of different waste streams, many of which are not suited for vermicomposting, primarily plastics. In addition, biodegradable plastic bags are nowadays used to collect biogenic waste and are disposed thereafter in the biowaste bin. Such impurities cannot be fully removed from the organic fraction from households and food and feed industry. Hence, the experiments presented in this master thesis aimed to examine the degradation of biodegradable and non-biodegradable plastics during vermicomposting or composting, and the quality of its products. In consequence following research questions were addressed:

1. How high is the degradation and disintegration degree of biodegradable and non-biodegradable plastics during vermicomposting and composting?
2. How is the particle size distribution of biodegradable and non-biodegradable plastics in compost and vermicompost?
3. What impact do biodegradable and non-biodegradable plastics have on the earthworm population?
4. How many heavy metals do earthworms ingest and egest during vermicomposting?
5. How do biodegradable and non-biodegradable plastic particles influence the rotting parameters and compost quality of the compost and vermicompost?
6. What are the major differences between compost and vermicompost related to compost quality parameters?

## **1.2 Structuring**

This master thesis is structured into three parts, namely theoretical background, empirical work, final discussion, and conclusion of the work. Chapter 2 provides an overview of composting, vermicomposting, and plastics. In chapter 3, the experimental setup and methods of analyses are explained in detail. Chapter 4 and 5 cover respectively the results, discussion and conclusion of the experiments that were conducted.



## 2 State of the art

### 2.1 Composting

A large quantity of solid waste comprises organic matter, which needs to be efficiently recycled. Composting presents a cost-efficient and simple method for treating biogenic waste. Hence, many countries have implemented composting into their waste management strategies, which furthermore prevents detrimental gas and leachate production on landfills (Diaz, 2007).

Composting is a biodegradation process of organic matter by different microbial populations under aerobic conditions (Insam & De Beroldi, 2007). It is characterized by microbial succession, in which the input material is successively degraded by distinct groups of microorganisms, and the degradation product of one group of microorganisms serves as input for the next group. This can also be described as syntrophy (also referred to as synergy), which is another key aspect in this process, and refers to groups of bacteria that grow as a mixed cultures and metabolic end-products of one microbial population is used as nutrition by another group of microorganisms (Domínguez & Edwards, 2011b).

These biodegradation processes produce energy in the form of heat, hence, temperatures rise within the composting windrow. The rise in temperature during the first three phases of composting can be subdivided into two mesophilic phases (25 - 40 °C) which precede and follow a thermophilic phase (35 - 65 °C). At first, easily degradable organic compounds are degraded, followed by more reluctant organic compounds, such as lignin and hemicelluloses. Moreover, complex processes are taking place, such as the humification of lignocellulosic compounds. In the course of this process carbon dioxide and water are released and the final product consists of minerals and stabilised organic matter (Insam & De Beroldi, 2007). In detail, the following processes occur during the four phases of composting:

1. Mesophilic phase (25 - 40 °C)  
This is the initial phase where fungi and bacteria compete for energy-rich, abundant, and easily degradable compounds, such as sugars and proteins. Alongside bacteria and fungi, compost worms, mites, and millipedes may appear. They play a minor role in the degradation process, but they support the mechanical breakdown, and provide an intestinal habitat for specialised microorganisms (Insam et al., 2010). Worms are one of the main drivers for the degradation process in the context of vermicomposting (Domínguez & Edwards, 2011b).
2. Thermophilic phase (35 - 65 °C)  
After the mesophilic phase, thermophilic microorganisms become more abundant and mesophilic ones are inactivated. Temperatures can rise to 65 °C and even higher and decomposition continues at a fast rate. Thermophilic fungi grow at temperatures up to 55 °C, but their growth is inhibited at higher temperatures (Insam et al., 2010).
3. Second Mesophilic phase  
Thermophilic temperatures cease as organic compounds run out, and mesophilic organisms repopulate the substrate. These feed upon starch and cellulose (Insam et al., 2010).

#### 4. Maturation and curing phase

In this phase more fungi inhabit the substrate since nutrients and water become scarce. Furthermore, compounds that are not further degradable, like lignin-humus complexes, are agglomerated (Insam et al., 2010).

Figure 1 shows the development of the microbial community over time during composting and illustrates the associated rise and decline in temperature. It highlights the tight connection between microbial activity and temperature. Heat, oxygen (O<sub>2</sub>), water (H<sub>2</sub>O) and nutrients are not evenly distributed in a composting pile. Therefore, composting piles need to be turned periodically to distribute heat and oxygen equally (Insam & De Beroldi, 2007).

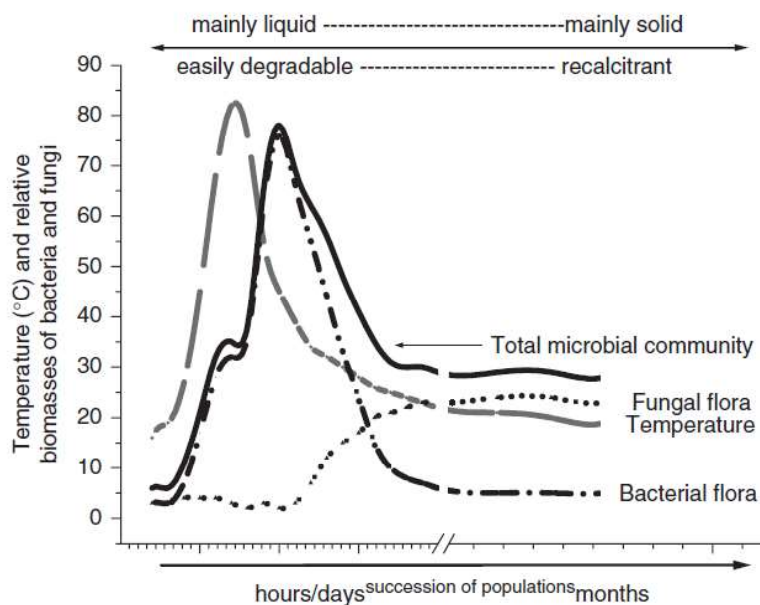


Figure 1: Development of the microbial community over time during composting and the associated rise and decline in temperature (Insam & De Beroldi, 2007)

##### 2.1.1 Microbial community

The composition of the microbial population strongly depends on the input material. However, some bacteria phyla are found in most composts. The majority of bacteria isolated from compost belong to the phyla Firmicutes, Actinobacteria and Proteobacteria. Moreover, the presence of Actinomycetes is often described. Most fungi belong to Ascomycota which can withstand high temperatures and a low water content. Among the phylum Ascomycota, Sordariomycetes and Saccharomycetes are most commonly found in compost (Gu et al., 2017; Jurado et al., 2014; Vargas-García et al., 2010).

Microbial and fungal activity is closely related to the prevailing temperatures. It changes in the course of composting and at each stage. The mesophilic phase presents a lower microbial biomass and diversity than the thermophilic phase. During this stage more Proteobacteria and fungi are present. In contrast, during the thermophilic phase, Firmicutes and Actinobacteria are more abundant. High temperatures during the thermophilic phase inhibit fungal growth, however, they seem to be dormant during this period, and recover in the mesophilic and maturation and curing phase. Microbial decomposition and, therefore, biomass reduction is greater

during the mesophilic phase than during the thermophilic phase (Gu et al., 2017; Tang et al., 2007).

Microorganisms degrade organic matter into different metabolites, which are further processed by other microbes. Nitrogen-fixing, ammonifying, xylanolytic, and cellulolytic microorganisms are mostly involved during composting. Whereas nitrifying bacteria counts are low as they favour different environmental conditions, id est (i.e.) different pH and temperature or inhibitory components for nitrification are present in the composting pile. Cellulolytic and hemicellulolytic microbes appear at a later stage of the biooxidation process, when easily degradable compounds are dissolved, and environmental and nutritional conditions favour them (Vargas-García et al., 2010).

An efficient degradation by microorganisms requires small particle sizes, hence, large surface areas of the raw material. The biodegradation process is directly proportional to the surface area available. Nevertheless, in practice there are limits to the particle size, since its porosity should still enable sufficient aeration (De Bertoldi et al., 1983).

### **2.1.2 Hygienisation**

Due to phytopathogenic and human pathogenic vectors in organic matter, hygienisation plays an important role during composting. If the composting process is not managed properly, these vectors can spread and effect potential hosts (Wichuk et al., 2011).

Human pathogen removal is determined by pH, temperature, water content and biochemical reactions, which are directly influenced by microbial activity and bulking agents. Mc Carthy et al. (2011) reported that Salmonella and E. coli were undetectable due to the rise in temperature and pH during composting, likewise Enterococci were below the limit of detection at the end of composting of pig manure. However, endospore-forming bacteria that are resistant to temperatures up to 100 °C and a potential health risk were not affected by the hygienisation procedure. Also, potentially hazardous fungal spores of yeasts and molds were found to be highly abundant in the final compost.

Other studies further emphasize the importance of temperature throughout composting. Millner et al. (2014) described that in composting piles, which were not managed, i.e. had not been turned or covered, had no bottom layer, and did not reach temperatures higher than 47 °C, faecal coliforms, E. coli and Listeria monocytogeneses were still detectable. Böhm (2007) further highlights the importance of maintaining a high temperature above 55 °C for at least two weeks.

The removal of plant pathogens depends entirely on the type and species of microorganisms present during composting. Phytopathogenic bacteria demonstrate heat-sensitivity, and die at temperatures above 55 °C. Moreover, most nematodes were shown to vanish when temperatures exceeded 55 °C for more than three days. These results suggest that maintenance of high temperatures during the thermophilic phase of composting is essential for hygienisation. However, fungi and fungus-like phytopathogens are more resistant to high temperatures during longer periods of time. Not all species can be eliminated at 55 °C and can even withstand higher temperatures. In practice not all vectors can be tested for assessing the hygienisation status of a composting pile. Hence, it is recommended to test for pests and diseases, which are relevant for a given regional fauna and flora (Wichuk et al., 2011).

The former ministry of agriculture, forestry, environment and water management published guidelines for the process operation of composting systems and

recommends the following temperatures, time spans, and number of turning events to achieve a thorough hygienisation of the compost, as shown in Table 1. However, temperature beyond 65 °C impair the degradation process since microbial species are limited. Therefore temperature should not be kept beyond 50 - 60 °C over an extended period of time (Amlinger et al., 2005).

Table 1: Recommendations for the minimum temperature, time spans, and number of turning events for the hygienisation of compost (Amlinger et al., 2005)

Minimum temperature	Duration
Open and in-vessel compost windrows with naturally or forced aeration	
55 °C	<u>Continuous measurement of temperature with a probe:</u> Minimum temperature must be kept over a time period of at least 10 days and measured 4 hours after at least 5 turning events of the compost
55 °C	<u>Discontinuous measurement of temperature with a probe on workdays:</u> Minimum temperature must be kept for at least 10 days including at least 3 turning events of the compost
60 °C	<u>Discontinuous measurement of temperature with a probe on workdays:</u> Minimum temperature must be kept 3 times on 3 days over a time period of 14 days including 2 turning events of the compost
65 °C	<u>Discontinuous measurement of temperature with a probe on workdays:</u> Minimum temperature must be kept 2 times on 3 days over a time period of 14 days including 1 turning event of the compost
Encapsulated intensive rotting process with forced aeration	
55 °C	<u>Continuous measurement of temperature with a probe:</u> Minimum temperature must be kept for 4 days over a time period of 10 days
65 °C	<u>Continuous measurement of temperature with a probe:</u> Minimum temperature must be kept for 3 days over a time period of 10 days

### 2.1.3 Operating parameters

Input or raw materials present different chemical and physical characteristics, which influence the entire composting process (Khater, 2015). The initial carbon (C) to nitrogen (N) ratio of the raw material is critical for composting. It influences temperature, biodegradation and N loss. For instance, a C to N ratio (C/N) of less than 20 leads to a fast biodegradation process, yet it provokes a high loss in nitrogen. In contrast, a C to N ratio of 30 results in a minimal loss of N (Tripetchkul et al., 2012). But a C to N ratio beyond 35 slows down the biodegradation process due to scarcity in N (Amlinger et al., 2005). N loss occurs when initial raw materials exhibit excessive N, close to the quantity of C. Naturally, the C to N ratio declines throughout the

biodegradation process and becomes more narrow (Larsen & McCartney, 2000). The optimal C to N ratio is between 25 and 35 (Amlinger et al., 2005)

Water content is influenced by feedstock materials, water addition, aeration, and the prevailing temperatures during the rotting process. A low to medium water content can indicate operational problems, which influence the stabilization of organic matter (Barrena et al., 2014). However, there is no universal optimal water content for every composting material as it depends on its physical, chemical, and biological characteristics. These factors impact water availability, particle size, porosity and permeability (Makan et al., 2013). The water content of kitchen waste with little bulking agents ranges between 45 - 60 % wet mass (wm). During composting water content should be held beyond 50 - 60 % (Amlinger et al., 2005).

The physical properties of the raw material in a composting pile are closely intertwined. Bulk density decreases with the increase of organic matter, i.e. the higher the total organic content the lower the bulking density. Porosity is determined by bulking density and water content. It is negatively correlated with bulking density. That means the greater the porosity the lower the bulking density (Khater, 2015). Hence, bulking agents should be added to the compost system which should account between 40 - 60 % of the volume (Amlinger et al., 2005).

#### **2.1.4 Monitoring parameters**

Different parameters are indicators for composting efficiency. These can be monitored throughout the degradation process. In general, bacteria prefer neutral conditions, whereas fungi favour a rather acidic environment. Optimal values for pH are lying between 5.5 to 8. During the mesophilic phase acid-forming bacteria break down carbonaceous material to fatty acid intermediates, mainly lactic and acetic acids. These are produced under anaerobic conditions and lower the pH. Whilst it increases during the thermophilic phase where fatty acids decompose under aerobic conditions. Thus, the pH depends also on the aeration rate (Beck-Friis et al., 2001; De Bertoldi et al., 1983; Sundberg & Jönsson, 2008).

Gaseous emissions are an essential monitoring parameter as they can indicate the condition of the composting pile. Oxygen is employed as electron acceptor by microorganisms for aerobic respiration and for the oxidation of several sorts of organic compounds. The optimal oxygen supply ranges between 15 and 20 volume (vol.) % and should not fall below 5 vol. % otherwise odours might appear (De Bertoldi et al., 1983). During composting organic compounds are mineralised into carbon dioxide (CO<sub>2</sub>) and water (Beck-Friis et al., 2001). Organic carbon, which is taken up by microorganisms is divided into microbial cell biomass production, metabolite excretion, and respiration. The mineralization of carbon strongly depends on the microbial growth and efficiency. If microorganisms are under stress, they employ most energy for cell maintenance and less on biosynthesis. Therefore, more carbon will be emitted as CO<sub>2</sub> and not bound in complex macromolecules (Domínguez, 2011). CO<sub>2</sub> emissions should not exceed 10 - 12 vol. % during composting as odours might appear due to insufficient oxygen supply (Amlinger et al., 2005).

Generally, organic nitrogen is mineralized into ammonium (NH<sub>4</sub>) and nitrate (NO<sub>3</sub>) when nitrification is taking place. Yet, some parts are incorporated into the microbial metabolism, some are assimilated into the organic matter during humification, and another part is released as ammonia (NH<sub>3</sub>) and nitrous oxide (N<sub>2</sub>O) (Larsen & McCartney, 2000). NH<sub>3</sub> is produced from NH<sub>4</sub> when pH is alkaline and microbial activity is low. Microorganisms can immobilize NH<sub>4</sub> and, thus, decrease NH<sub>3</sub> emissions. N<sub>2</sub>O

emissions occur in the course of the denitrification process. Hence, it strongly depends on the nitrate nitrogen ( $\text{NO}_3\text{-N}$ ) concentration and the prevailing temperatures since high temperatures inhibit denitrification (Beck-Friis et al., 2001). However,  $\text{NH}_4$  and  $\text{NO}_3$  might also be lost due to leaching (Brown et al., 2013; Romero et al., 2013).

During the composting process humification takes place and humic substances are built up during the composting process. Their formation depends on the composition of the input material as well as the process operation. Humic substances are brown, high molecular compounds that are formed by different chemical fractions. The reactants that are converted into humic substances can be divided into primary reactants and secondary reactants. Primary reactants are aromatic compounds, which can easily be transformed into radicals. Secondary reactants are not classified by a certain chemical structure class, but they need to react with humic substance fractions. Primary and secondary compounds comprise metabolites of microbial degradation, such as lignin, fats, carbohydrates, proteins et cetera (etc.). A mixture of biogenic and yard waste offers many compounds that can be used for humic acid formation. The end-products are stable humins that are difficult to solve and little reactive. Humification can be influenced and controlled by different parameters. For instance, the microbiological composition determines the humification process since certain microorganisms enhance it. But also, abiotic factors such as aeration and composting duration impact humification. After a composting time of 40 - 45 days the maximum of humic acids are formed, hence more organic material can be accumulated. Nevertheless, intensive aeration leads to a faster mineralization rate of organic matter (Binner et al., 2011; Ziechmann, 1996). The evolution of humic substances also plays an important role for the immobilization of heavy metals (Ciavatta et al., 1993).

### 2.1.5 Austrian Compost Ordinance

The Austrian Compost Ordinance handles the quality standards and the sources and type of input materials for composting. It classifies compost into three different categories, namely quality standard A<sup>+</sup>, A, and B. These are distinguished by their heavy metal content. Heavy metal content needs to stay in a certain range in order to be used for different areas, such as agriculture and horticulture. Quality standard A<sup>+</sup> is eligible for organic farming, quality standard A is authorized for conventional farming, and B should not be used for food and feed production (BGBl. II Nr. 292/2001). Foods, processed foods and green wastes are a major sources for heavy metals which are mobilized by mineralization processes (Barrena et al., 2014). Table 2 exhibits the limiting values for cadmium (Cd), chrome (Cr), mercury (Hg), nickel (Ni), lead (Pb), copper (Cu), and zinc (Zn) in compost of quality A<sup>+</sup>, A, and B.

Table 2: Limiting values for the heavy metal content in quality standard A<sup>+</sup>, A, and B (BGBl. II Nr.292/2001)

Limit value	Cd	Cr	Hg	Ni	Pb	Cu	Zn
Quality standard A <sup>+</sup> accepted for organic farming							
mg/kg dm	0.7	70	0.4	25	45	70	200
Quality standard A accepted for conventional farming							
mg/kg dm	1	70	0.7	60	120	150	500

	Quality standard B not accepted for any food and feed production						
mg/kg dm	3	250	3	100	200	500	1800
						400*	1200*

\* guide value: if this value is exceeded, the value needs to be indicated in the labelling

Moreover, it gives limiting values concerning the degree of hygienisation for the application in different areas. The limiting values comprise four different pathogens, i. e. *E. coli*, *Salmonella* sp., *Campylobacter*, and *Listeria* sp.. For instance, laboratory testing for the degree of hygienisation for commercially bagged compost, needs to be conducted when the production reaches 500 m<sup>3</sup> of compost. All four pathogens shall be undetectable in a 50 g sample (BGBl. II Nr. 292/2001).

Plastic particles larger than 2 mm are restricted by 0.2 % dry mass (dm) for agricultural use and by 0.4 % dm for landscape construction and conservation or recultivation layers on landfills. Apart from limiting values for pollutants, foreign matter and plant compatibility, the Austrian Compost Ordinance does not determine favourable properties for composts. Nutrient values should be indicated on the packaging, but minimum requirements are not specified (BGBl. II Nr. 292/2001).

## 2.2 Vermicomposting

Vermicomposting is a mesophilic and aerobic decomposition process, where earthworms and microorganisms jointly bio oxidise and stabilise organic matter. While only microorganisms are involved in the biochemical degradation process, earthworms are essential catalysts. They aerate, condition, and fragment the substrate, and therefore, drastically increase microbial activity. Consequently, earthworms break down organic material, raise the surface area exposed to the microorganisms and transport fragments and bacteria-rich excrements through the biogenic waste, and homogenize the organic material (Domínguez & Edwards, 2011b).

It involves a two-step process; first the active phase where the earthworms transform the waste, and change its physical state and microbial composition; and secondly the maturation phase, where earthworms seek fresher input material and only microorganisms are involved in the stabilization and humification of organic matter (Castillo et al., 2013; Domínguez & Edwards, 2011b). In consequence, vermicompost does not need to be turned periodically, leading to a low to no energy input. It is a waste management tool that can be used to transform different biogenic waste streams, i.e. wastes from on- and off-farm, food processing, wood processing, sewage sludge, and industrial and municipal wastes, into nutrient rich vermicompost (Sinha, 2011).

### 2.2.1 Earthworms

Approximately, 3,000 earthworm species are known which live across the biosphere under different climatic conditions. In each region earthworms have adapted to the specific environmental conditions (Butt & Lowe, 2010). They are macroscopic clitellate oligochaete annelids and their natural habitat is soil (Domínguez & Edwards, 2011a). Moreover, they are cross-fertilizing hermaphrodites. This means they reproduce by transferring and receiving sperm in their clitellum in the same copulation. Then the clitellum is taken off and fertilization is taking place in the cocoon. One or more

juveniles are produced in one cocoon (Cosin et al., 2010). The earthworm population depends on the physical soil conditions and availability of organic matter. They reproduce until food is a limiting factor (R. P. Singh et al., 2011). There are three categories describing earthworms; epigeic, endogeic and anecic (Bouché, 1977). Endogeic and anecic earthworms feed on a mixture of soil and organic matter, whereas epigeic species live on litter and transform it into holorganic faecal pellets. The most employed epigeic earthworms in vermicomposting are *Eisenia Fetida* (Bouché), *Eisenia Andrei* (Savigny) *Dendrobaena Veneta* (Savigny), and to a lesser extent *Eudrilus Euginae* (Savigny) and *Perionyx Excavates* (Perrier) (Domínguez & Edwards, 2011a).

Earthworms are detritivorous and feed on the biofilm covering organic materials, which is produced by microorganisms and fungi in the course of degradation and consists mainly of their metabolites (Curry & Schmidt, 2007). Furthermore, earthworms recover most of their nutrients from processing fungi, protozoa, and bacteria (Swati & Hait, 2017a). Yet, Aira and Domínguez (2009) disagree with these findings that earthworm *Eisenia Fetida* thrives on microorganisms. In conclusion, digestion of microorganisms strongly depends on the earthworm species. They can consume half or more of their body weight as organic matter per day (Evans & Furlong, 2003). Earthworms can feed on a variety of biogenic wastes, from both municipal, and industrial streams. This includes:

1. Municipal solid waste or biogenic waste containing fruits and vegetables. Also a small amount of cooked kitchen leftovers (Lleó et al., 2013)
2. Animal manure, like cattle dung and pig manure (Gunadi & Edwards, 2003; Lazcano et al., 2008)
3. Green waste (Cai et al., 2018)
4. Sewage sludge (Sinha et al., 2010)

Citrus, garlic, onions, meat, dairy products, fish and beans are not suitable for vermicomposting (Pirsaheb et al., 2013). Excessive N content might require amendment of carbon rich bulking agents to maintain appropriate C to N ratio. C to N ratio should not exceed 40:1 (Sinha, 2011). Earthworms need finely cut materials for ingestion (Curry & Schmidt, 2007).

The majority of epigeic earthworms seek fresh organic matter and, therefore, are located in the top layers of vermicompost (Monroy et al., 2009). They ingest feed and soften it by excreting mucus in their mouth. The softened feed is passed on to the oesophagus, where it is neutralized with calcium secreted by the walls of the oesophagus. Sequentially, it is finely crushed into two to four  $\mu\text{m}$  sized particles by the musculus gizzard with the aid of stones. Lastly, it is enzymatically dissolved by proteases, lipases, amylases, celulasas and chitinases. The end process involves humification in which large organic particles are converted into complex amorphous colloids and then excreted in casts (Sinha et al., 2010). Only 5 to 10 % of the digested and ingested material remains are used as nutrients for the earthworm. The rest is excreted in form of cast which is high in nitrates, phosphates and potash (Sinha, 2011). In Figure 2 the gut and cast associated digestion processes within the earthworm are shown.



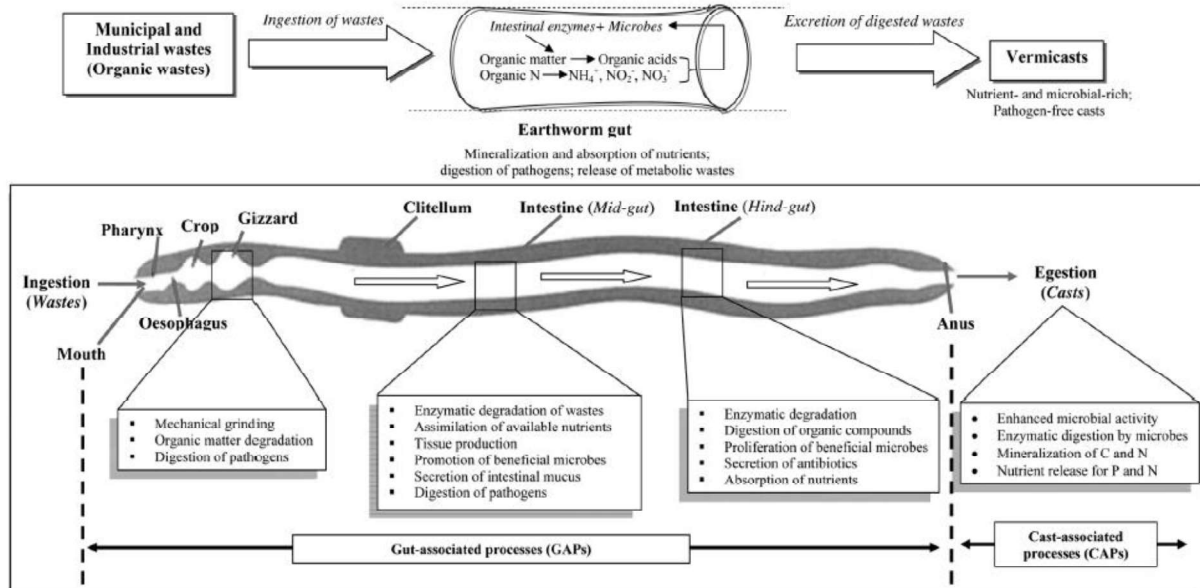


Figure 2: Gut and cast associated processes of earthworms during vermicomposting (Swati & Hait, 2017a)

Earthworms require temperatures between 20 and 30 °C, thus, vermicomposting is classified as mesophilic composting (Sinha, 2011). Below 10 °C ingestion of organic matter is reduced and below 4 °C cocoon production is stopped. When extremely low temperatures prevail, earthworms hibernate and tend to move to deeper layers for protection. Temperatures above 30 °C provoke a high microbial activity, therefore, competition for oxygen is high and it has a negative effect on the earthworm survival (Domínguez & Edwards, 2011a). However, optimal temperature depends on the earthworm species (Ali et al., 2015). Earthworms thrive best on moderate temperatures and moist conditions. Optimum water content ranges between 50 and 90 % dm (Domínguez & Edwards, 2011a). Also, they need an aerobic environment which provides adequate flow of air. However, they provide spatial aeration systems by forming burrows (Lleó et al., 2013). Earthworms do not hold specialized respiratory organs and take up gases through diffusion of their body walls (Domínguez & Edwards, 2011a).

The majority of epigeic earthworms are relatively tolerant to pH. They bear pH levels between 5 and 9. Yet, they prefer more acidic materials with a pH of 5 (Domínguez & Edwards, 2011a). To maintain pH at a certain level, earthworms excrete calcium salts. Nevertheless, it is recommended to add lime to control pH and to supply calcium carbonate to the earthworms (Sinha, 2011). Additionally, earthworms cannot survive in environments with high ammonia content and salt content (Gunadi & Edwards, 2003). Ammonia content should not exceed 0.5 mg/g and salt content should not exceed 0.5 % (Domínguez & Edwards, 2011b).

#### 2.2.1.1 *Eisenia Fetida* (Savigny 1826) and *Eisenia Andrei* (Bouché 1972)

Both *Eisenia Fetida* (Savigny) and *Eisenia Andrei* (Bouché) belong to the lumbricid earthworm species and are often employed in vermicomposting and vermiculture since they are ubiquitous, feed on organic substrates, have a short life cycle, tolerate wide temperatures and moisture variations, are resilient, and easy to handle. They are morphologically similar, demand the same environmental conditions, and are found to be syntopic. Hence, they often appear together. However, *Eisenia Andrei* is

recommended more frequently, since their growth and reproduction rates are higher. Their optimum temperature is 25 °C and optimum ambient water content is 85 % dm. It takes them 45 to 51 days to grow from newly laid cocoon to clitellate adult earthworms. 48 hours after copulation *Eisenia Andrei* and *Eisenia Fetida* lay cocoons. Their average life span is 594 days at 18 °C and 589 days at 28 °C and have a maximum life expectancy of 4.5 to 5 years (Domínguez & Edwards, 2011a). More information is given in Table 3.

Table 3: Additional information about *Eisenia Fetida* and *Eisenia Andrei* (Domínguez & Edwards, 2011a)

<b>Epigeic earthworm species</b>	<b><i>Eisenia Fetida</i></b>	<b><i>Eisenia Andrei</i></b>
Colour	Brown and buff bands	Red
Size of adult earthworms [mm]	4 - 8 to 50 - 100	4 - 8 to 50 - 100
Mean weight of adults [g]	0.55	0.55
Time to maturity [days]	28 - 30	21 - 28
Number of cocoons [day <sup>-1</sup> ]	0.35 - 0.5	0.35 - 0.5
Mean size of cocoons [mm]	4.85 x 2.82	4.8 x 2.82
Incubation time [days]	18 - 26	18 - 26
Hatching viability [%]	73 - 80	72
Number of worms [cocoon <sup>-1</sup> ]	2.5 - 3.8	2.5 - 3.8
Self-fertilization	+	+
Life cycle [days]	45 - 51	45 - 51
Optimal Temperature [°C]	25	25
Optimal moisture [% dm]	80 - 85	80 - 85

### 2.2.2 Microbial composition

On the one hand, microbial diversity and richness are enhanced by vermicomposting (Cai et al., 2018; Suthar & Gairola, 2014). On the other hand, earthworms reduce total microbial biomass compared to the raw material (Lazcano et al., 2008). At first bacteria native to the raw material are present in the top layers which are unaltered by the presence of earthworms. After passing through the gut of the earthworm, bacterial composition changes, and microbial biomass declines due to the digestion and feeding activity of the earthworm (Aira et al., 2009; Dominguez et al., 2019). Bacteria are spread in all different layers of vermicompost. However, they are more ubiquitous in the top layers where the earthworm population is located, as they thrive on the earthworm cast, which contains more readily available and soluble nutrients (Monroy et al., 2009).

Microorganisms are not only present in vermicast but also in the earthworm gut. They produce essential enzymes that the earthworms need in order to digest feed (Negi & Suthar, 2013). The earthworm gut can be described as a micro-ecological niche in which different microorganisms live. Organic feed and anaerobe conditions favour a certain subset of microorganisms during gut passage, mostly the denitrifying and fermentative flora. In this environment complete nitrogen and sulphur cycles are conducted. Singh et al. (2015) found a high abundance of ammonia oxidisers and nitrogen fixers in metagenomes of *Eisenia Fetida*. Furthermore, lignocellulolytic biomass degraders, specifically xylan degraders, and chitin degraders were widely spread. Most processes in the gut of *Eisenia Fetida* are dehalogenation, aromatic hydrocarbon degradation, chlorophenol degradation, atrazine metabolism and lastly naphthalene degradation.

Both in vermicomposting as well as in aerobic composting the most abundant phylum is Proteobacteria. In contrast, the population of Actinobacteria and Bacteroidetes were found to be greater in vermicomposting than in composting. Acidobacteria, Chloroflexi and Saccharibacteria are present in both (Cai et al., 2018; Suthar & Gairola, 2014). Actinobacteria are abundant in the gut of *Eisenia Fetida* and, therefore, are frequently found in the vermibed. Some genera of Actinobacteria are known to produce antibiotics which decimate or eliminate other bacteria or fungi as well as pathogenic bacteria, such as *Streptomyces scabiei* (Palaniyandi et al., 2013).

### **2.2.3 Fungal distribution**

Fungal richness is enhanced by vermiculture. The modification of organic matter into more readily available soluble nutrients forms a perfect medium for fungal growth (Negi & Suthar, 2013; Suthar & Gairola, 2014). The high biodiversity in fungi can be explained by the mesophilic conditions that are beneficial to most fungal phylum (Anastasi et al., 2005). Similarly, to the reduction in microbial biomass, fungal biomass decreases as well in the course of vermicomposting. Furthermore, it has been reported that fungal abundance is smaller than microbial (Huang et al., 2013). This can be attributed to the earthworm's preference of fungi over microorganisms as nutrient source (Curry & Schmidt, 2007). Fungal growth is mostly found at the maturation phase, which indicates that they are thriving on recalcitrant compounds (Castillo et al., 2013).

According to Huang et al. (2013) the most abundant fungal phylum during vermicomposting is Sordariomycetes which belongs to the fungal phylum Ascomycota. This strain is also most frequently found in composting. Alongside Ascomycota there is Basidiomycota, Chytridiomycota, Zygomycota, and Cryptomycota (Anastasi et al., 2005; Cai et al., 2018).

### **2.2.4 Indoor vermicomposting**

There are many vermicomposting techniques that can be either applied on a larger or smaller scale. However, they can be separated into open vermicomposting systems and container vermicomposting systems (Domínguez & Edwards, 2011b). Container vermicomposting systems can be applied indoors. They have several advantages, as biogenic waste can be composted at home in simple containers or more sophisticated composting bins. Its vermicompost shows good values for organic matter, ash value, total organic carbon, total nitrogen, C to N ratio, phosphate, water content and pH (Pirsahab et al., 2013). Organic material is added to the vermicomposting systems in periodical intervals, since earthworms can only process a certain amount of organic matter a day (see chapter 2.2.1). When vermicomposting systems are overloaded, foul

odours can arise due to insufficient oxygen supply, and hence anaerobic conditions (Lleó et al., 2013; Sinha et al., 2010).

### **2.2.5 Vermicompost and vermicompost tea**

During the vermicomposting process biogenic waste is converted into vermicompost (Salter & Edwards, 2011). The vermicompost is characterized by a dark-brown colour, which indicates its soil nutrient richness (Suthar & Gairola, 2014). After vermicomposting the mass of treated waste can reduce up to 72 %, whereas during composting the biomass can reduce up to 41 % on dry matter basis respectively (Lleó et al., 2013).

Vermicompost tea is the concentrated essence of vermicompost. Both depend on the initial raw material that is added and the prevailing environmental conditions. Vermicompost tea is produced by either passively or mechanically controlled steeping of vermicompost in water (mostly recommended 1:20 or 1:5) (Salter & Edwards, 2011). However, it has also been reported that leachate evolves during the vermicomposting process that can be collected in a container underneath the vermicomposting system (Suthar & Gairola, 2014). Vermicompost tea will not be further discussed in this chapter as the focus lies on vermicompost.

### **2.2.6 Physico-chemical parameters**

When earthworms feed on organic matter, they excrete vermicast, which is then processed by microorganisms. Microorganisms further mineralize the nutrients present in the cast (Domínguez, 2011). Vermicomposting changes the pH of the raw material. It slightly turns from neutral to acidic after vermicomposting (Cai et al., 2018; Garg et al., 2012; Lazcano et al., 2008). The drop in pH is thought to be the result of mineralization of N and phosphor (P) compounds, the release of CO<sub>2</sub>, organic acids from microbial metabolisms, and the production of humic and fulvic acids during vermicomposting (Kaushik & Garg, 2004; Ndegwa & Thompson, 2001). On the contrary, Majlessi et al. (2012) report that pH turns neutral or partially alkaline, which is a sign for the stabilization of vermicompost. The electrical conductivity (EC) is a good parameter to measure salinity of biogenic waste. Salinity is a phytotoxic parameter in soil. The electrical conductivity declines during vermicomposting due to less soluble metabolites and precipitation of soluble salts (Lazcano et al., 2008). However, it has also been reported to increase after vermicomposting due to the accelerated decomposition of organic matter by earthworms (Suthar & Gairola, 2014).

Degradation of organic matter is widely expressed by the C to N ratio. C is lost subsequently by biooxidation, whereas N-compounds are decomposed at a lower rate. Therefore, the C to N ratio tends to decrease during vermicomposting, as it does during composting. However, C was found to reduce at a faster rate during vermicomposting than during composting, thus, total organic carbon (TOC) tends to be low. The TOC loss can be explained by microbial respiration and assimilation of easy degradable carbon as worm tissue (Suthar & Gairola, 2014). In contrast, total nitrogen (TN) increases even more compared to composting (Garg et al., 2012; Lazcano et al., 2008; Suthar & Gairola, 2014). Additionally, available phosphor (P) is as well increased during vermicomposting as phosphatases is taking place in the earthworm gut and P-solubilizing microbes are present in vermicast (Cai et al., 2018; Suthar & Gairola, 2014). Vermicomposting augments ammonium nitrate (NH<sub>4</sub>-N) and NO<sub>3</sub>-N concentration (Suthar & Gairola, 2014; Wu et al., 2015). Nevertheless, ammonium loss can occur due to nitrification, which is enhanced in the cast, or denitrification processes taking place in the anaerobic earthworm gut (Aira & Domínguez, 2009). Exchangeable

potassium (K) has been reported to increase during the course of vermicomposting by Negi and Suthar (2013). In contrast, Suthar and Gairola (2014) stated that exchangeable K content declined after vermicomposting because of leachate. Due to the availability of inorganic nutrients in vermicast, the mineralization process of calcium (Ca) and magnesium (Mg) are enhanced (Domínguez, 2011). Also humic acid (HA) fractions are higher than in the raw material (Castillo et al., 2013).

### **2.2.7 Human pathogens**

In academic research the defence mechanisms of earthworms have been widely investigated and discussed. In contrast to composting, temperatures during vermicomposting should not exceed 30 °C. This means that vermicomposting does not undergo a thermophilic phase where pathogens are removed. However, there is evidence that human pathogens are ingested by earthworms (Aira et al., 2009; Swati & Hait, 2017a).

Secondly, pathogens are suppressed or eliminated through the joint action of earthworms and the prevailing microbial population. Monroy et al. (2009) concluded that total number of coliforms are reduced in the presence of *Eisenia Fetida*. This is proven by a decrease in coliform population in deeper layers after passing through the earthworm gut. Still, it might also be connected to the reduction in available carbon by the feeding activity of earthworms and enough aeration due to burrowing activity of earthworms. These environmental factors favour certain subsets of microorganisms which include Actinobacteria. They can produce antibiotics leading to the depression and elimination of pathogens (Castillo et al., 2013). Not only total coliforms are depressed by the presence of *Eisenia Fetida*, but also faecal coliforms, *Salmonella*, *Enterococcus* and Helminth ova (Hait & Tare, 2011).

In summary, earthworms eliminate and reduce human pathogens through different mechanisms. Firstly, they actively inhibit microbes through their intestinal enzymatic action, secretion of coelomic fluids with antibacterial properties and selective grazing. Secondly, they play an indirect role by stimulating growth of endemic or other non- pathological microbes, which leads to competition and stimulation of phagocytic activity among the microbial population by means of antimicrobial substances. However, it has to be noted that each earthworm species may interact differently with different pathogens (Swati & Hait, 2017a).

### **2.2.8 Heavy metals**

The effects of vermicomposting on heavy metal content and their bioavailability have been widely studied. Earthworms are capable of decreasing the content of several heavy metals in vermicompost, such as Cr, Cu, Ni, Pb, Zn, Hg, iron (Fe), Cd and Mg. By decomposing organic matter, heavy metals bound to ions and carbonates are released. Earthworms can accumulate them in their body during intestinal and dermal passage. This causes a stress response due to prolonged exposure to heavy metal contaminated wastes. Numerous metals can be either bound to cysteine-rich metal binding proteins or accumulated in cutaneous tissues in earthworms. Chloragogen cells seem to immobilize heavy metals in small spheroidal chloragosomes and debris-containing vesicles. When earthworms are exposed to a high concentration of heavy metals, the rate of metal excretion exceeds immediate metal uptake. As a result, they excrete more heavy metals than they immediately ingest. This is likely part of the earthworms' stress response as it tries to alleviate the stress by releasing heavy metals from internal stores within the tissues (Li et al., 2009; Morgan & Morgan, 1999; Niyazi & Chaurasia, 2014; Sinha et al., 2010). Not only can they bioaccumulate heavy metals,

but earthworms can also decrease their bioavailability by modifying their chemical specification into lesser available forms, hence immobilising them (Swati & Hait, 2017b).

Essential metals, like Cu and Zn, are taken up fast by earthworms before they reach an equilibrium, and are subsequently excreted over time, which suggests physiological control over uptake and secretion. In contrast, xenobiotic heavy metals such as Cd, Ni and Pb are excreted slowly or not at all after uptake (Liu et al., 2012). Vermicomposting has been used to stabilize and decompose sewage sludge in Australia since 1997 as it is suitable to remove pathogens and heavy metals. The first facility was installed in Redland Shire in Queensland and processed 400 - 500 tons of sewage sludge a week (Sinha et al., 2010).

### **2.2.9 Greenhouse gas emissions**

During vermicomposting direct greenhouse gas emissions, namely methane (CH<sub>4</sub>), and N<sub>2</sub>O evolve. In addition to direct greenhouse gas emissions, NH<sub>3</sub> and volatile organic compounds are also emitted. Compared to home and technical composting processes, these are relatively low. This is due to burrowing activity of earthworms as they aerate the substrate and anaerobic zones are minimised (Lleó et al., 2013). Nevertheless earthworms enhance denitrification and, therefore, N<sub>2</sub>O may increase respectively by vermicomposting (Wu et al., 2015).

### **2.2.10 Phytosanitary properties**

Adding fertilizers strongly influences the bacterial and fungal community structures. The addition of vermicompost provokes an increase in microbial population as well as diversity compared to chemical fertilizers (NPK) and no addition of fertilizer. This can be explained by the priming effect, which results from a higher nutrient availability. The priming effect describes that a microbial community is stimulated through a richer nutrient pool. In soils, where nutrients are limited, one microbial group adapts quicker to the circumstances and dominates the other. Hence, the dominated group becomes dormant at this point. However, vermicompost increases the nutrient availability upon which dormant microbial strains can thrive (Abbadie, 2003; Maji et al., 2017).

Along with microbial activity, enzymatic activity is increased by vermicompost. This includes ureases, invertases, cellulases and catalases. But also, other positive effects on the growth and health of plants are observed. For instance, nodulation and arbuscular mycorrhizal fungi counts are improved (Maji et al., 2017). Not only the favourable microbial population makes it a good medium for crop development, but also its supply with plant growth hormones, such as auxins, gibberellins, and cytokines (Arancon et al., 2011).

All those factors lead to a positive development in root, shoot, and total biomass in plants. Blouin et al. (2019) made a comparative literature review between different studies on the positive effects of vermicompost on plants. They state that the optimal amendment of vermicompost lays between 20 and 60 % of the medium volume. The largest increase in root biomass is achieved by adding between 20 and 40 % of vermicompost to the soil. At a higher rate the positive effects reverse, which could be due to an overdose of hormone-like-molecules, soil compaction, or competition for nutrients among microorganisms. Furthermore, the initial raw material plays a major role on the nutrient availability in vermicompost. Most beneficial effect on plant development are yielded with cattle manure and pig manure as raw material. But also, food waste shows promising effects as it generates a boost of 44 % in shoot biomass.

However, no general conclusions can be made since the positive effects depend strongly on the plant species.

Moreover, vermicompost helps to prevent and suppress pests and diseases in plants. Among them are phytopathogenic fungi, insects, and nematodes (Arancon et al., 2005; Mu et al., 2017; Xiao et al., 2016). These positive effects are hypothesized to originate from beneficial microbes in vermicompost. As mentioned before, Actinobacteria are abundant in vermicompost and produce antibiotic substances. These are proven to inhibit and control fungal and bacterial plant diseases (Monroy et al., 2009; Raaijmakers & Mazzola, 2012).

## 2.3 Composting versus vermicomposting

Composting and vermicomposting are both aerobic biodegradation processes that result in a stabilized and nutrient-rich end-product. However, there are a couple of differences. Firstly, vermicomposting only includes a mesophilic phase where earthworms suppress and eliminate unfavourable microorganisms, which would otherwise increase temperatures beyond 30 °C. Therefore, the microbial community is composed of a different sub-set of bacteria during vermicomposting compared to composting. Secondly, these temperatures do not enable a thermophilic phase as with composting. As a result of it, human and plant pathogens are not removed by prevailing temperatures beyond 55 °C. Nevertheless, there is evidence that earthworms remove pathogens by selective feeding activity, nutrient availability, and excretion of antibacterial compounds. Thirdly, earthworms can accumulate heavy metals in their body and change their chemical properties and consequently, immobilize them, whereas in composting the immobilization of heavy metals strongly depends on the humification process. Fourthly, earthworms aerate and fragment the input material, hence, no turning or active aeration is needed as with composting. Furthermore, they increase the surface area for further degradation. Table 4 compares key features of vermicomposting and composting.

Table 4: Comparison of key features between vermicomposting and composting (Amlinger et al., 2005; Domínguez & Edwards, 2011b; R. P. Singh et al., 2011)

Parameters	Composting	Vermicomposting
Waste characteristics	Source separately collected biogenic waste	Any biogenic waste which is not appreciably oily, spicy, salty or hard, and that do not have excess alkalinity or acidity
Initial particle size	10 - 15 mm for agitated systems or forced aeration	10 - 20 mm
Optimum C to N ratio	25 - 35	25 - 30
Water content	55 - 60 %	80 - 85 %
Aeration	0.6 - 1.8 m <sup>3</sup> /day kg	Earthworms aerate the system
pH	-----	>5 to <9

Temperature	55 - >65 °C	15 - 25 °C
Heavy metals	Risk of heavy metals in the compost	Heavy metals are partly removed and accumulated within the earthworm's tissue
Human pathogens	Removed by the thermophilic phase	Removed after 70 days

## 2.4 Plastics

### 2.4.1 Biodegradability and compostability

Plastics are considered to be biodegradable when they can be completely mineralized to CO<sub>2</sub>, water and converted into biomass by naturally occurring microorganisms. Therefore, it does not matter if they are based on non-renewable fossil resources or renewable biomass resources. It should not be confounded with eco-friendly or bio-based plastics that are non-biodegradable. These plastics are materials that are carbon neutral. Hence, CO<sub>2</sub> produced with their disposal, incineration for instance, is again converted to biomass through photosynthesis (Iwata, 2015).

Aerobic degradation is described in the following equation (Zee, 2014)



Apart from being biodegradable some polymers are compostable, which suggests that their chemical structure is designed for biological decomposition processes. They must be mineralized and disintegrated during the composting process and fulfil their biodegradation during the end-use of the compost without exhibiting any harmful effect on ecosystems (Rudnik, 2008).

### 2.4.2 Classification and composition of biodegradable plastics

#### 2.4.2.1 Bio-based plastics from renewable resources

Bio-based plastics are based on renewable carbon resources. They contain extracted components from plant and wood biomass, such as starch, cellulose, hemicellulose, lignin, or plant oil (Iwata, 2015). Three different production pathways for bio-based plastics exist. Firstly, natural occurring polymer chains, such as starch polymers, are used or modified, yet, a large part remains intact. Secondly, monomers are produced by fermentation and further polymerization (polylactic acid). Thirdly, bio-based polymers are directly formed in microorganisms or in genetically modified crops. These pathways produce the following biodegradable polymers (Rudnik, 2008)

- Polylactide (PLA)
- Polyhydroxyalkanoates: poly(3-hydroxybutyrate) (PHB)
- Thermoplastic starch
- Cellulose
- Chitosan
- Proteins



#### 2.4.2.2 Fossil-fuel based plastics

Biodegradable petroleum-based polymers comprise.

- Aliphatic polyesters and copolyesters (e.g. poly(butylene succinate)- PBS, poly(butylene succinate adipate)- PBSA)
- Aromatic copolyesters (e.g. polybutylene adipate-co-terephthalate)- PBAT)
- Poly( $\epsilon$ -caprolactone)- PCL
- Polyesteramides- PEA
- Poly(vinyl alcohol)- PVA

Bio-based polymers are mostly blended with fossil-fuel based plastics to improve their properties or lower their cost (Rudnik, 2008).

#### 2.4.3 Microbial and fungal degradation

Microorganisms and fungi can produce enzymes that can break down long polymer chains. Microbial degradation of polymers includes two major steps. Firstly, depolymerisation occurs outside of the organism as the polymer chains are too big, and insoluble. Therefore, extracellular enzymes degrade these chains either in an endo-enzymatic or exo-enzymatic manner. Endo-enzymatic degradation means that random internal linkages and exo-enzymatic degradation that terminal monomers of the polymer chains are attacked (Zee, 2014). These extracellular enzymes perform either oxidation or hydrolysis on the polymer. During hydrolysis the enzyme binds to the polymer and secondly, subsequently catalyses a hydrolytic cleavage (Endres & Siebert-Raths, 2009; Tokiwa & Calabia, 2004). Water is critical for hydrolysis, hence, disintegration of plastics is faster in media with high water holding capacity, such as compost (Karamanlioglu & Robson, 2013).

As soon as the polymers are broken down into oligomeric or monomeric fragments that are sufficiently small sized, they are carried into the cell. This is where the mineralization process is taking place which results in the production of metabolic energy for the microorganism. Apart from adenosine triphosphate, gases, water, salts, minerals, and biomass are produced. The degradation process of polymers does not depend on the total mineralisation, but also on the biomass accumulated (Zee, 2014).

The biodegradation process is dependent on the readily available surface area since microbial degradation rate increases with the surface area to attack (Chinaglia et al., 2018). Furthermore, soil temperature and total N content play a major role. Biodegradable plastics mainly consist of C, H and O atoms, consequently, microorganisms need additional N for their metabolism (Hoshino et al., 2001). Moreover, microorganisms prefer amorphous over crystalline regions in polymers (Barragán et al., 2016).

#### 2.4.4 Disposal of plastics by earthworms

Academic research has just recently been focusing on the impact of microplastics on earthworms. However, some authors have conducted studies on living earthworms, such as Huerta Lwanga et al. (2016) who studied the influence of polyethylene microparticles sized between 200 - 300  $\mu\text{m}$  on *Lumbricus Terrestris*. They found that earthworms died when 25 and 60 % of microparticles were added to plant litter. Furthermore, their growth rate was significantly lower at microparticle levels that were higher than 28 %. Surprisingly, more microplastic was found in vermicasts at concentration levels of 7 %. Sizes of microparticles were significantly decreased in the casts compared to the beginning of the experiment. Another study by Cao et al. (2017)

found similar results in their study when exposing *Eisenia Fetida* to polystyrene microspheres with a particle size of 58  $\mu\text{m}$ . Concentration levels higher than 1 % caused a growth rate inhibition, and mortality among the population rose with microparticle concentration.

Rodríguez-Seijo et al. (2018) showed that *Eisenia Fetida* is negatively impacted when exposed to low-density polyethylene (LD-PE) micro particles. By testing different biomarkers after the experiment, they proved that *Eisenia Fetida* suffered from oxidative stress. This means that microplastics caused an overproduction of reactive oxygen species, which leads to the peroxidation of lipid tails in the membrane structure. Moreover, Rodríguez-Seijo et al. (2017) proved that after being exposed to polyethylene microparticles, *Eisenia Andrei* suffered histopathological damages. They ranged from gut damages to atrophy or detachment of gut epithelium. Additionally, inflammatory processes in the gut epithelium and the chloragogen tissue were recorded, leading in some cases to fibrosis and congestion. Furthermore, polyethylene micro particles were found in the gut of *Eisenia Andrei*. Nevertheless, some individuals did not incorporate any plastic microparticles. This is due to the fact that earthworms are selective feeders, i.e. they prefer different organic material properties over others, which they egest within 5.5 hours. Therefore, they might not feed on plastic particles, or simply egest them too rapidly for detection (Curry & Schmidt, 2007).

Lwanga et al. (2018) showed in their study that bacteria isolated from the earthworm gut of *Lumbricus Terrestris* reduced LD-PE particles significantly. The extracted bacteria belonged to the phylum Actinobacteria and Firmicutes. They were inoculated in a mixture of sterile, sandy soil and LD-PE microparticles. After 21 days they were able to degrade 60 % of the microplastics. The rest was reduced to smaller particles and nanoparticles. Since earthworms are detritivorous, they are susceptible to micro- and nanoplastics produced as biproduct by microorganisms and fungi (Helmberger et al., 2020).

### **2.4.5 Microplastics**

During biodegradation of plastics, micro particles and nanoparticles might be produced. Microparticles are smaller than 5 mm and nanoparticles smaller than 0.1  $\mu\text{m}$ . They can be either visible for the naked eye or detectable by microscopical analysis (Sintim et al., 2019). Microplastics in aquatic systems have been widely investigated throughout the past 8 years. However, microplastic pollution in soils has just recently caught more attention from academia and methods for analysing microplastic concentrations in soil still need to be developed. Its impact on soil biota and fauna is merely known. There is evidence that soil biota enhances plastic fragmentation, hence microplastics, and even transports microplastics through the soil (Helmberger et al., 2020). It was proven that microparticles of polyethylene can adhere to the skin of *Lumbricus terrestris* L. which further transports it into deeper layers. Above it all the smallest particle fraction sized between 710 and 850  $\mu\text{m}$  were transported to the deepest layer (Rillig et al., 2017).

Nevertheless, microparticles are not only found in soils, but also in compost. A study conducted by Weithmann et al. (2018) investigated the microplastic concentration in compost originating from a German composting plant. Although, the compost was sieved to remove impurities before and after composting, 20 to 24 particles/kg compost sized between 1 to 5 mm were still detectable in the two compost samples respectively. Most plastic particles originated from food packaging that entered the composting process. These plastic particles are then introduced into soil through horticultural and

agricultural application. The authors of this study estimate that 35 billion to 2.2 trillion microplastic particles enter the environment by this pathway.

In practice, impurities are removed from the compost by sieving, manual sorting, a metal separator, and an air separator (Amlinger et al., 2005). These procedures can significantly reduce contaminants, but not completely remove them (Weithmann et al., 2018).

#### **2.4.6 Certification and standardisation**

The European Union has set a regulative framework for biodegradable and compostable plastics in the “European Directive on Packaging and Packaging waste”. There it is stated that “biodegradable packaging waste shall be of such nature that it is capable of undergoing physical, chemical, thermal, or biological decomposition such that most of the finished compost ultimately decomposes into carbon dioxide, biomass and water” (Directive 94/62/EC). EN 13432 defines guidelines that biodegradable and compostable plastics need to fulfil. These are a list of input materials used for production, biodegradability, disintegration during biological treatment, effect on the biological treatment, and effect on the quality of the resulting compost.

##### **List of input materials used for production**

Volatile solid contents must make up for at least 50 % and heavy metals are restricted for compostable packaging. In Table 5 the limiting values for compostable packaging according to EN 13432 are presented.

Table 5: Limiting values for heavy metal content in compostable packaging according to EN 13432

<b>Heavy metal</b>	<b>Zn</b>	<b>Cu</b>	<b>Ni</b>	<b>Cd</b>	<b>Pb</b>	<b>Hg</b>	<b>Cr</b>	<b>Mo</b>	<b>Se</b>	<b>As</b>	<b>Fe</b>
mg/kg dm	150	50	25	0.5	50	0.5	50	1	0.75	5	100

##### **Biodegradability**

For testing the biodegradability of packaging ISO 14855, ISO 14851, and ISO 14852 are recommended standards. The packaging of interest needs to be biodegraded to at least 90 % within less than six months under defined conditions. 90 % of TOC of the original packaging needs to be transformed into CO<sub>2</sub> and water.

##### **Disintegration**

This means the fragmentation and loss of visibility of biodegradable plastics in compost. The assessment shall be conducted on a pilot or full-scale composting plant where the packaging of interest shall be composted together with biogenic waste within three months. Afterwards, the compost should be sieved with a 2 mm sieve and the residual fractions of packaging should not exceed 10 % of the original mass.

##### **Effect on the composting system**

The biodegradation of the packaging should not have any negative impacts on the composting system which needs to be verified by the composting trials.







##### **Effect on the quality of the resulting compost**

Compost samples shall be withdrawn from two different composting trials: one with packaging and one without packaging. Their results should be comparable and should include the volumetric weight density, total dry solids, volatile solids, salt content, pH,

and presence of N, NH<sub>4</sub>-N, P, Mg and K. Moreover, plant growth tests must be conducted.

In Table 6 frequently used labels for plastics that are awarded by TÜV Austria, formerly Vinçotte, are shown. However, more labels and even counterfeited labels exist, and the worldwide harmonisation in labelling has been a polemic over the past decades.

Table 6: Labelling for biodegradable and compostable plastics (TÜV AUSTRIA HOLDING AG, 2020)

Labels	Requirements
	<p>Based on a certain amount of biobased carbon. Up to four stars are awarded for different total amounts of biobased carbon.</p> <ul style="list-style-type: none"> <li>• 1*- 20 - 40 %</li> <li>• 2**- 40 - 60 %</li> <li>• 3***-60 - 80 %</li> <li>• 4****- &gt;80 %</li> </ul>
	<p>Based on EN 16785-1 which measures the bio-based content based on biomass.</p>
	<p>Products are compostable in a technically operated composting system. This includes all components, ink and additives. Label requirements comply with EN 13432.</p>
	<p>Products are compostable in home operated composting systems which reach lower temperatures (20 - 30 °C) than industrial ones.</p>
	<p>Products are compostable according to EN 13432. The label is issued by Bioplastic Europe.</p>
	<p>Biodegradable in soil.</p>

### 2.4.7 Testing methods

Different methods are available to determine biodegradation of polymers. It is necessary to assess mineralisation of organic matter into H<sub>2</sub>O, CO<sub>2</sub>, and new biomass. Therefore, mere changes, damage or reduction of the surface of plastics does not indicate total biodegradation (Zee, 2014).

#### 2.4.7.1 Visual observations

Visual changes can be detected easily in every set-up. They encompass roughening of the surface, formation of holes or cracks, defragmentation, changes in colour, or formation of biofilms on the surface. These changes do not necessarily mark biodegradation processes. Nevertheless, it can be the first indication for microbial attack. Degradation can be investigated more thoroughly by microscopy. When polymers are biodegraded, crystalline spherulites appear on the surface as microorganisms prefer amorphous over crystalline polymer fractions (Shah et al., 2008).

#### 2.4.7.2 Mechanical, physical and chemical properties

The degradation process of polymers is closely associated with changes in mechanical, physical and chemical properties (Zee, 2014). Weight loss is a good indicator. It can be measured as the percentage of the initial sample weight (Barragán et al., 2016).

$$\% \text{ Weight loss} = \frac{W_0 - W_i}{W_0} * 100$$

W<sub>0</sub>.... Weight of the sample before the test

W<sub>i</sub>.... Weight at a given point of time i

Apart from weight loss, molecular weight can be easily determined. A decrease in average molecular weight and broadening of molecular weight can demonstrate an ongoing degradation process (Karamanlioglu & Robson, 2013; Zee, 2014).

Chemical parameters can be detected by different methods. Often a Fourier-transform infrared (FTIR) spectrophotometer is used to determine different chemical components. A decrease in the absorbance of bands indicates a change in chemical properties (Barragán et al., 2016).

Mechanical properties can be measured by assessing the tensile strength. Decreasing tensile strength expresses the biodegradation process going on (Karamanlioglu & Robson, 2013).

#### 2.4.7.3 Respiration test

In order to degrade organic material, microorganisms need enough oxygen in aerobic environments. The biological oxygen demand can be measured with respiratory tests that measure CO<sub>2</sub> production or O<sub>2</sub> consumption. CO<sub>2</sub> evolution can be measured by respirometers and O<sub>2</sub> consumption by measuring the flow rate of oxygen (Aspray et al., 2015).

#### 2.4.7.4 Gas evolution test

The evolution of CO<sub>2</sub> and CH<sub>4</sub> are direct parameters indicating the mineralisation process. Hence, measuring the amount of gases evolved is widely used in academic research. Testing methods can differ in medium composition, inoculum, the way substrate is introduced, and in methods measuring gas evolution. In addition to the detection of gaseous carbon, the soluble, and solid products need to be recorded. They

can be measured as dissolved organic carbon or as chemical oxygen demand, which describe soluble products, oligomers, intermediates and proteins produced by microbial cells (Zee, 2014).

#### *2.4.7.5 Enzyme assay*

In an enzyme assay, a polymer substrate is applied to a buffered or pH-controlled system that contains one or more purified enzymes. The type of enzyme used in the test depends on the analysed polymer. Within minutes or hours quantitative information can be obtained about enzymatic degradation. It is useful in describing polymerization kinetics or oligomer or monomer release from polymer chains. However, it does not describe mineralisation rates (Zee, 2014).

#### *2.4.7.6 Clear-zone technique*

For this testing method, a fine suspension of polymer is dispersed onto the surface of an agar gel in a petri dish. Different microorganisms are inoculated in wells bored into the agar. After an incubation period, degradation of the polymer suspension is indicated by a clear zone that evolves around the well. This clear zone can be either detected visually or instrumentally. Still, a positive result does not ultimately mean that the polymer is biodegradable since the organisms can also grow on contaminants, plasticisers etc. (Gould et al., 1990; Zee, 2014).

#### *2.4.7.7 Radiolabelling*

Radiolabelling includes incorporating radioactive  $^{14}\text{C}$  into test materials, such as polymers. These marked materials are exposed to a microbial population and sequentially mineralised to  $\text{CO}_2$  in aerobic environments. Continuously, the amount of  $^{14}\text{CO}_2$  is captured by a scintillation counter. This method is simple, non-destructive, measures ultimate biodegradation and is insensitive to biodegradable impurities and additives in the polymer. However, marked materials are expensive and issues concerning licensing and waste disposal are major drawbacks (Shah et al., 2008; Sharabi & Bartha, 1993).

#### *2.4.7.8 Laboratory-scale simulated accelerating environments and field trails*

Natural environments can be mimicked at laboratory scale by exposing polymers to a biotic medium, such as soil or compost. In this case biodegradation can be assessed by various methods, already described in the sections 2.4.7.1 - 2.4.7.7 (Chinaglia et al., 2018). In laboratory scale experiments there is a maximum control over different variables, such as temperature, pH, microbial community, mechanical agitation and supply of oxygen (Zee, 2014). In contrast, field trails are conducted in a natural environment. This includes soil burial in different sites with different soil properties. With field trails little information on the degradation process itself can be retrieved and only weight loss, and total disintegration can be monitored (Hoshino et al., 2001).

## **2.5 Fourier transform infrared (FTIR) spectroscopy**

Infrared spectrometry is a method to quantify and identify chemical bonds. The method is based on the theory that every molecule incorporates energy consisting of translational, rotational and vibrational energy. Each chemical bond within a molecule has got a specific natural vibrational frequency. When a molecule is excited with the broad spectrum of infrared light, the covalent bonds can absorb certain characteristic frequencies and start to vibrate. This process is called adsorption of the infrared

radiation. An adsorption range is characteristic for different functional groups and molecules can be characterized by their functional groups (Colthup et al., 1975).

### 2.5.1 FTIR spectroscopy of compost

Smidt & Schwanninger (2005) described the decomposition process by periodically examining compost with a FTIR spectroscopy. The indicator bands serve as a reference to determine different stages during the decomposition process. The end of the rotting process is characterized by a constant presence of certain band-heights and absence of other bands, i.e. bands at 1560, 1320, 1260 - 1240  $\text{cm}^{-1}$  in fully matured compost. During the first few weeks, indicator bands of easily degradable compounds decrease the fastest. For instances, the indicator band at 1740  $\text{cm}^{-1}$ , which characterises C=O stretch of aldehydes, ketones, carboxylic acids and esters, disappears very rapidly. Bands of aromatic amines at 1320  $\text{cm}^{-1}$  diminish first but increase after the first 6 - 10 weeks. A decrease in the final compost indicates low microbial activity and inefficiency in transformation rates to more resistant molecules. Aromatic C=C bands at 1512  $\text{cm}^{-1}$  indicate lignocellulosic materials. In Table 7 indicator bands and their changes throughout the rotting process are presented.

Table 7: Changes in characteristic indicator bands in the infrared spectrum throughout the rotting process (Smidt & Schwanninger, 2005)

Wavenumber ( $\text{cm}^{-1}$ )	Vibration	Functional group or compound	<16 weeks	>16 weeks
3400	<i>C – O stretch</i>	Bonded and nonbonded hydroxyl groups and water		
2920	<i>C – H stretch</i>	Methylene	↓	→
2850	<i>C – H stretch</i>	Methylene	↓	→
2520		Carbonate	↑	→
1740-1720	<i>C = O</i>	Aldehyde, ketone, carboxyl acids, esters	↓	
1640	<i>C = O</i>	Amide I, carboxylates	↓	→
	<i>C = C</i>	Aromatic ring modes, alkenes	↑	→
1635	<i>O – H bending</i>	Adsorbed water		
1560, 1546	<i>N – H in plane</i>	Amides II	↓	→
1515 - 1505	Aromatic skeletal	Lignin		
1425	<i>COO<sup>-</sup> stretch</i>	Carboxylic acids	↓	→
	<i>C – O stretch</i>	Carbonate	↑	→

1384	<i>N – O stretch</i>	Nitrate		↑↓
1320	<i>C – N stretch</i>	Aromatic primary and secondary amines	↑↓	
1260 - 1240	<i>C – O</i>	Carboxylic acids	↓	
	<i>C – N</i>	Amide III	↓	
1250 - 900	<i>C – O – C, C – O</i>	Polysaccharides	↓	→
	<i>C – O – P</i>	Phosphodiester		
1080		Quartz		
1030	<i>Si – O stretch</i>	Clay minerals	↑	→
	<i>Si – O – Si stretch</i>	Silica		
875	<i>C – O out of plane</i>	Carbonate	↑	→

↑ increase ↓ decrease → constant

### 2.5.2 FTIR spectroscopy of low-density polyethylene and thermoplastic starch poly(butylene adipate-co-terephthalate)

Low-density polyethylene (LD-PE) products contain four characteristic peaks. The most pronounced peaks are found at  $2914\text{ cm}^{-1}$  that is attributed to the C-H asymmetrical stretch in ethene, and at  $2847\text{ cm}^{-1}$ , which is assigned to the C-H symmetrical stretch in ethene. A bending deformation is found at  $1468\text{ cm}^{-1}$ , a symmetric deformation at  $1373\text{ cm}^{-1}$ , and a rocking deformation at  $718\text{ cm}^{-1}$  (Rajandas et al., 2012). Rajandas et al. (2012) report that pre-aging or pre-treatment of LD-PE products is necessary to facilitate biodegradation since it would otherwise take decades to decompose.

Many studies have analysed thermoplastic starch poly(butylene adipate-co-terephthalate) (TPS-PBAT) using FTIR spectroscopy. However, indicator bands height and width can vary vastly between TPS-PBAT products due to their composition and production (Brandelero et al., 2011). In Table 8 characteristic indicator bands of TPS-PBAT are presented. Barragán et al. (2016) tested the biodegradability of agricultural mulch films in soil under laboratory conditions. Among the mulch films, a Mater-Bi® film was used which is composed of TPS-PBAT. Biodegradation was monitored by FTIR spectroscopy. After 158 days, the Mater-Bi® mulch film saw a decrease in absorbance of -OH at wavenumber  $3450\text{ to }3300\text{ cm}^{-1}$  and C=O at wavenumber  $1840\text{ to }1640\text{ cm}^{-1}$ . Hydroxyl group bonds originate from hydroxyl endings of starch and carbonyl groups are part of the ester bonds.



Table 8: Characteristic indicator bands in the infrared spectrum of TPS-PBAT (Barragán et al., 2016; Brandelero et al., 2011; Elfehri Borchani et al., 2015; Kijchavengkul et al., 2008; Yaacob et al., 2016)

Wavenumber (cm <sup>-1</sup> )	Vibration	Functional group or compound	Source
3900 - 3300	<i>O – H stretch</i>	Hydroxyl, mainly attributed to starch	(Elfehri Borchani et al., 2015)
3400	<i>O – H stretch</i>	Hydroxyl groups and water	(Barragán et al., 2016)
3000	<i>O – H stretch</i>	Aliphatic and aromatic compounds	(Kijchavengkul et al., 2008)
1710	<i>C = O stretch</i>	Carbonyl group in ester compound	(Kijchavengkul et al., 2008)
1573	<i>C – H stretch</i>	Phenylene group	(Elfehri Borchani et al., 2015)
1495	<i>C – H stretch</i>	Phenylene group	(Elfehri Borchani et al., 2015)
1480 - 1350	<i>C – H bending</i>	Methyl group	(Barragán et al., 2016)
1456	<i>C – H stretch</i>	Phenylene group	(Elfehri Borchani et al., 2015)
1267	<i>C – O stretch</i>	Carbonyl group in ester	(Kijchavengkul et al., 2008)
1190 - 1087	<i>O – C = O stretch</i>	Carbonyl group in ester	(Yaacob et al., 2016)
1080, 1020	<i>C – O stretch</i>	Glucose ring	(Brandelero et al., 2011)
1020 - 880	<i>C – H bending</i>	Substituted Benzene ring	(Kijchavengkul et al., 2008)
1019	<i>C – H stretch</i>	Phenylene group	(Elfehri Borchani et al., 2015)
725	<i>C – H rocking</i>	Four or more adjacent methylene	(Elfehri Borchani et al., 2015)

### 3 Material and methods

#### 3.1 Experimental set-up

The current thesis investigated the degradation degree and impacts of biodegradable and non-biodegradable plastics on vermicomposting and composting. The experiments were designed to compare composting and vermicomposting under three different conditions. Therefore, composting reactors and vermicomposters were prepared for each experimental group. A reactor was spiked with non-biodegradable plastic foils, another one was spiked with biodegradable foils and the third was not spiked and served as control. Laboratory compost reactors and vermicomposters were monitored over a period of 120 days. For compost reactors, all input material was added at the beginning of the experiment, whereas for vermicomposting fresh input material was added every week since earthworms can consume half or more of their body weight in biogenic waste a day. Figure 3 summarizes the experimental set-up.

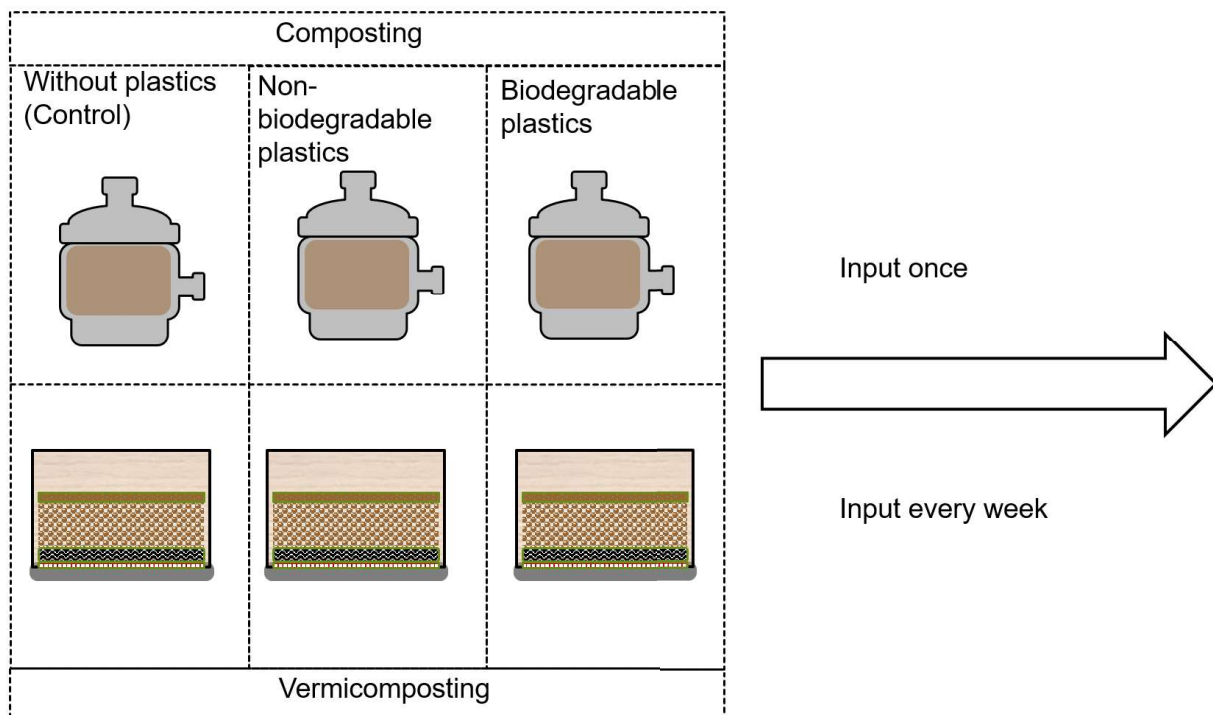


Figure 3: Experimental set-up of the compost and vermicompost experiment including three experimental groups; not spiked with foils, spiked with non-biodegradable foils and spiked with biodegradable foils

##### 3.1.1 Input materials

###### 3.1.1.1 Biogenic waste

Biogenic waste was provided by the Wiener Tafel- Verein für sozialen Transfer (a non-profit organisation that collects food from wholesalers and restaurants for social institutions) and served as input material for compost reactors and vermicomposters. The biogenic waste was composed of fruits and vegetables that were chopped into 2 cm pieces. For vermicomposting, the biogenic waste was weighted and frozen at - 22 °C, because input material had to be added continuously. Using frozen organic material caused excessive moisture to collect in the vermibed during thawing and led to the appearance of unwanted red mites. Therefore, the experimental set up was adapted, and input material was then collected freshly from MERKUR Warenhandels

AG, a Viennese supermarket that was close to the institute. This material varied in composition due to seasonal availability of fruits and vegetables. Only seasonal and regional fruits and vegetables were chopped into about 2 to 5 cm pieces.

### 3.1.1.2 Bulking agent

Compost reactors were supplied with 29.3 % of woodchips as bulking agent that was necessary to ensure sufficient aeration to the composting experiments.

### 3.1.1.3 Non-biodegradable plastic bag

The non-biodegradable plastic bag that was added to the compost reactors and vermicomposters was analysed by ATR-FTIR spectroscopy to record its infrared spectrum. The spectrum revealed typical indicator bands which are shown in Figure 4. The spectrum of the non-biodegradable plastics bag shows the typical pronounced peaks at  $2914\text{ cm}^{-1}$  (C-H asymmetrical stretch), and at  $2847\text{ cm}^{-1}$  (C-H symmetrical stretch). A bending deformation is found at  $1468\text{ cm}^{-1}$  and a rocking deformation at  $718\text{ cm}^{-1}$  (Rajandas et al., 2012). A small peak at  $875\text{ cm}^{-1}$  revealed its reinforcement with calcium carbonate as reported by Adeosun et al. (2014). These bands indicate that the bag was made of LD-PE.

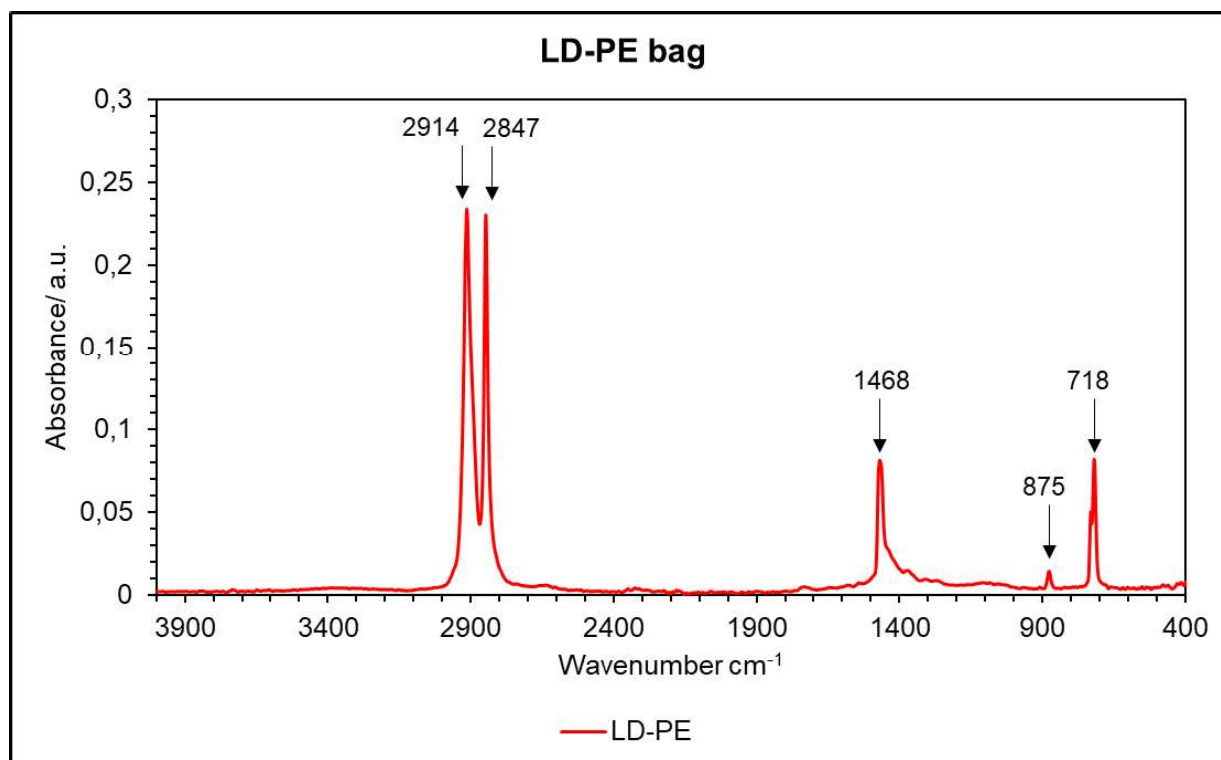


Figure 4: Infrared spectrum of the LD-PE bag

LD-PE is produced under high pressure polymerization of ethylene and is characterized by its relatively low molecular weight. It is semi-crystalline and has got a crystalline melting point at  $108\text{ }^{\circ}\text{C}$ . Furthermore, it is hydrophobic. Many shopping bags and trash bags are made from LD-PE (Brandsch & Piringer, 2008; Oliveira Gama et al., 2018). LD-PE bags were obtained from MERKUR Warenhandels AG. They were cut into 2 – 10 mm pieces and added to the input material.

### 3.1.1.4 Biodegradable plastic bag

The infrared spectrum of the biodegradable plastic bag revealed its original composition as illustrated in Figure 5. It is composed of thermoplastic starch (TPS) and

poly(butylene adipate-co-terephthalate) (PBAT). The broad band between  $3700 - 3300 \text{ cm}^{-1}$  represents O-H stretching vibrations of hydroxyl functions. These belong to hydroxyl endings of starch that are typically found in TPS (Elfehri Borchani et al., 2015). Moreover, at  $1079$  and  $1018 \text{ cm}^{-1}$  a C-O stretch, which is part of a glucose ring is found (Brandelero et al., 2011). The following adsorption bands in the spectrum represent PBAT. A sharp band between  $3000 - 2840 \text{ cm}^{-1}$  indicates C-H stretching vibrations which are attributed to aliphatic and aromatic compounds. Another sharp band at  $1711 \text{ cm}^{-1}$  is attributed to a C=O stretch which is ascribed to the carbonyl group in an ester compound (Kijchavengkul et al., 2008). Between  $1480$  and  $1350 \text{ cm}^{-1}$  a characteristic C-H bending for PBAT is seen, which is a reference to methyl groups (Barragán et al., 2016). A phenylene group is represented by wavenumber  $1454 \text{ cm}^{-1}$  (Elfehri Borchani et al., 2015). Two typical carbonyl groups in ester are found at  $1269 \text{ cm}^{-1}$  (Kijchavengkul et al., 2008) and at  $1154 \text{ cm}^{-1}$  (Yaacob et al., 2016). At  $725 \text{ cm}^{-1}$  C-H rocking is found which is assigned to four or more adjacent methylene compounds (Elfehri Borchani et al., 2015).

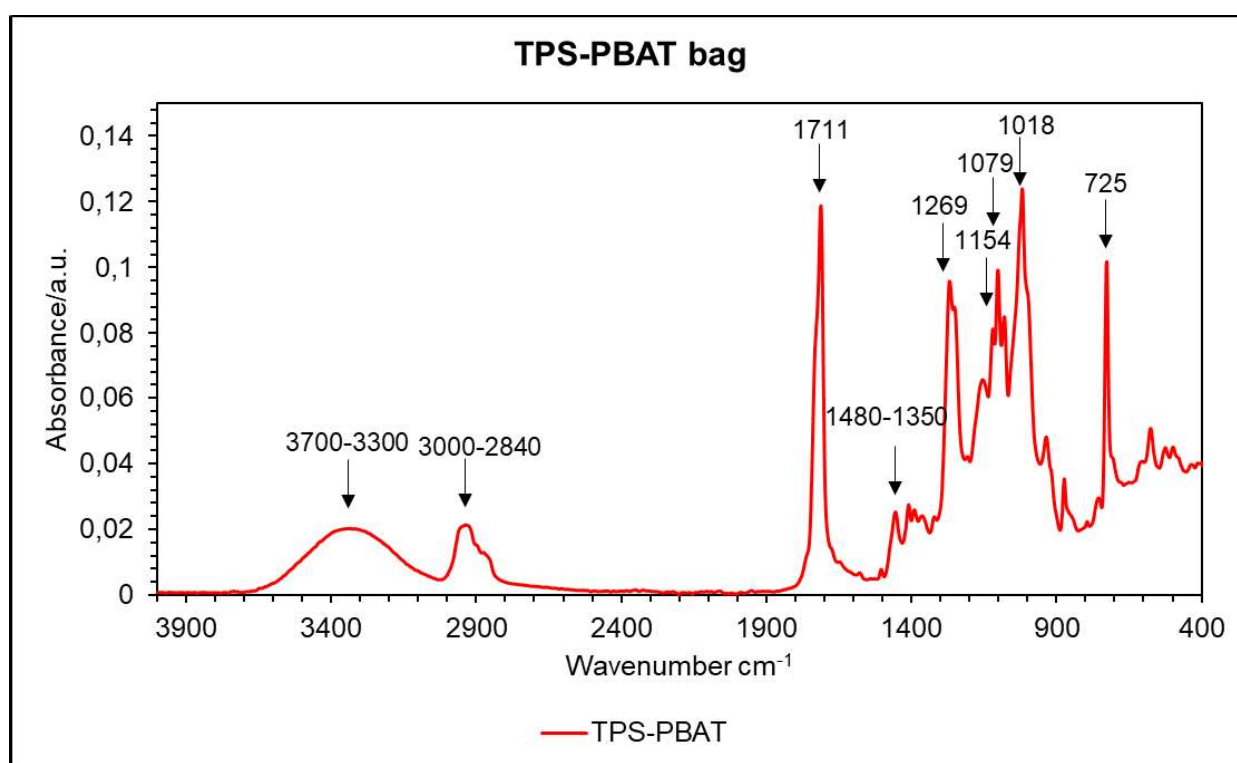


Figure 5: Infrared spectrum of the TPS-PBAT bag

Biodegradable plastic bags, namely the so called “Bio-Kreislauf-Sackerl”, were obtained from the Kompost & Biogas Verband Österreich. Mater-Bi<sup>®</sup> produced by Novamont S.p.A. is a thermoplastic polymer based on starch and is commercially available in different grades depending on the given amount of starch. Each composition exhibits different properties. Mater-Bi<sup>®</sup> N is a blend of starch and poly(butylene adipate-co-terephthalate) (Elfehri Borchani et al., 2015). Therefore, it is both bio-based and fossil-fuel based. According to the producer it is biodegradable and compostable in line with EN 13432 (Novamont S.p.A., 2015). The TPS-PBAT bags had a Seedling and OK compost HOME labelling on them. They were cut into approximately 2 - 10 mm in diameter pieces and added to the input material.

Figure 6 shows a picture of the LD-PE and TPS-PBAT bag. Both were printed. The LD-PE bag was transparent, and its texture was brittle, whereas the TPS-PBAT bag had an opaque colour and was more elastic than the LD-PE bag.

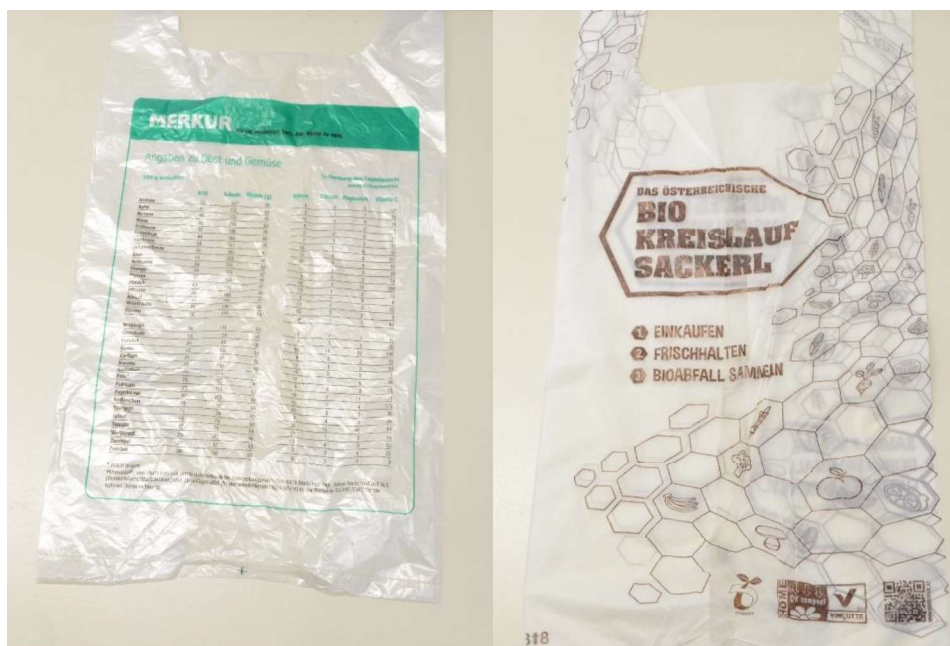


Figure 6: LD-PE bag (on the left) and TPS-PBAT bag (on the right)

### 3.1.2 Composting experiment

12 adapted glass desiccators were used as rotting reactors for this experiment. In Figure 7 a schematic drawing of the compost reactors is provided. The compost reactors were airtight. Hence, they were actively aerated through a tube that reached the bottom of the composting system and connected it to the outside. The airflow was adjusted according to the CO<sub>2</sub> concentrations in order to provide proper oxygen supply. Waste air was collected through a tube at the top of the compost reactor that was connected to a cold trap, which was located in a water bath at room temperature. While the vapour condensed, gases were collected in a plastic bag. CO<sub>2</sub> was recorded by an infrared CO<sub>2</sub>-detector every three hours. The condensate was quantified at every turning event.

Input material was placed on a grid covered by fleece inside of the compost reactor in order to collect leachate at the bottom. The 12 compost reactors were placed on three levels within a climatic chamber. Temperature was regulated externally in order to simulate the centre of a realistic composting pile. The temperature of each compost reactor was determined by a thermo-element minimum twice a day. Temperature of the climatic chamber was adjusted to below 1 °C of the lowest measured temperature of the compost reactors at the top level. This procedure was used to prevent heat loss and to simulate conditions in a composting windrow.

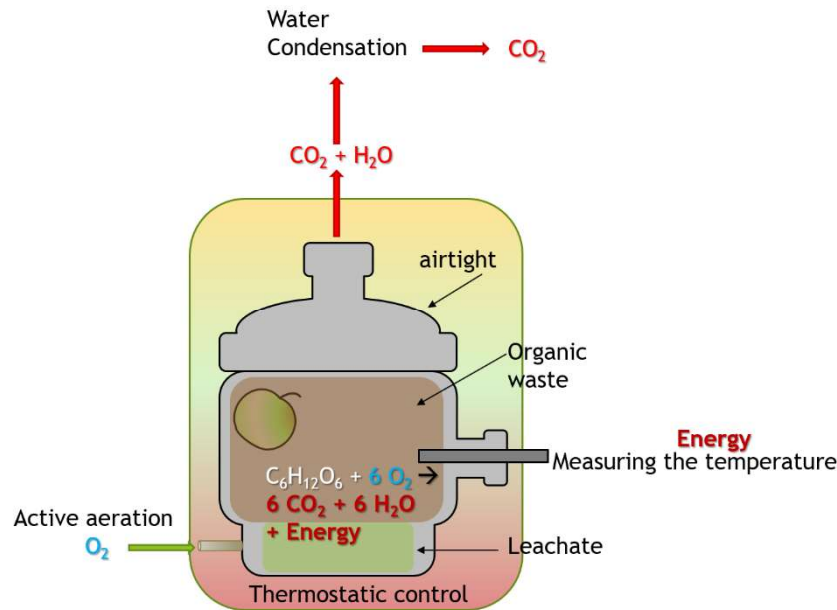


Figure 7: Schematic drawing of the compost reactors

From the 12 compost reactors, R1, R4, R5, and R9 were filled with input material only (control), R2, R6, R8, and R10 with input material and 1 % LD-PE foils, and R3, R7, R11, and R12 were filled with input material and 1 % TPS-PBAT foils. In Table 9, Table 10, and Table 11 the ratio between biogenic waste and bulking agent is shown as well as the weight of total input material and plastic particles in each compost reactor.

Table 9: Composition of the input material of composting without foils

1.Composting of pure biogenic waste				
Composting reactors	R1	R4	R5	R9
Bulking agent [%]	29.3	29.3	29.3	29.3
Biogenic waste [%]	70.7	70.7	70.7	70.7
Input material [kg]	3.02	3.06	3.02	3.04
Plastic [kg]	0.00	0.00	0.00	0.00

Table 10: Composition of the input material of composting with LD-PE foils

2.Composting of biogenic waste and LD-PE foils				
Composting reactors	R2	R6	R8	R10
Bulking agent [%]	29.3	29.3	29.3	29.3
Biogenic waste [%]	70.7	70.7	70.7	70.7
Input material [kg]	3.04	3.01	3.03	3.06
Plastic [kg]	0.03	0.03	0.03	0.03



Table 11: Composition of the input material of composting with TPS-PBAT foils

3.Composting of biogenic waste and TPS-PBAT foils				
Composting reactors	R3	R7	R11	R12
Bulking agent [%]	29.3	29.3	29.3	29.3
Biogenic waste [%]	70.7	70.7	70.7	70.7
Input material [kg]	3.03	3.04	3.03	3.03
Plastic [kg]	0.03	0.03	0.03	0.03

At the beginning, at least one compost reactor of each experimental group was placed on the first, second and third level of the climatic chamber. In Figure 8 the timeline of the composting experiment is presented. The rotting material was turned after 8 days and then approximately every 14 days and samples were taken at the beginning of the experiment, on day 8, 22, 48, 90 and 124 which marked the end of the experiment. Water was added to compost reactors, when required. After 8 days the rotting material in the compost reactors lost significantly in mass, R4 and R9 were merged with R1 and R5, R8 with R2 and R6, and R11 and R12 with R3 and R7 to maintain the biodegradation process. R10 was merged with R2 and R6 after 22 days since the material loss was too low in this reactor. Finally, the compost reactors in each experimental group were united into one, i.e. R1, R2 and R3, on day 90, and the experiment ended with 3 compost reactors, each of which contained the output material of the entire experimental group respectively.

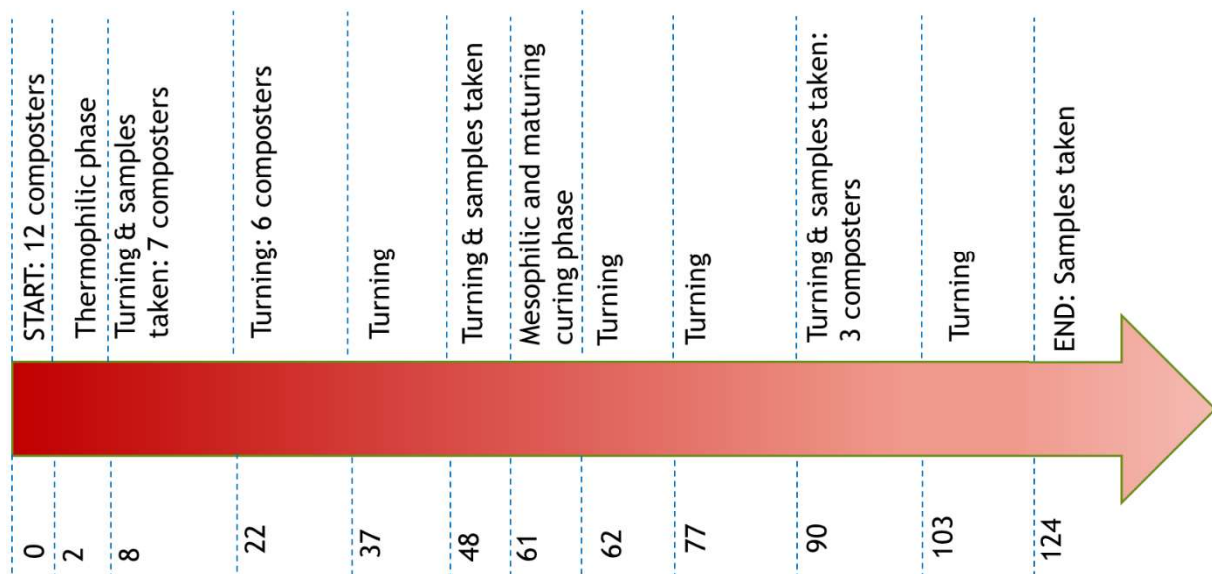


Figure 8: Timeline of the composting experiment

### 3.1.3 Vermicomposting experiment

3 vermicomposters were acquired from Wormsystems GmbH. They were made of spruce and impregnated with flax oil before the start of the experiment. Additionally, earthworms, mineral blend and 3 hemp mats were obtained from the same company. According to the CEO, BSc. David Witzeneder, the earthworm species delivered by Wormsystems GmbH are *Eisenia Fetida*, *Eisenia Andrei* and *Eisenia Hortensis* (*Dendrobena Veneta*). In order to maintain constant and favourable ambient temperature for earthworms, the 3 vermicomposters were placed either in a climatic chamber with a steady temperature between 22 and 23 °C or in the basement of the Institute with moderate temperatures from the 6<sup>th</sup> day onwards. The schematic drawing

in Figure 9 illustrates the set-up of the vermicomposters. It is a wooden box with a lid to close. The vermibed is placed on a grid (net covered by a fleece) in order to prevent earthworms from escaping and allow leachate collection in a plastic tank on the bottom. 4 holes in the upper part and the grid at the bottom of the box guarantee enough aeration.

The input material was continuously added on top of the vermibed and was covered with the hemp mat to avoid drying of the input material. In the first 5 days the input material started to mould, and the mat of hemp was also affected. Therefore, it was replaced by printing paper, which was substituted as soon as most of it had degraded. Every 4 weeks, 42 g of a mixture of rock flour and lime was added, as recommended by the supplier. The mixture allows to maintain pH at a favourable level and rock flour supplies the earthworms with essential minerals that they need to grow and reproduce (Wormsystems GmbH, n.d.-b).

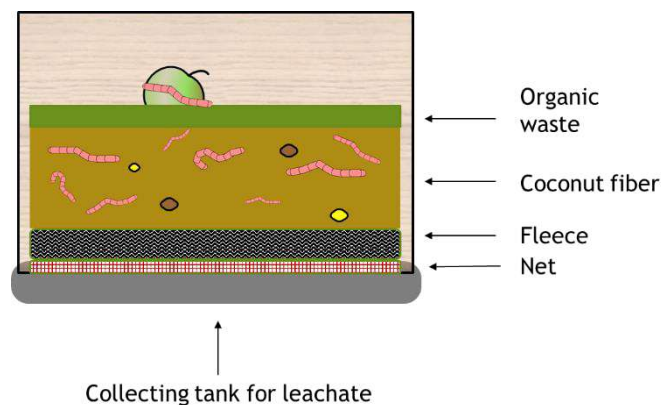


Figure 9: Schematic drawing of the vermicomposters

At the beginning of the experiment, 2,000 g of coconut fibre were placed in each vermicomposter to serve as vermibed. The worms were weighted and evenly distributed among the three vermicomposters. 563.6 to 564.6 g of earthworms were put in each one. In the 1<sup>st</sup> vermicomposter only input material, in 2<sup>nd</sup> vermicomposter 1 %TPS-PBAT foils and input material, and in 3<sup>rd</sup> vermicomposter input material and 0.01 % LD-PE foils were added. The load of LD-PE foils was reduced prior to the start of the experiment, as it was assumed that a higher percentage of LD-PE foils would hinder aeration and overburden the earthworms. Figure 10 shows a picture of the 3 vermicomposters.



Figure 10: Vermicomposters from the company Wormsystems GmbH



During the vermicomposting experiment different parameters were quantified. Firstly, vermicomposters were weighted before and after addition of input material. Secondly, temperature was measured by a thermo-element and water content was examined by fist test. Thirdly, leachate was gathered in the collecting tank at the bottom of the vermicomposter and was quantified. By inserting a tube into the vermibed at a 30 mm depth  $\text{CO}_2$ ,  $\text{CH}_4$ , and  $\text{O}_2$  were extracted and quantified by a gas-detector. At the end of the vermicomposting experiment the height of the final vermicompost in all three vermicomposters was examined and divided into half in order to separate it into a top and bottom layer. Figure 11 shows the height measurement of the vermicompost with a ruler.



Figure 11: Ruler measuring height of the vermicompost

### 3.2 Sampling

For further analysis samples were taken from compost reactors and vermicomposters at different timepoints throughout the experiments. Samples were collected from compost reactors at the beginning, on day 8, 22, 48, 90 and 124. The samples were withdrawn, after the rotting material had been turned. During the turning procedure, the material was thoroughly homogenised. Furthermore, samples were taken from the input material that was initially applied to both experiments. Table 12 presents the samples that were collected from the composting experiment and their consecutive analyses. Analyses comprised quantifying water content (WC), loss on ignition (LOI), total organic carbon (TOC), total inorganic carbon (TIC), total nitrogen (TN), pH, electrical conductivity (EC), Attenuated total reflection-Fourier transform infrared (ATR-FTIR) spectroscopy, respiration activity ( $\text{RA}_4$ ),  $\text{NH}_4\text{-N}$ ,  $\text{NO}_3\text{-N}$ , humic acids (HA), heavy metal content, total phosphor (TP), K, and total Kjeldahl nitrogen (TKN).

Table 12: Samples taken from the composting experiment and their consecutive analyses

Days	Sample	Analyses
1-Start	R1, R2, R3	WC, LOI, TOC, TIC, TN, pH, EC, ATR-FTIR
1-Start	Input material	WC, LOI, TOC, TIC, TN, pH, EC, ATR-FTIR, $\text{RA}_4$ , $\text{NH}_4\text{-N}$ , $\text{NO}_3\text{-N}$
8	R1, R2, R3, R5, R6, R7	WC, LOI, TOC, TIC, TN, pH, EC, ATR-FTIR

22	R1, R2, R3, R5, R6, R7	WC, LOI, TOC, TIC, TN, pH, EC, ATR-FTIR, HA
48	R1, R2, R3, R5, R6, R7	WC, LOI, TOC, TIC, TN, pH, EC, ATR-FTIR, HA
90	R1, R2, R3, R5, R6, R7	WC, LOI, TOC, TIC, TN, pH, EC, ATR-FTIR, HA
124-End	R1, R2, R3	WC, LOI, TOC, TIC, TN, pH, EC, ATR-FTIR, HA, RA <sub>4</sub> , NH <sub>4</sub> -N, NO <sub>3</sub> -N

Sampling from vermicomposters included samples of the original coconut fibre and, fresh input material, whenever new material was added. For subsequent sampling of the vermicompost in later stages, material from each layer was collected, spread out on an aluminium tray and the earthworms were removed by hand. Thereby samples were collected from each layer of the vermicomposters for further analysis. Since sample collection and earthworm removal was very time-consuming, the samples of each vermicomposter were collected on three different days. Additionally, about 20 g of earthworms were collected at the beginning and at the end of the experiment, frozen at -22 °C, and analysed for heavy metals. Furthermore, leachate from the three vermicomposters was collected and stabilized in a refrigerator at 4 °C. Table 13 summarizes sampling days, type of sample, and analyses that were conducted.

Table 13: Samples taken from the vermicomposting experiment and their consecutive analyses

Days	Sample	Analyses
0	Coconut fibre	WC, LOI, TOC, TIC, TN, pH, EC, ATR-FTIR, HA
0	Earthworms	Heavy metal content
0 - 116	V-Input material	WC, LOI, TOC, TIC, TN, pH, EC, ATR-FTIR, NH <sub>4</sub> -N, NO <sub>3</sub> -N
32	Leachate 1	NH <sub>4</sub> -N, NO <sub>3</sub> -N, TP, TKN, K
123	Leachate 2	NH <sub>4</sub> -N, NO <sub>3</sub> -N, pH, EC, TP, TKN
125	V1-Top, V1-Bottom	WC, LOI, TOC, TIC, TN, pH, EC, ATR-FTIR, HA, RA <sub>4</sub> , NH <sub>4</sub> -N, NO <sub>3</sub> -N
125	V1-earthworms	Heavy metal content
125	Leachate 2	NH <sub>4</sub> -N, NO <sub>3</sub> -N, pH, EC, TP, TKN
127	V3-Top, V3-Bottom	WC, LOI, TOC, TIC, TN, pH, EC, ATR-FTIR, HA, RA <sub>4</sub> , NH <sub>4</sub> -N, NO <sub>3</sub> -N
127	V2-earthworms	Heavy metal content
130	Leachate 2	NH <sub>4</sub> -N, NO <sub>3</sub> -N, pH, EC, TP, TKN

131	V2-Top, V2-Bottom	WC, LOI, TOC, TIC, TN, pH, EC, ATR-FTIR, HA, RA <sub>4</sub> , NH <sub>4</sub> -N, NO <sub>3</sub> -N
131	V2-earthworms	Heavy metal analysis

### 3.2.1 Sample preparation

For WC, LOI, TOC, TIC, TN, pH, EC, ATR-FTIR the sample was airdried or dried at 105 °C in a compartment drier (Memmert) for more than 40 hours. Subsequently, the sample was grinded in a cutting mill (Retsch SM 200). The material was mechanically grinded until it was small enough to pass through a series of sieves with filter sizes of 10, 4 and 0.5 mm.

For LOI, TOC, TIC, TN, pH, EC and ATR-FTIR the initial samples were further grinded by a centrifugal mill (Retsch ZM 200) at 14,000 rpm to reach a smaller than 0.5 mm particle size. Since the centrifugal mill generates excessive heat in the course of the grinding process which leads to the distortion of the photometric analysis for humic acids, another device was used to prepare samples that were to be analysed for humic acids.

Instead in the centrifugal mill the material was grinded in a vibratory disc mill (Retsch RS1), whose equipment was made from agate and then sieved through a 0.63 mm sieve. The residual particles that were too large were again grinded in the vibratory disc mill and again sieved. A large part of the samples that were taken on day 22 and 48 from the composting experiment remained as residual particles after sieving. They were mostly composed of bulking agent. It was not feasible to further grind these particles in the vibratory disc mill. Therefore, they were collected and analysed separately for LOI, TOC, TIC, and TN. Data from the before mentioned samples were weighted in reference to their weight and a mean value was formed. During grinding, plastic particles adhered to the metal walls of the cutting mill and partially melted and stick together in the centrifugal and vibratory disc mill. Thus, their contribution to the results of the analyses done with samples that were prepared in that way, was most probably lower than expected.

For RA<sub>4</sub> measurements 200 g and for NH<sub>4</sub>-N and NO<sub>3</sub>-N 100 g of compost and vermicompost were taken and frozen at -22 °C. Further sampling preparation is described in chapter 3.3.5, 3.3.7, and 3.3.8.

Additional samples from compost reactors and vermicomposters were collected in plastic bags and stored in the refrigerator at 4 °C for plastic particle analysis. The earthworms that were frozen at the beginning and the end of the vermicomposting experiment were freeze-dried with a TELSTAR CRYODOS at -48 °C and then grinded in a vibratory disc mill.

## 3.3 Compost quality

Different parameters were determined for the samples taken during the compost and vermicompost experiment. All analyses except for the heavy metal content analysis were conducted at the Institute of Waste Management at the University of Natural Resources and Life Sciences Vienna.

### 3.3.1 Water content

To determine the water content (WC), samples were weighted before and after drying. They were either dried in a compartment drier at 105 °C for 40 hours ( $WC_{105^{\circ}C}$ ) or airdried at room temperature until they did not lose any more weight ( $WC_{airdried}$ ). The residual water content, which resulted from the loss of ignition analysis, was subtracted from the dry matter of  $WC_{airdried}$ . The difference between the wet matter and dry matter was expressed as percentage dry matter (% dm).

$$WC_{105^{\circ}C} [\% \text{ dm}] = \frac{(\text{wet matter} - \text{dry matter}) * 100}{\text{wet matter}}$$

$$WC_{airdried} [\% \text{ dm}] = \frac{(\text{wet matter} - \text{dry matter} - \text{residual water content}) * 100}{\text{wet matter}}$$

### 3.3.2 pH and electric conductivity

Samples were eluted in deionized water at a ratio of 1:10 and put on an overhead shaker for 3 hours. After 3 hours the eluate was filtered with folded filters and then pH and electric conductivity (EC) were recorded.

pH was determined using a pH meter (WTW pH 531). Before conducting the analysis, the device was calibrated for the necessary measuring range, acidic (pH 4) and neutral (pH 7) or alkaline (pH 10). Results were referred to 20 °C. EC was recorded with an EC-meter (WTW LF 318) that measures the ohmic resistance of the eluate and calculates the EC referred to 25 °C. To calculate the EC at 20 °C the value was further multiplied by 0.90446.

### 3.3.3 Loss on ignition

Loss on ignition (LOI) was determined in duplicate. Approximately 10 g of sample was weighted in two ceramic vessels and dried at 105 °C in a compartment drier to assess residual water content. After that the samples were placed in a muffle furnace from Nabertherm® and combusted at 550 °C for 5 hours. The muffle furnace was preheated for 7 hours until 550 °C were reached.

After combustion in the muffle furnace, the inorganic part of the sample remained as ash content in the ceramic vessels as the organic components are burned at 550 °C. The difference between dry matter and ash value is the loss on ignition and is expressed in percentage dry matter [% dm].

$$LOI [\% \text{ dm}] = \frac{(\text{dry matter} - \text{ash value}) * 100}{\text{dry matter}}$$

### 3.3.4 Total organic carbon, total nitrogen and C to N ratio

To obtain the total organic carbon (TOC) and total inorganic carbon (TIC) the analytical device vario MAX CNS from the company ELEMENTAR was employed. Total carbon (TC) was quantified in the original sample and the total inorganic carbon (TIC) was determined from the ash content that remained after combustion in the muffle furnace. Each analysis was conducted in duplicate. Approximately 200 mg of the sample and 40 mg of ash were used as input for the measurement. The samples were burned at 900 °C in a combustion tube while oxygen was constantly supplied. The evolved CO<sub>2</sub> and nitrogen oxides (NO<sub>x</sub>) were then carried by Helium to the post-combustion tube (900 °C) and reduction tube (830 °C). After passing the combustion tubes, the gases were further carried to a CO<sub>2</sub>-absorber, where CO<sub>2</sub> is absorbed, and NO<sub>x</sub> is carried to a thermal conductivity detector where N<sub>Dumas</sub> (TN) is quantified. After the quantification

of TN, the CO<sub>2</sub>-absorber is heated to 250 °C and CO<sub>2</sub> is desorbed. CO<sub>2</sub> is then detected by the thermal conductivity detector.

TOC is determined by the difference between TC and TIC.

$$TOC [\% dm] = TC [\% dm] - TIC [\% dm]$$

TN, TC, TOC and TIC are expressed as percentage of dry matter [% dm].

The ratio between carbon and nitrogen (C/N) is obtained by dividing TOC by TN.

$$C/N = \frac{TOC [\% dm]}{TN [\% dm]}$$

### 3.3.5 Respiration activity

Respiration activity (RA<sub>4</sub>) measurements were set up with fresh frozen samples that were stabilized by freezing at -22 °C. Sample preparation and analysis were conducted based on ÖNORM S 2027-4. The analysis was carried out using a Sapromat from Voith Sulzer, which measures oxygen consumption at 20 °C over a 4-day time period. The frozen sample was slowly thawed overnight in a refrigerator at 4 °C and moistened until optimal water content for aerobic biodegradation was achieved. The samples were spread out onto an aluminium tray and left to pre-aerate for 5 - 7 hours. Excessive drying was avoided by monitoring the samples periodically. Finally, the samples were mixed again and 30 - 50 g were put in 500 ml glass reaction bottles. The analysis was carried out in duplicates.

When microorganisms degrade organic matter, they consume oxygen and emit CO<sub>2</sub>. The volume of CO<sub>2</sub> is equivalent to the consumed O<sub>2</sub>. During the analysis CO<sub>2</sub> emissions were absorbed by sodium hydroxide (NaOH) granules, which were located in a small basin above the sample. Therefore, a negative pressure was generated in the glass reaction bottles filled with samples. As soon as a negative pressure was detected, O<sub>2</sub> was produced electrochemically by electric energy and a copper sulphate (CuSO<sub>4</sub>) solution to balance pressure. The electrical energy needed to generate O<sub>2</sub> was monitored every 36s. In the end RA is calculated by the electrical energy used.

$$RA [mg O_2/g dm] = \frac{c * 0.25 * f}{dm [g]}$$

c....counts which equvalate 0.25 mg of O<sub>2</sub>

f...factor depending on the reactivity of the sample where 0.1 indicates a very stable and 2 a very reactive sample.

RA<sub>4</sub> was given in mg O<sub>2</sub>/g dm. O<sub>2</sub> consumption was calculated for each hour and every three hours an average is formed. In line with ÖNORM S 2027-4, lag-phase ended whenever the three-hour average exceeded 25 % of the previously assessed maximum three-hour average. The hourly RA was accumulated, and the RA of the lag- phase was subtracted from RA<sub>4</sub>.

### 3.3.6 Humic acids

Humic acids were analysed according to the modified method by Gerzabek et al. (1993). Airdried samples were grinded in the vibratory disc mill to avoid excessive heat generation during the grinding process and were further analysed.

The following solutions were used for the analysis:

Sodium pyrophosphate solution0.1 M Na<sub>4</sub>P<sub>2</sub>O<sub>7</sub>Buffer solutionSolution A: 7.5 g Glycin + 5.8 g NaCl/l H<sub>2</sub>O

Solution B: 0.1M NaOH

310 ml Solution A + 190 ml Solution B

10 g of the sample were weighted into 250 ml plastic bottles and diluted in 50 ml of sodium pyrophosphate solution. Since the composting samples soaked up the whole solution on the first day, 80 ml of sodium pyrophosphate solution were used instead of 50 ml that were used in the original method. The following three days 50 ml of sodium pyrophosphate solution were added, as previously described. Then the 250 ml plastic bottles were placed overnight on an overhead shaker. The next day the liquid extract was separated from the solid residue by centrifuging at 5,000 rpm for 20 minutes and then the supernatant at 13,500 rpm for 20 minutes. The solid residues, from both centrifugation steps, were re-dispersed with sodium pyrophosphate solution and then incubated overnight on the overhead shaker.

After centrifugation, the extract was transferred into a 100 ml flask and the rest was filled up to 100 ml with deionized water. Two extractions were conducted to obtain total humic acids and fulvic acids (FA). Firstly 25 ml of the initial extract were mixed with 0.5 ml of hydrochloric acid (HCl) 37 %. After some minutes, the brown and grey humic acids precipitated and were separated from the fulvic acids by centrifuging at 8,000 rpm for 5 minutes. The supernatant containing fulvic acids, was then filled into 50 ml flasks and 0.6 ml of sodium hydroxide was added to adjust the pH to 10. Afterwards, the rest was filled up with buffer solution to the 50 ml mark.

Secondly, the initial solution was diluted with buffer solution either 1:5, 1:10, 3.5:25, 1:25 in a 25 ml flask depending on the colour of the initial extract, as the initial extract had acquired a very dark tone that is not suitable for photometric analysis. Subsequently, humic and fulvic acids were determined using a photometer (HACH LANGE DR 500). With the photometer the optical density (OD) was measured at 400 nm wavelength. The optical density was calculated as follows. The result is given in OD<sub>400</sub>/g organic dm (odm).

$$FA [OD_{400}/g\ odm] = \frac{\text{Absorbance of fulvic acids} * \text{dilution} * 100}{odm [g]}$$

$$HA [OD_{400}/g\ odm] = \frac{(\text{Absorbance of initial extract} * \text{dilution} * 100) - FA [OD_{400}/g\ odm]}{odm [g]}$$

**3.3.7 Nitrate nitrogen**

The nitrate nitrogen (NO<sub>3</sub>-N) analysis was carried out with a photometer (HACH LANGE DR 500). In a highly acidic environment NO<sub>3</sub>-N reacts with the colour reagent 2,6-Dimethylphenol, and a reddish solution is produced. As a result, the absorbance of the solution can be measured in the ultraviolet range at 324 nm wavelength. All samples were analysed in duplicates.

The following solutions were used for the analysis:

Acid mixture1:1, H<sub>2</sub>SO<sub>4</sub>+H<sub>3</sub>PO<sub>4</sub>

Colour reagent

0.12 g 2.6 Dimethylphenol + 100 ml glacial acetic acid

Standard solution

0.3609 g KNO<sub>3</sub> dried at 105 °C + 1000 ml H<sub>2</sub>O

100 g fresh sample was taken from the compost, vermicompost or input material and frozen at -22 °C. The sample was diluted in 1000 ml of deionized water and incubated on the overhead shaker for 2 hours. The leachate from the vermicomposters was first filtered through folded filters to separate solid particles and insects that got trapped in the collecting tank from the leachate. The analysis was carried out in duplicate.

Afterwards 1 ml or 2 ml of the eluate, depending on the expected concentration of NO<sub>3</sub>- N (concentrations ranging between 5 mg/l, 10 mg/l), were pipetted into a 25 ml flask and 3 - 5 granules of amidosulfonic acid (H<sub>3</sub>NSO<sub>4</sub>) were added. After its dissolution, 8 ml of acid mixture and colour reagent were added. Due to the heat production following the exothermic reaction, the flask was left to cool for 10 minutes. After 10 minutes the absorbance is photometrically measured at 324 nm wavelength. For each sample, a blank sample was produced by mixing all reactants except for the eluate which was replaced by 1 or 2 ml of deionized water. The difference between the absorbance rate of the sample and the blank value, resulted in the actual absorbance value of the given sample.

For the analysis a calibration curve was developed using 5 dilutions of a standard solution with known concentrations of NO<sub>3</sub>-N. The calibration curve is presented in the appendix in Figure 73. The result is given in mg/l and for solid samples in mg/kg dm.

### **3.3.8 Ammonium nitrogen**

Ammonium nitrogen (NH<sub>4</sub>-N) was determined using a photometer (HACH LANGE DR 500). In an alkaline environment a reaction between ammonium, sodium nitroprusside, and sodium dichlorisocyanurate produces a green solution. The absorbance of this solution can be measured by a photometer at 655 nm wavelength.

The following solutions were used for the analysis:

Salicylate and Citrate solution

13 g sodium salicylate (C<sub>7</sub>H<sub>5</sub>O<sub>3</sub>Na) + 13g trisodium citrate (C<sub>6</sub>H<sub>5</sub>O<sub>7</sub>Na<sub>3</sub>\*2H<sub>2</sub>O) + 0,097 g sodium nitroprusside (Na<sub>2</sub>Fe(CN)<sub>5</sub>NO\*2H<sub>2</sub>O) + 1000 ml deionized water

NaOH solution

3.2 g NaOH + 0,2 g sodium dichlorcyanate (C<sub>3</sub>Cl<sub>2</sub>N<sub>3</sub>NaO<sub>3</sub>) + 100 ml deionized water

Standard solution

0.4717 g (NH<sub>4</sub>)<sub>2</sub>SO<sub>4</sub> (dried at 105 °C) + 1000 ml deionized water

For analyses the same eluate extracted for NO<sub>3</sub>-N analyses was used. In order to determine NH<sub>4</sub>-N, 0.025 - 1 ml of the eluate were pipetted into a 25 ml flask. The volume of sample that was pipetted into the flask was determined by the estimated concentration of NH<sub>4</sub>-N. It was diluted with deionised water, and 2 ml of Salicylate/Citrate. Afterwards the flask was shaken for 20 seconds to mix it and 2 ml of NaOH solution was added. It was filled up to 25 ml with deionized water and incubated at room temperature for 1 hour. The absorbance was then measured with the photometer at 655 nm wavelength. A blank sample was produced as described above for each sample.

A calibration curve was generated using 6 standards with known concentrations of 0 - 1.2 mg/l  $\text{NH}_4\text{-N}$ . The calibration curve is presented in Figure 74 in the appendix. The results are given in mg/l and for solid samples in mg/kg dm.

### 3.3.9 Kjeldahl nitrogen

Kjeldahl nitrogen is a quantitative method to determine organic nitrogen and inorganic nitrogen, i.e. ammonia and ammonium. The method was first developed by Kjeldahl J. (1883). It was used to determine total Kjeldahl nitrogen (TKN) in the leachate of the vermicomposters. The sample was filtered with a folded filter in order to remove all solid particles and insects that got trapped in the collecting tank.

25 ml of the leachate were pipetted into a 250 ml flask and 15 ml of sulfuric acid ( $\text{H}_2\text{SO}_4$ ) that oxidizes the organic matter and binds the reduced nitrogen as ammonium sulphate was added. In addition, Kjeldahl tablets were added as catalyser to accelerate the oxidation process. The solution was heated for 2 hours at 230 °C and then for 2 hours at 400 °C. During the procedure fumes evolved, which were removed using a water jet pump. After 4 hours the solution clarified.

After the reaction with sulfuric acid ( $\text{H}_2\text{SO}_4$ ), the solution was steam distilled in a Behrotest® WP 12. NaOH 33 % was added step wise to form  $\text{NH}_3$  from  $\text{NH}_4$ , until no gas was evolved anymore.  $\text{NH}_3$  bubbled through the acidic solution and was led to another flask filled with 2 % boric acid ( $\text{H}_3\text{BO}_3$ ) where it was bound as ammonium salt. Kjeldahl nitrogen was then determined by titration. 5 drops of a colour reagent (Tashiro) was added to the solution which turns from green to rose-violet when the solution turns acidic. 0.1 molar HCl was slowly titrated to the solution and it turned rose or violet. The amount of HCl used for achieving a neutral pH is proportional to the Kjeldahl nitrogen. Results are given in mg/l.

The results were calculated by the following equation

$$TKN[mg/l] = \frac{0.14007 * vol. HCl * 1000}{leachate [ml]}$$

### 3.3.10 Total Phosphor

Total phosphor was assessed by photometric analysis. 5 ml of leachate were mixed with 15 ml peroxide sulphate. The resulting solution is heated in a microwave (MARS 6) for 60 minutes. The device is preheated for 20 minutes, then the solution is steadily heated at 180 °C for 20 minutes and the device is left to cool down for another 20 minutes. After heating, total phosphor was measured using a photometer (HACH LANGE DR 500).

The following solutions were used for the analysis:

#### Ammonium heptamolybdate standard solution

12.6 g of ammonium heptamolybdate tetrahydrate ( $(\text{NH}_4)_6\text{Mo}_7\text{O}_{24} \cdot 4\text{H}_2\text{O}$ ) was dissolved in 400 ml of hot deionized water. After cooling down the solution, 140 ml of sulfuric acid ( $\text{H}_2\text{SO}_4$ ,  $\rho_{20}=1,84\text{g}\cdot\text{ml}^{-1}$ ) were added. Finally, it was filled up with 900 ml deionized water and 100 ml of 0.5 g Potassium antimony(III) oxide tartrate ( $\text{K}(\text{SbO})\text{C}_4\text{H}_6\text{O}_6 \cdot 0.5 \text{H}_2\text{O}$  dissolved in hot deionized water) was added.



#### Ammonium heptamolybdate application solution

1:10 Ammonium heptamolybdate standard solution + deionized water.

#### Ascorbic acid

4.4 g ascorbic acid + 1000 ml deionized water.

To 1 ml of the phosphorous solution 16 ml ammonium heptamolybdate application solution and 2 ml of ascorbic acid were added. The reaction is conducted at ambient air temperature for 15 minutes. Thereby, a blue molybdic acid-complex was produced, which was further quantified using the photometer at a wavelength of 660 nm. Results are given in mg/l.

### **3.3.11 Heavy metal analysis**

Heavy metals were analysed from the earthworm samples. The samples were digested by aqua regia. It was applied to dissolve Cd, Cr, Cu, Hg, Ni, Pb und Zn. 23 mg of the sample were dissolved in 9 ml HCl 37 % and 3 ml nitric acid (HNO<sub>3</sub>) 85 %. It was heated for 20 minutes at 160 °C in a microwave (MARS 6). The solution was then further analysed by ESW Consulting WRUSS Ziviltechnikergesellschaft mbH through the inductively coupled plasma optical emission spectrometry (ICP-OES) according to ÖNORM EN ISO 11885.

### **3.3.12 Plastic particle analysis**

Fresh samples were wet sieved in a sieve tower (Retsch AS 200). The particles which remained in the sieves were separated into larger than 6.3 (>6.3), 6.3 - 2 and 2 - 0.63 mm particle sizes and dried at 105 °C in a compartment drier until no further weight loss was recorded. TPS- PBAT particles got stuck on the aluminium trays, therefore, they were removed with ethanol (C<sub>2</sub>H<sub>5</sub>OH). After that, plastic particles with diameter >6.3, 6.3 - 2 and 2 - 0.63 mm were collected manually. Some plastic particles were then further examined with ATR-FTIR to determine the plastic species and its biodegradation degree.

### **3.3.13 Attenuated total reflection-Fourier transform infrared (ATR-FTIR) spectroscopy**

For the analysis of compost, vermicompost and plastic particles, the Attenuated total reflection-Fourier transform infrared (ATR-FTIR) spectroscopy was applied. Plastic particles were washed with ethanol if dirt adhered. The samples were pressed against a diamond ATR crystal, that was illuminated by an infrared beam at a grazing angle. This optical setup creates evanescent waves that penetrate only a few µm into the material. The sample partially absorbs the beam and a detector records the absorption spectra (Guerrero-Pérez & Patience, 2020). The device used for analysis was a Bruker ALPHA-P with a detection range of 4,000 to 400 cm<sup>-1</sup>. Each sample was measured 4 times, and the average absorption spectra were corrected against ambient air as background. The spectra of the compost samples taken at different days were compared to each other to assess their stability and identify changes in the functional groups present in the composts over time. Infrared spectra of vermicompost samples of the top and bottom layer were compared with the infrared spectrum of the input material. Plastic particles were measured only once and corrected against ambient air as background. Bruker software OPUS 7.5 was used for graphic representation of the results.

## 4 Results and Discussion

### 4.1 Rotting parameters of the composting experiment

In the course of the composting experiment several parameters were measured. In the first 69 days temperature of the compost reactors was quantified several times a day. Data of the compost reactors of the experimental groups, which were distributed on different levels in the climatic chamber, i. e. composting without foils “C1”, composting with LD-PE foils “C2”, and composting with TPS-PBAT foils “C3” were averaged and are shown in Figure 12. It is to be noted that some variability in temperature between compost reactors was caused by the position of the compost reactors on different levels within the climatic chamber. The effects of this temperature difference within the climatic chamber are discussed in the following section.

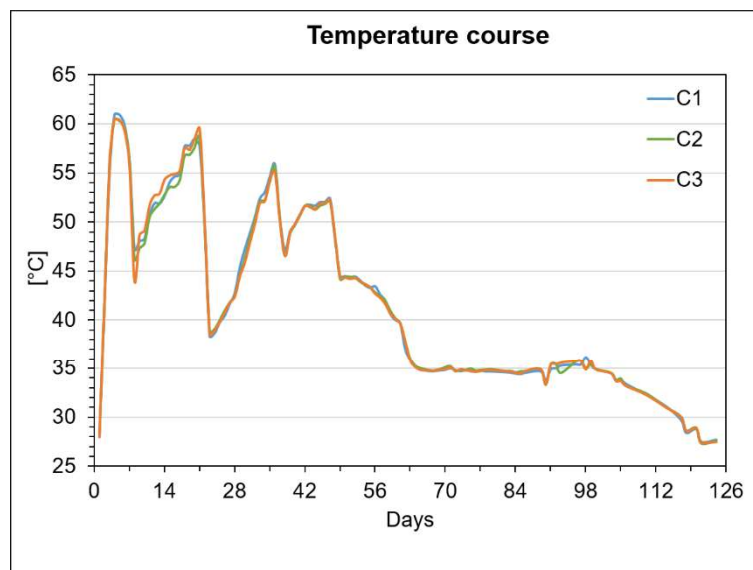


Figure 12: Averaged temperature course of C1- Composting without foils, C2- Composting with LD-PE foils and C3- Composting with TPS-PBAT foils

The initial temperature of all compost reactors was 28 °C and rose very quickly within the first four days. On the fourth day temperatures reached more than 60 °C. After that they steadily declined until the 8<sup>th</sup> day when the rotting material was turned. Rotting material was turned at ambient temperature, therefore, they lost heat. However, temperatures increased again thereafter, and again reached more than 58 °C on day 21. Similarly, the required turning on day 22 and day 37, also caused a decrease in temperature to around 38 °C, which rose again to 55 °C on day 36 and day 47 respectively. After day 47 temperatures steadily declined until the last day when they reached around 27 °C. Overall, the highest recorded temperature was 62.8 °C on the 5<sup>th</sup> day in R3, and the lowest temperature was 27.3 °C in R2 on day 120. According to the temperature profile, the thermophilic phase started on the 2<sup>nd</sup> day, and the mesophilic phase on the 61<sup>st</sup> day. The rapid increase in temperature within the first four days is a sign of degradation of easily degradable organic compounds by microorganisms. Hence, microbial activity was very high from day 0 to day 60, when temperatures rose between 40 and 60 °C. After that temperatures slowly decreased, and the temperature of the climatic chamber was adjusted to 35 °C in order to maintain a constant temperature that would simulate a larger composting pile until the end of the experiment. Temperatures fell below 30 °C on day 118. This means microbial activity had decreased.

Temperatures varied slightly between the compost reactors due to their placement on three different levels within the climatic chamber. Data of compost reactors at the top, middle and bottom level were averaged and plotted in Figure 13.

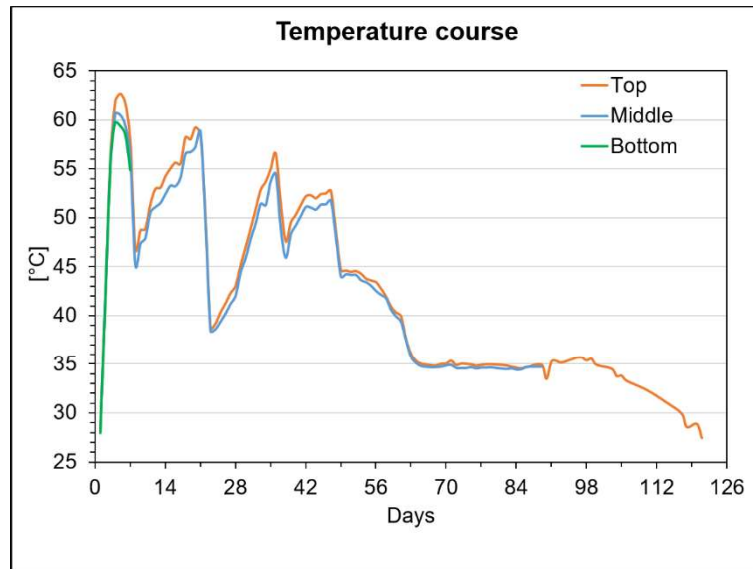


Figure 13: Averaged temperature course on different levels; Top, Middle, Bottom

On average a difference of 0.4 °C was detected for compost reactors placed on different levels of the climatic chamber. Most compost reactors which were located at the bottom level were merged with the other compost reactors at the top and middle level on the 8<sup>th</sup> day, since they had lost significantly in weight. However, R10 was placed on the middle level from the 8<sup>th</sup> day onwards and was merged with R2 and R6 on the 22<sup>nd</sup> day. On day 90 the compost reactors of the middle level were distributed among the compost reactors of the top level. From then onwards compost reactors were only located on the top level. In general, temperatures of the compost reactors at the top level were higher than those of compost reactors on the middle and bottom level, as hot air is transported upwards. However, on the 8<sup>th</sup> day temperatures at the top level were lower than at the middle and from the 47<sup>th</sup> day onwards temperatures of the top and middle level became similar.

Temperatures did not exceed 55 °C for 14 days in any of the experimental groups. Therefore, hygienisation of the compost according to Böhm (2007) was not achieved. Moreover, the Austrian guidelines for hygienisation provided by the former ministry of agriculture, forestry, environment and water management were as well not fulfilled (Amlinger et al., 2005). C1 reached temperatures beyond 55 °C in 13 days, C2 in 9 days, and C3 in 13 days. Nevertheless, temperatures reached more than 55 °C in the compost reactors at the top level within 14 days.

CO<sub>2</sub> concentrations were similar among C1, C2 and C3. Data of the CO<sub>2</sub> concentrations of compost reactors were averaged among the three experimental groups and plotted as seen in Figure 14.

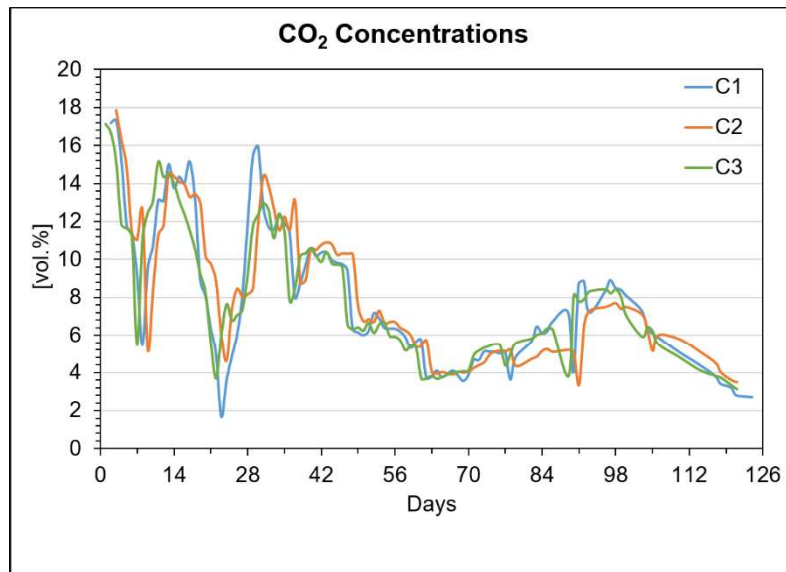


Figure 14: CO<sub>2</sub> concentrations of C1- Composting without foils, C2- Composting with LD-PE foils and C3- Composting with TPS-PBAT foils

First, CO<sub>2</sub> concentrations were measured on the 2<sup>nd</sup> day and they were around 17 vol. %. They declined whenever the input material was turned but rose very quickly after that. It was intended to keep CO<sub>2</sub> concentrations at about 15 vol. % at first and then at around 10 vol. %. Until day 37, CO<sub>2</sub> concentrations were at approximately 15 vol. % and then around 10 vol. %. Yet, the recorded data shows that CO<sub>2</sub> concentrations dropped below these values several times throughout the experiment. Highest CO<sub>2</sub> concentrations were recorded on the 2<sup>nd</sup> day with 18.3 vol. % in R6 and lowest concentrations were recorded on the 23<sup>rd</sup> day after turning which were 1.5 vol. % in R1. Between the 2<sup>nd</sup> and 48<sup>th</sup> day CO<sub>2</sub> concentrations were beyond 10 to 12 vol. % which might have caused foul odours due to insufficient oxygen supply according to Amlinger (2005). The data of the compost reactors which were distributed among the top, middle and bottom level were averaged and are exhibited in Figure 15. On average they varied 0.2 vol. %, which is less pronounced than the variability in temperature.

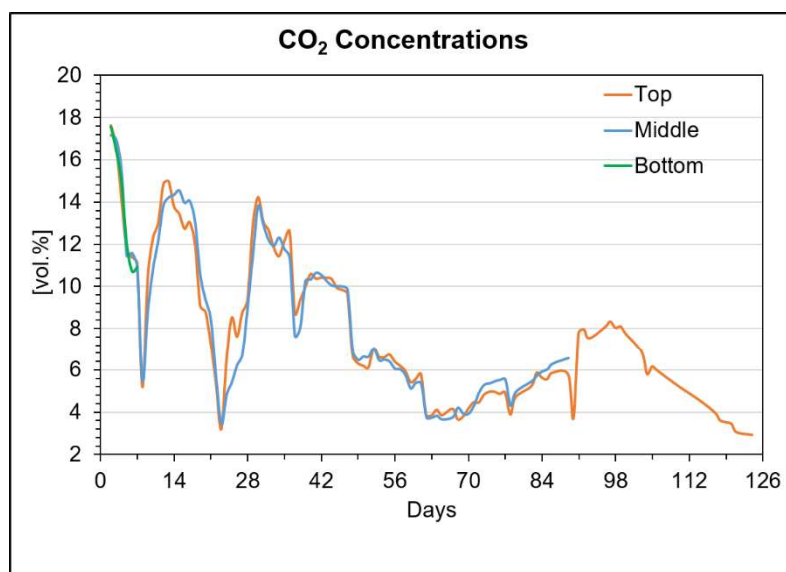


Figure 15: CO<sub>2</sub> concentrations on different levels; Top, Middle, Bottom

Applying a linear regression model to the collected data from C1, C2, and C3 shows a positive correlation between increased temperature and increased CO<sub>2</sub> concentrations with a p-value of 0.  $R^2$  is 0.51 for C1,  $R^2$  is 0.65 for C2, and  $R^2$  is 0.66 for C3. In Figure 16 the linear regression models of temperatures and CO<sub>2</sub> concentrations for C1, C2, and C3 are plotted. As expected, CO<sub>2</sub> concentrations rise with increasing temperatures, since microbial respiration drives the rise in temperature and is accompanied by an increase in CO<sub>2</sub> concentrations.

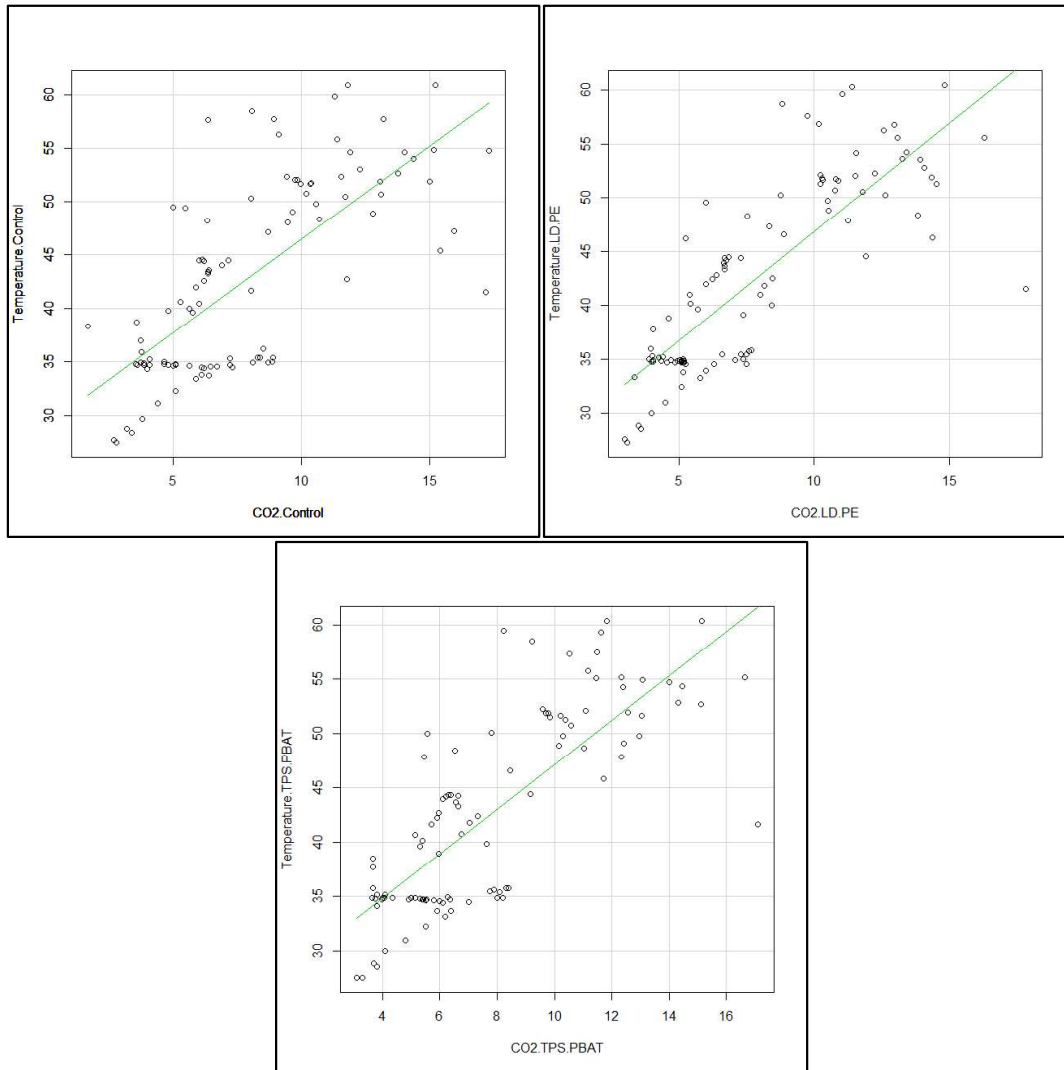


Figure 16: Linear regression model of temperatures and CO<sub>2</sub> concentrations for C1- Composting without foils, C2- Composting with LD-PE foils and C3- Composting with TPS-PBAT foils

As can be seen in Figure 17, mass reduction increased throughout the composting experiment. The compost reactors were weighted every second week. There is a positive correlation between CO<sub>2</sub> concentrations and mass reduction. As expected, mass reduction was proportional to the CO<sub>2</sub> concentrations, as mass reduction was most pronounced when the CO<sub>2</sub> concentrations were highest. When CO<sub>2</sub> concentrations declined during the mesophilic phase, also mass reduction decreased. During the degradation process organic matter is inter alia mineralized into CO<sub>2</sub>. Nevertheless, C1's and C2's mass reduction between the 22<sup>nd</sup> and 37<sup>th</sup> day, which accounted for only 1.9 and 3.2 % wet matter (wm) respectively, are contradictory. However, it then increased again to 7.94 and 4.94 % wm respectively. Between day 62 and 77 mass reduction accounted for almost 0 % wm in all experimental groups.

The decrease might be connected to the low water content in the compost reactors that caused low microbial activity. Additional 60 ml of water had to be added. C3 had a steadier decrease in mass. C1 and C2 had a similar total mass reduction. Mass decreased by 39 % dm in C1, by 39 % dm in C2, and by 53 % dm in C3.

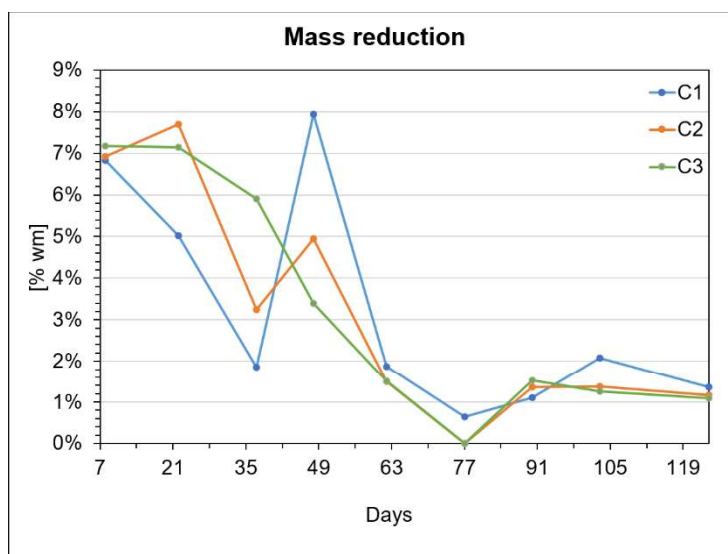


Figure 17: Mass reduction during the composting experiment in C1- Composting without foils, C2- Composting with LD-PE foils and C3- Composting with TPS-PBAT foils

In Figure 18 a diagram of the condensate that was collected in a cold trap is exhibited.

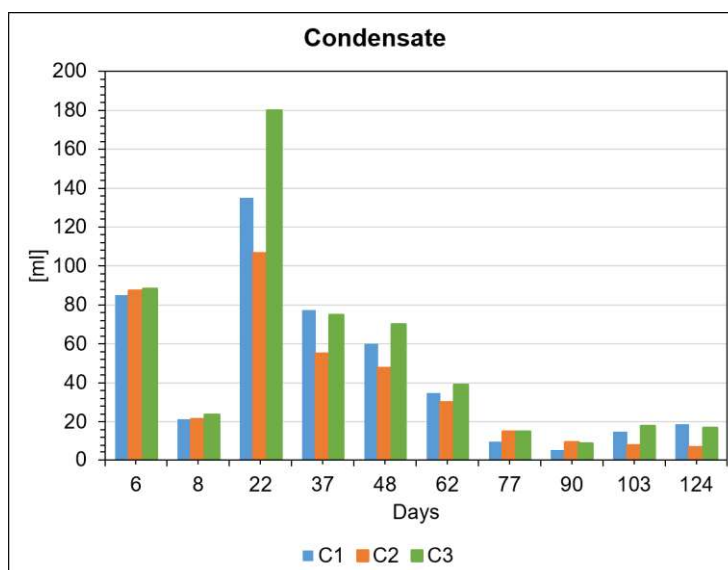


Figure 18: Condensate that evolved during the composting experiment in C1- Composting without foils, C2- Composting with LD-PE foils and C3- Composting with TPS-PBAT foils

Most condensate was recovered from C3 (535 ml), second most condensate was obtained from C1 (463 ml), and least was collected from C2 (387 ml). Although most water was added to C2, least water was collected as condensate from it. Of note, C1 received 130 ml, C2 220 ml and C3 208 ml of additional water. Leachate was collected only on the 8<sup>th</sup> day at the bottom of the compost reactors and its volume was assessed for all three experimental groups. It was 208 ml for C1, 129 ml for C2, and 153 ml for C3. Condensate collection was higher on the 22<sup>nd</sup> day than on the 6<sup>th</sup> and 8<sup>th</sup> together and then steadily decreased on the following days when leachate was collected.



## 4.2 Rotting parameters of the vermicomposting experiment

This was the first vermicomposting experiment that was conducted at the Institute of Waste Management at the University of Natural Resources and Life Sciences Vienna. Thus, the experimental set-up was dominated by trial and error. Although, an instruction manual was provided by the manufacturer, some issues ensued during the experiment, hence, part of this section is devoted to presenting the successful trouble shooting and adaptations made to the experimental set-up.

The three experimental vermicomposting groups were “V1” vermicomposting without foils, “V2” vermicomposting with 0.01 % LD-PE foils, and “V3” vermicomposting with 1 % TPS-PBAT foils. Alongside the earthworms, different insects appeared throughout the vermicomposting experiment. In Figure 19 a timeline of the vermicomposting experiment is presented with the marked occurrence of insects. After 12 days red oribatid mites appeared in the vermicomposters which are a sign of excessive water content according to the producer. Until day 28 defrozen input material was added which had a high water content. After changing to fresh input material on day 29, the red oribatid mites disappeared again. White hydrachna globosa were recorded on the input material in V2 on day 34 and then in V1 and V3 on the 61<sup>st</sup> day. They are also a sign of excessive water content (Wormsystems GmbH, n.d.-a). On day 75 fruit flies appeared in V3. On day 90 pupa from fruit flies surfaced on all walls of the vermicomposters. Thus, fly traps containing water, cider vinegar and washing-up liquid, were installed. These seemingly controlled the fruit fly population. After that many enchytraeids were seen from day 113 onwards.

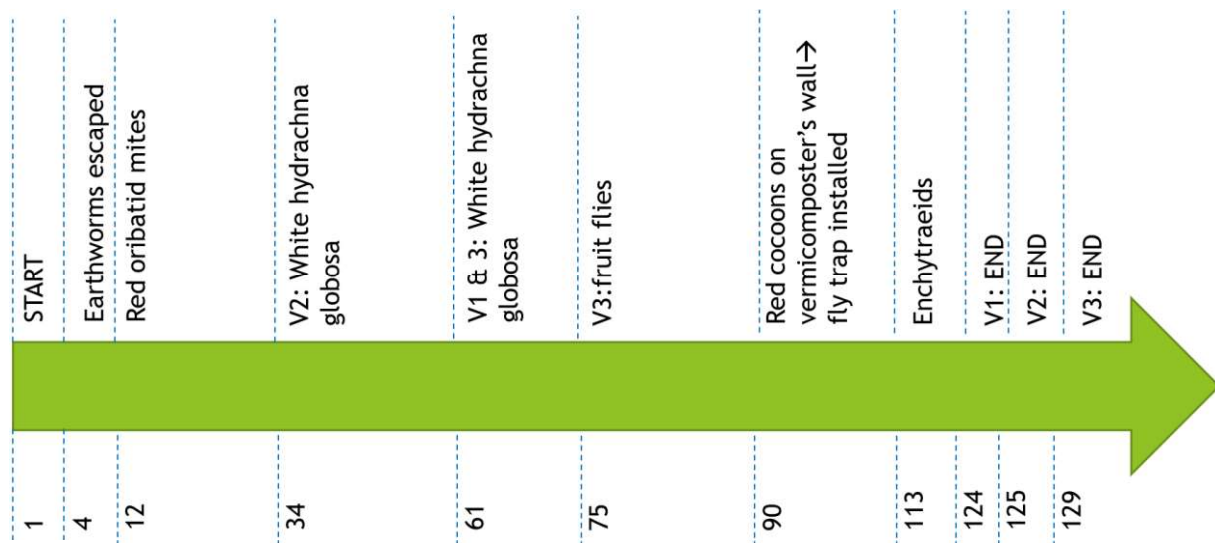


Figure 19: Timeline of the vermicomposting experiment for V1- Vermicomposting without foils, V2- Vermicomposting with LD-PE foils and V3- Vermicomposting with TPS-PBAT foils

As can be seen in Figure 20 the amount of input material was variable from the 2<sup>nd</sup> to the 120<sup>th</sup> day. Initially it was aimed to calculate the input material that earthworms consumed per day. However, this approach was dismissed after 9 days since earthworms were overburdened with this amount of input material. The input material was affected by fungi and was hence removed from V1 and V2 after weighing. The parts removed were subtracted from the input material. Hence, the bar of V1 and V2 is lower than the one of V3 after 2 days, which was not affected by fungi. Input load was modified each week according to the degradation rate of the previously added input material. Nevertheless, input load tends to increase throughout the experiment.

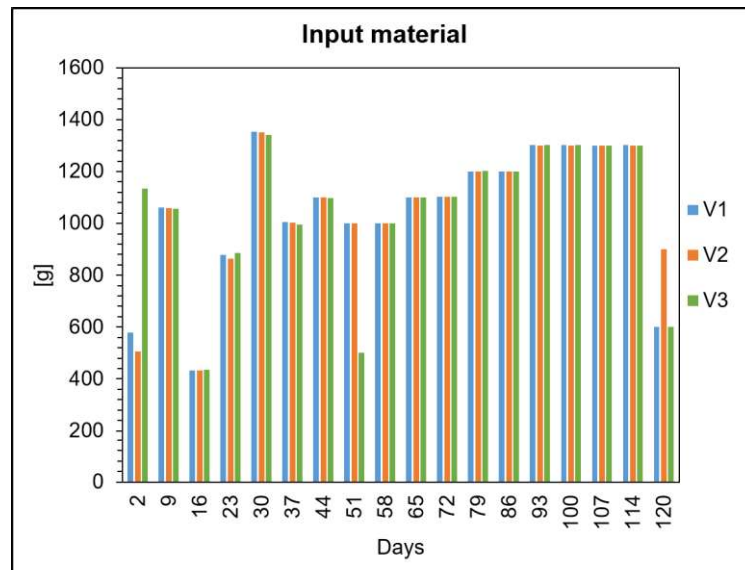


Figure 20: Input material of the vermicomposting experiment for V1- Vermicomposting without foils, V2- Vermicomposting with LD-PE foils and V3-Vermicomposting with TPS-PBAT foils

Between the 44<sup>th</sup> and 51<sup>st</sup> day, less input material was added in V3 since earthworms seemed to be overloaded. Between the 114<sup>th</sup> and 120<sup>th</sup> day, V2 was fed with an additional load of 300 g, as it was the last vermicomposter to be analysed, and, thus, had a longer running time. At the end of the experiment 18,822 g of biogenic waste was added to V1, 19,024 g to V2, and 18,854 g to V3. After 41 days, no further plastic particles were added, as no biodegradation of plastics was apparent, and it was feared that earthworms would be overburdened. In total 6 g of LD-PE particles and 60.7 g of TPS-PBAT particles were added to V2 and V3 respectively. On day 116 input material was added for the last time to V1 and V3 and on day 120 to V2.

Since the vermicomposters were kept in a climatic chamber that ensured ambient temperatures between 22 and 23 °C, or the basement where temperatures were moderate, the temperature of all three vermicomposters remained between 20 and 25 °C, except for the first four days as described in Figure 21.

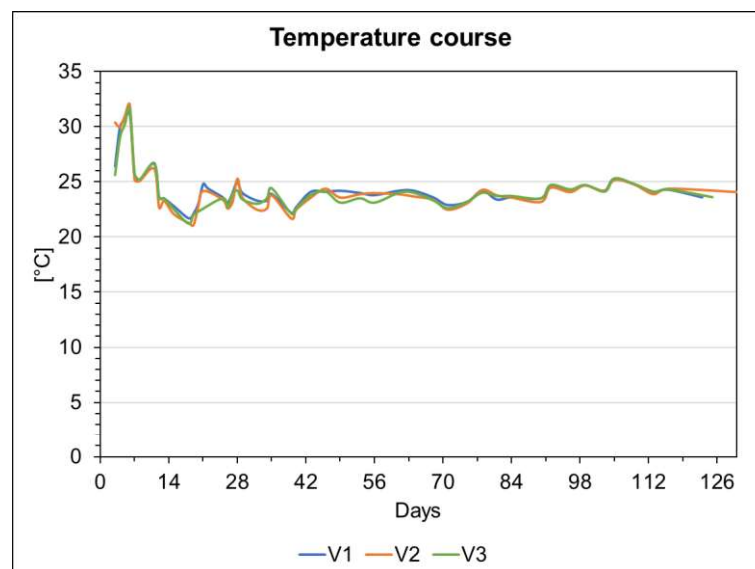


Figure 21: Temperature course of the vermicomposting experiment for V1- Vermicomposting without foils, V2- Vermicomposting with LD-PE foils and V3-Vermicomposting with TPS-PBAT foils



On average temperature was 24.4 °C for V1, 24.2 °C for V2, and 24.2 °C for V3. No significant difference was detected between the three experimental groups. As reported by Sinha (2011) earthworms need temperatures between 20 and 30 °C. Optimal temperatures for *Eisenia Fetida* and *Eisenia Andrei* are 25 °C (Domínguez & Edwards, 2011a). In conclusion, temperatures were kept within an optimal range during the vermicomposting experiment.

When vermicomposters were supplied with 500 g fresh input material, its degradation was already visible after 6 days of vermicomposting as illustrated in Figure 22. These mere observations already proved a high degradation rate with vermicomposting.



Figure 22: Degradation of 500 g of biogenic waste within 6 days by vermicomposting

Vermicomposting is known to reduce mass through mineralization processes to mostly CO<sub>2</sub>, water, and incorporation of carbon into biomass. Every time input material was added to the vermicomposters, its content was weighed before and after input material addition. Thereby, mass reduction for each week was assessed, and is shown in Figure 23. The weekly degradation rate steadily increased throughout the vermicomposting experiment. At first the reduction was only 2.36 % wm in V1, 2.63 % wm in V2, and 1.92 % wm in V3. Towards the end of the experiment, it was between 10 and 18 % wm. The highest weekly degradation rate was observed for V3 after 121 days which was 20.2 % wm. In the 6<sup>th</sup> and 7<sup>th</sup> week an overestimation of mass reduction might have occurred due to leachate. The collecting tank was emptied on the 32<sup>nd</sup> day and the 40<sup>th</sup> day and this might have contributed to the weight difference rather than an actual reduction in mass. These datapoints are highlighted in red in Figure 23, as to exclude them from interpretation. In order to avoid this issue, the collecting tanks were thereafter emptied every time before the vermicomposters were weighted to obtain a more accurate result. In total V1 has lost 66 % dm, V2 59 % dm, and V3 67 % dm without considering earthworm biomass. The values were very similar among the 3 experimental groups and higher compared to the results of the composting experiment, which resulted in a 39 - 53 % dm loss. These results are in line with LLéo et al. (2013) who also stated that mass reduction of vermicomposting was higher than of composting.

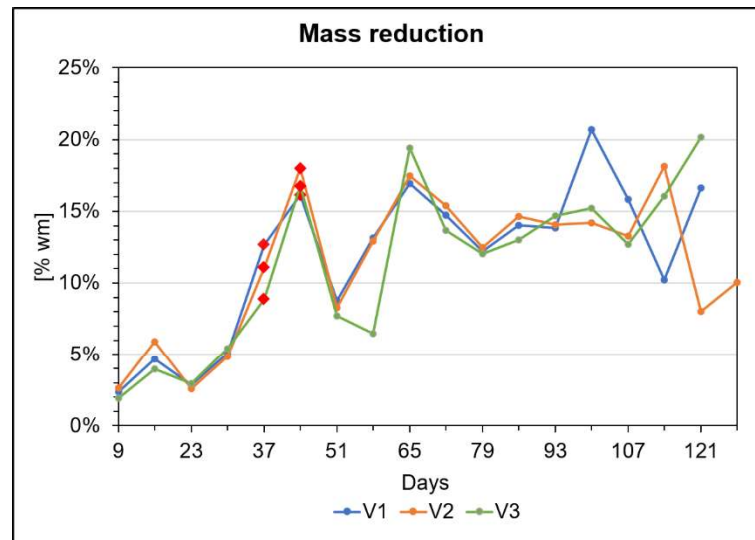


Figure 23: Mass reduction during the vermicomposting experiment for V1- Vermicomposting without foils, V2- Vermicomposting with LD-PE foils and V3- Vermicomposting with TPS-PBAT foils

In the course of the vermicomposting experiment a large amount of leachate was collected in the collecting tank as illustrated in Figure 24. The amount of leachate was mostly similar among the experimental groups. In total 9,575 ml of leachate was collected in V1, 9,1190 ml in V2, and 8,290 ml in V3. Although the three vermicomposters received almost the same amount of input material and had the same temperature, leachate differs between V1 and V3. This might result from the addition of TPS-PBAT particles. Thermoplastic starch is known to be hydrophilic, therefore, blends of TPS-PBAT absorb water which could explain the differences in leachate within the experimental groups (Shirai et al., 2013).

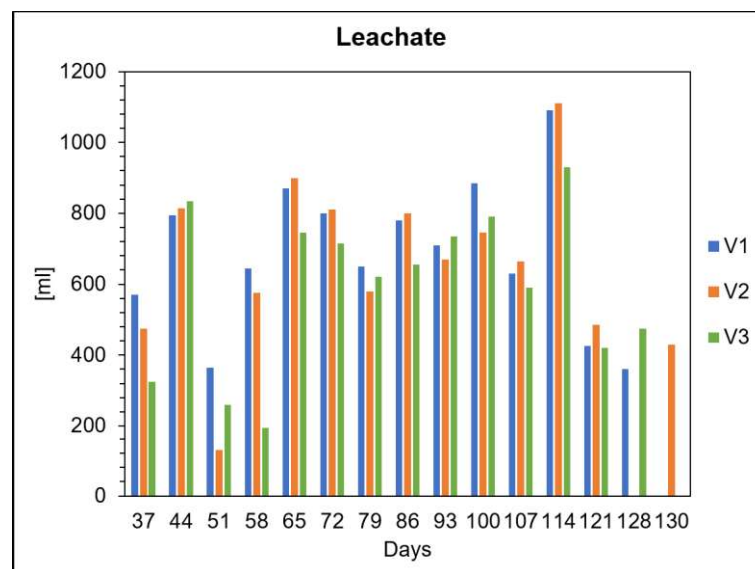


Figure 24: Leachate collection during the vermicomposting experiment for V1- Vermicomposting without foils, V2- Vermicomposting with LD-PE foils and V3- Vermicomposting with TPS-PBAT foils

Measurements of CO<sub>2</sub> concentrations were stopped after the 20<sup>th</sup> day due to excessive water content in the vermicomposters. It caused the gas-detector to pump too much water into the device. Given the potential damage to the device the measurements, were stopped and have, thus, been dismissed.

### 4.3 Plastic particle analysis

All vermicompost and compost samples were separated into fractions containing particles larger than 6.3 mm (>6.3 mm) and particles between 6.3 - 2 mm and 2 - 0.63 mm. Plastic particles were separated from the fractions by hand, counted and washed with ethanol. In compost without foils (C1) two particles of polypropylene (PP), two particles of polyethylene terephthalate (PET) and one undefined green particle were found. Fruits and vegetables that were obtained from the Wiener Tafel were packed in plastic packaging. Thus, some plastic particles might have remained in the input material. In vermicompost without foils (V1) only 1 particle of PP sized between 2 - 0.63 mm was found, which could originate from the input material or coconut fibre. However, these impurities can be considered negligible.

In this chapter the number of particles per kg compost or vermicompost on dry matter basis are presented. The number of particles was calculated in ratio to 1 kg dm of compost or vermicompost for comparability. LD-PE foils did not disintegrate since many particles were found in the compost (C2) and vermicompost (V2) where LD-PE foils were added. In Figure 27 the number of LD-PE particles that were found in C2 and V2 are presented. The number of particles in general and those larger than 6.3 mm was particularly high in C2 compared to the other composts and vermicomposts. 2,975 particles/kg dm larger than 6.3 mm, 201 particles/kg dm sized 6.3 - 2 mm and 126 particles/kg dm sized 2 - 0.63 mm were found. In total 3,301 particles/kg dm were retrieved which made a total of 6.5 % dm. LD-PE foils accounted for 4 % dm in compost at day 1. This means the ratio between LD-PE particles and compost had increased, as LD-PE particles did not degrade and the compost reactors were merged whenever they had lost in mass. A picture of the LD-PE particles that were found in C2 is provided in Figure 25.

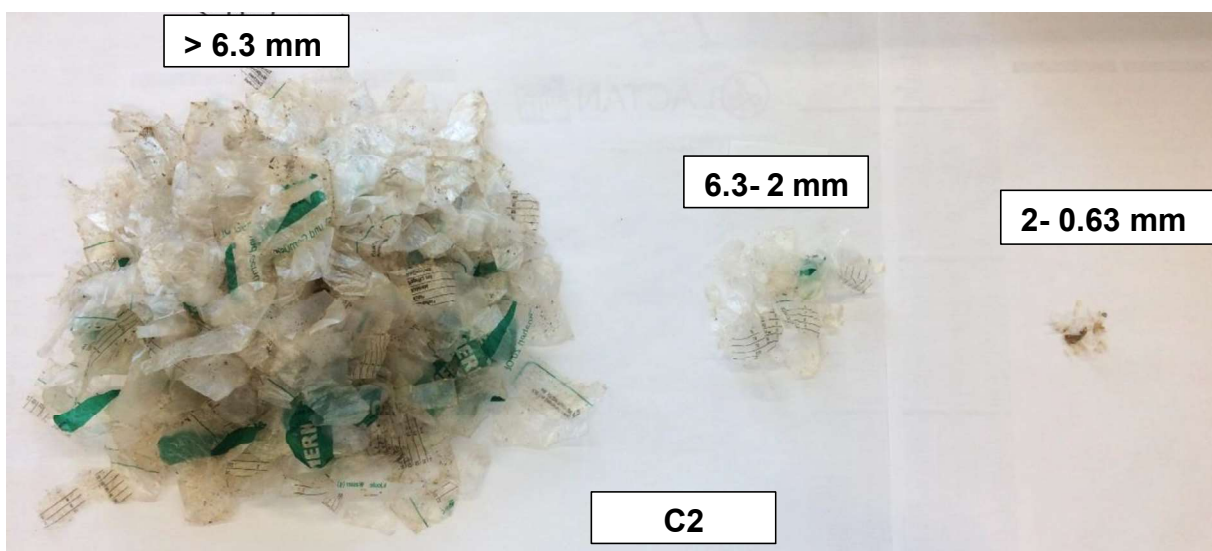


Figure 25: LD-PE particles sorted by their particle size; > 6.3 mm, 6.3 – 2 mm, and 2 - 0.63 mm in C2-Composting with LD-PE foils

LD-PE particles were only found in the top layer of the vermicompost. 1,979 particles/kg dm sized 6.3 - 2 mm and 216 particles/kg dm sized 2 - 0.63 mm. Total number was 2,195 particles/kg dm which made up for 1.95 % dm. Initial ratio between LD-PE foils and vermicompost was 0.9 % dm. Therefore, the relative value increased as biogenic waste degraded on the one hand and LD-PE foils did not decompose on

the other hand. In Figure 26 a picture of LD-PE particles that were retrieved from the top layer of V2 are presented

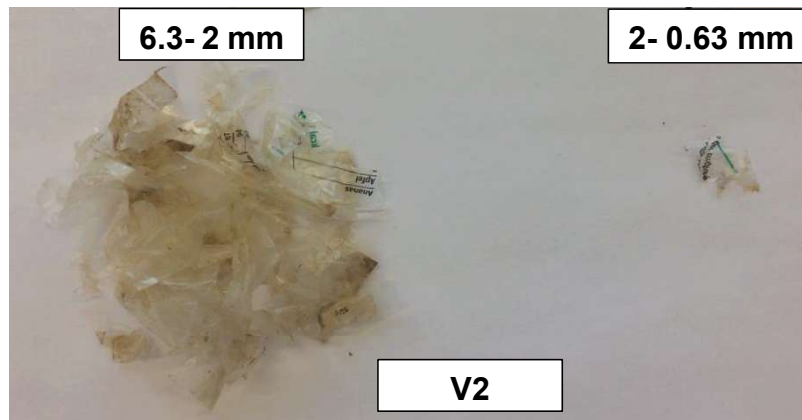


Figure 26: LD-PE particles sorted by their particle size; 6.3 – 2 mm and 2 - 0.63 mm in the top layer of V2- Vermicomposting with LD-PE foils

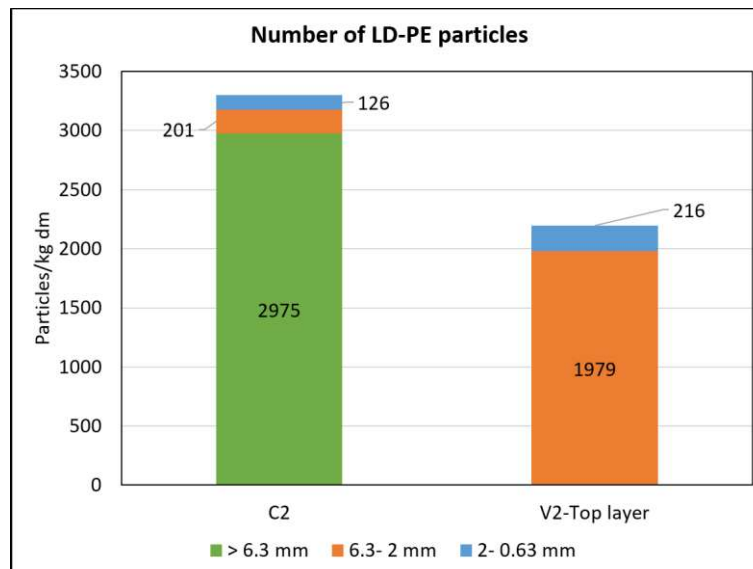


Figure 27: Number of LD-PE particles/kg dm in C2- Composting with LD-PE foils and in the top layer of V2- Vermicomposting with LD-PE foils at the end of the experiments

TPS-PBAT particles were almost entirely disintegrated during composting with TPS-PBAT foils (C3) and no pieces were visible by the naked eye after 7 days of composting. Only 21 particles/kg dm were found sized 2 - 0.63 mm which makes up for 0.021 g/kg dm. Thus, TPS-PBAT foils decreased by 99.93 % in mass. This means that TPS-PBAT foils disintegrated in line with EN 13432 which requires that a maximum 10 % of the original mass of packaging remains as particles larger than 2 mm in the course of composting within 3 months. However, more micro particles might have evolved and fractions below 0.63 mm were not examined in this thesis. Figure 29 exhibits the TPS-PBAT particles/kg dm found in C3 and in V3.

In contrast, many TPS-PBAT particles were found in the vermicompost where TPS- PBAT foils were added (V3). They were more abundant in the top layer than in the bottom layer. 10,037 TPS-PBAT particles/kg dm sized between 6.3 - 2 mm and 2,634 particles/kg dm sized between 2 - 0.63 mm were retrieved from the top layer. 553 particles/kg dm sized between 2 - 0.63 mm were found in the bottom layer. The smallest particle fraction probably got transported by the earthworms to the bottom



layer. Rillig et al. (2017) described the phenomenon that smaller particles are more likely transported through soil by earthworms.

In total, TPS-PBAT particles made up for 13.7 % dm in V3. Initial ratio between TPS- PBAT foils and vermicompost was 8 % dm. Therefore, the ratio between TPS-PBAT particles and vermicompost has increased due to loss in mass. In Figure 28 a picture of the TPS-PBAT particles found in the top layer of V3 is shown.

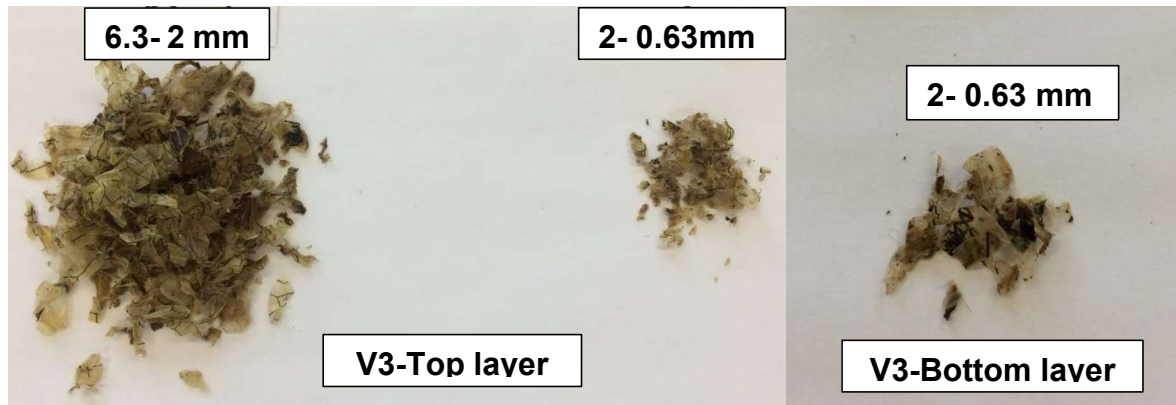


Figure 28: TPS-PBAT particles sorted by their particle size; 6.3 – 2 mm and 2 - 0.63 mm in the top layer (on the left) and bottom layer (on the right) of V3- Vermicomposting with TPS-PBAT foils

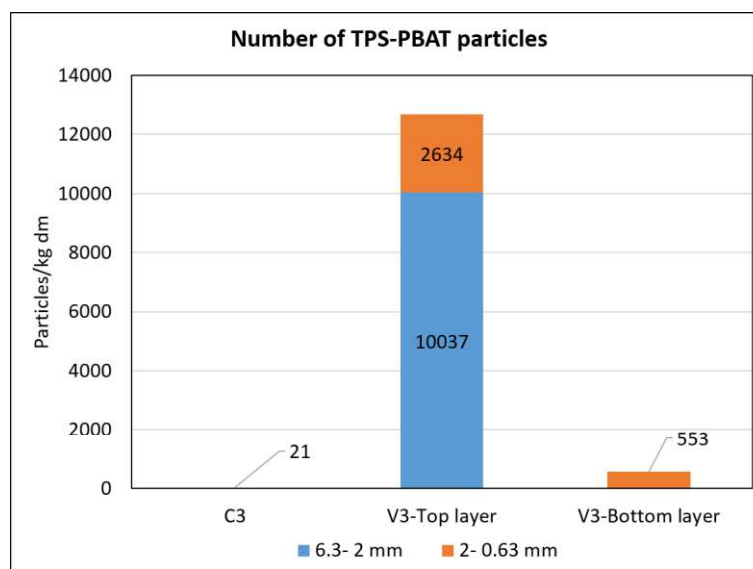


Figure 29: Number of TPS-PBAT particles/kg dm in C3- Composting with TPS-PBAT foils (21 TPS- PBAT particles sized 2 - 0.63 mm) and in the top and bottom layer of V3- Vermicomposting of TPS- PBAT foils at the end of the experiments

## 4.4 ATR-FTIR spectroscopy

### 4.4.1 Compost

ATR-FTIR spectroscopy was conducted on both, compost, vermicompost and plastic particles, to determine their degradation degree. Infrared spectra of compost samples from day 1, 8, 22, 48, 90 and 124 are compared with each other and plotted in a diagram. Indicator bands and degradation degree were determined as described by Smidt and Schwanninger (2005). Indicator bands of compost and vermicompost samples are marked by arrows. Red arrows indicate a decrease, and black arrows indicate an increase in absorbance. Figure 30, Figure 31, and Figure 32 show the infrared spectra of C1, C2 and C3 respectively.

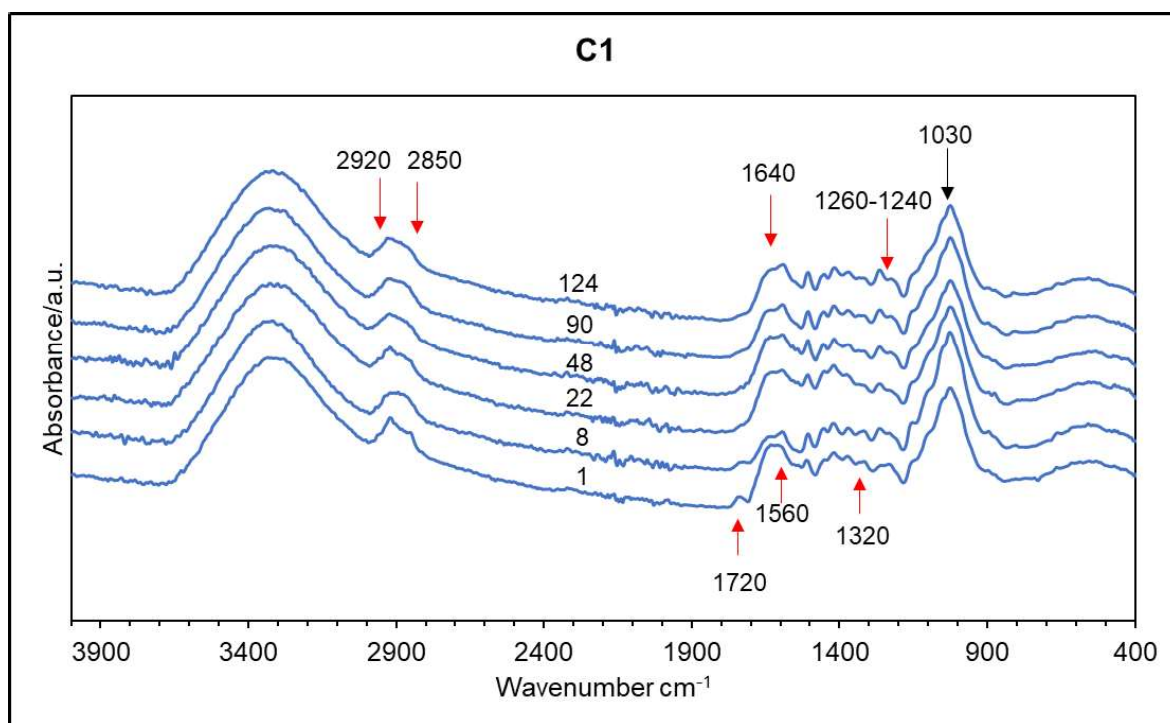


Figure 30: Infrared spectra showing the degradation process of C1- Composting without foils, located at the top level from day 1 - 124

Mostly red arrows dominate the diagrams since absorbance of indicator bands have generally decreased, like C-H stretching found at 2920 and 2850  $\text{cm}^{-1}$ . They represent methyl groups that decline during the degradation process since organic material is broken down. Furthermore, a small peak at 1720  $\text{cm}^{-1}$  disappeared after 22 days, which is attributed to aldehydes, ketones, carbonic acids and/or esters. Its peak is clearly visible in the fresh input material.

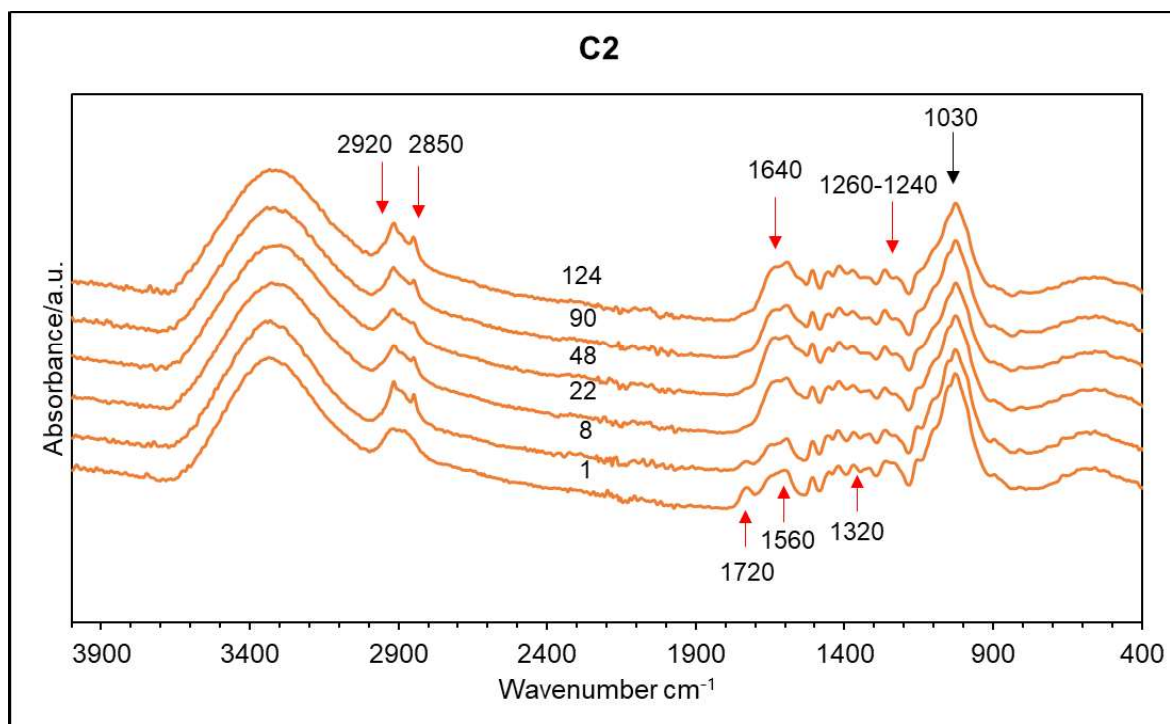


Figure 31: Infrared spectra showing the degradation process of C2- Composting with LD-PE foils, located at the top level from day 1 - 124

A very pronounced decrease in absorbance is evident at 1650 and 1630  $\text{cm}^{-1}$  between the input material and the first week, especially in C1. At these wavenumbers carboxylate, amides, alkenes, and aromatic compounds are found. At wavenumber 1540  $\text{cm}^{-1}$  also a decline in absorbance is evident that is attributed to amide II vibration band. After 22 days the band at wavenumber 1320  $\text{cm}^{-1}$  flattened, which is an indication for degradation of aromatic primary and secondary amines. In the course of the degradation process the bands at 1260 to 1240  $\text{cm}^{-1}$  reduced as well, which are assigned to carboxylic acids and the amide III band. Only the bands of clay minerals have slightly increased, which are found at 1032  $\text{cm}^{-1}$  and indicate their accumulation as the organic material reduced.

C1, C2 and C3 present similar changes in their composition. However, methyl bands at 2920 and 2850  $\text{cm}^{-1}$  are not as pronounced in C2 and C3 compared to C1 on the 1<sup>st</sup> day.

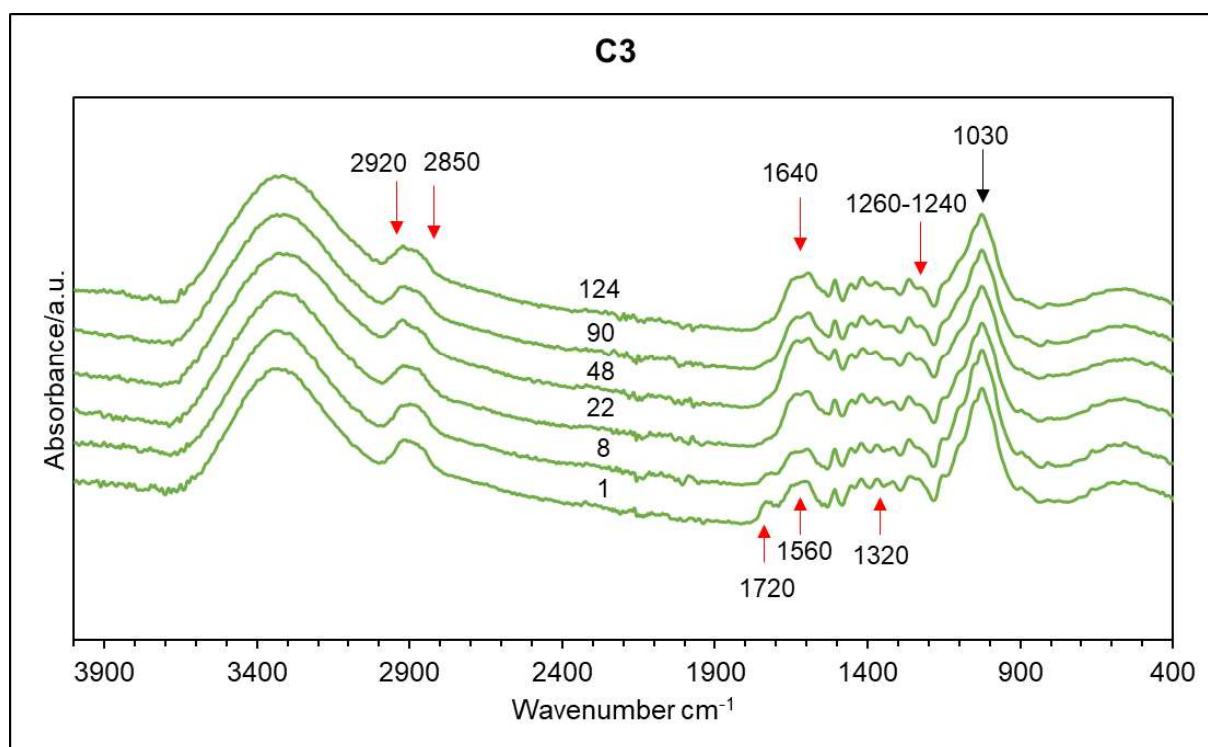


Figure 32: Infrared spectra showing the degradation process of C3- Composting with TPS-PBAT foils, located at the top level from day 1 - 124

In the final composts after 124 days almost all indicator bands are similar among the different experimental groups except for the two peaks at 2914  $\text{cm}^{-1}$  and 2847  $\text{cm}^{-1}$  that are found in the spectrum of C2. In the spectrum of the pure LD-PE bag 2914 and 2847  $\text{cm}^{-1}$  are the strongest indicator bands (Figure 33). However, the peaks were not as pronounced on day 1 and 48 which might be attributed to the number of LD-PE particles in C2. During grinding, plastic particles adhered to the metal walls of the cutting mill and partially melted and stick together in the centrifugal and vibratory disc mill. Therefore, it is possible that the quantity of plastic particles varied after they underwent milling processes. This might explain why these peaks were visible on day 8, 22, 90 and 124 and not on day 1 and 48. Nevertheless, these findings indicate that LD-PE particles can be detected at 1 % in compost by ATR-FTIR analysis and did not significantly degrade during composting, as their concentration increased as a result of decreasing mass. Therefore, the results confirm the findings showed earlier for hand collected particles that remained in the compost.

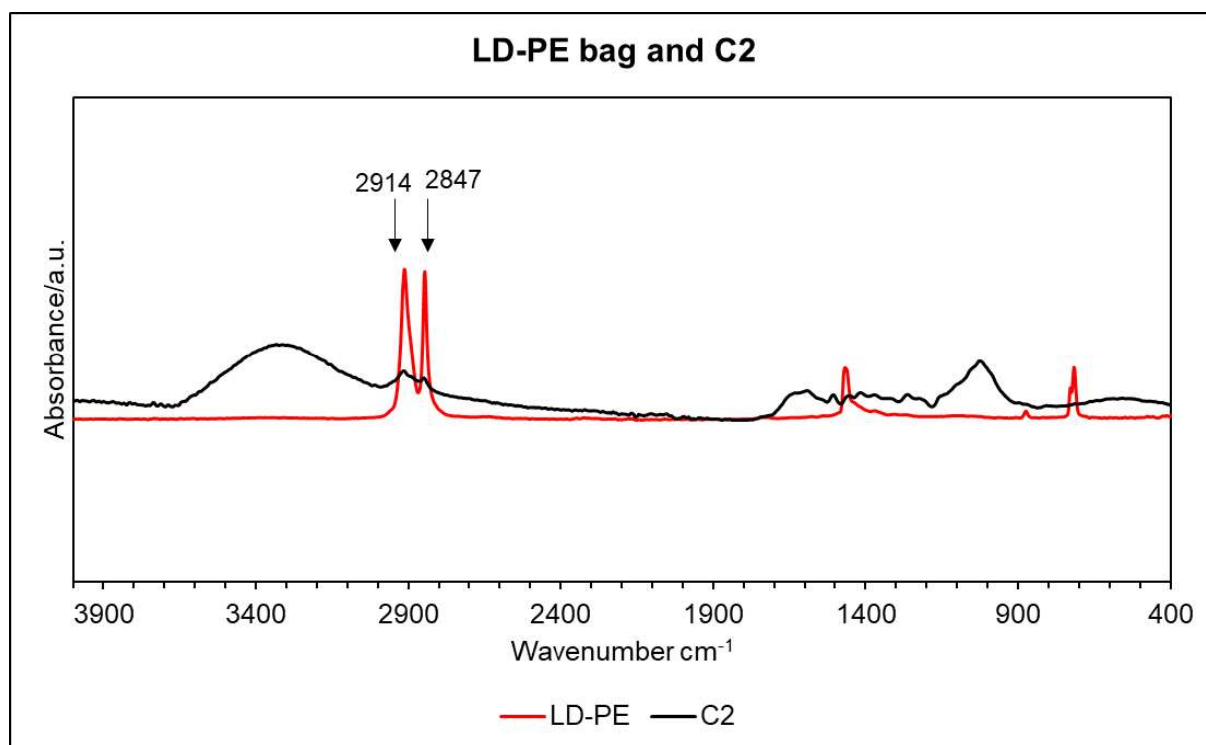


Figure 33: Comparison between LD-PE bag and final compost on day 124 of C2- Composting with LD-PE foils, located at the top level

#### 4.4.2 Vermicompost

Infrared spectra of vermicompost samples from the top and bottom layer were compared to the input material that was added from the 29<sup>th</sup> day onwards. They are plotted in Figure 34, Figure 35, and Figure 36.

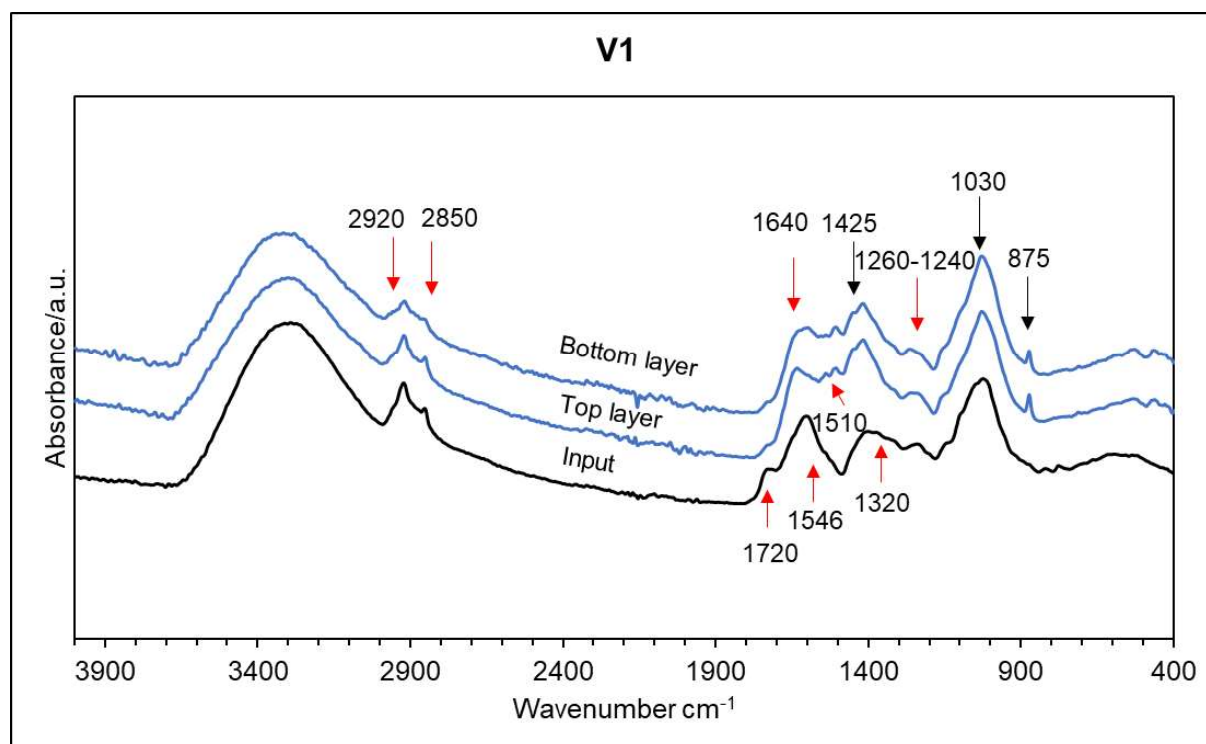


Figure 34: Infrared spectra showing the degradation process of V1- Vermicomposting without foils from input material to the bottom layer



Indicator bands and degradation degree were determined as described by Smidt and Schwanninger (2005). They are marked by arrows. Red arrows indicate a decrease and black arrows an increase in absorbance.

Within all three vermicomposters absorbance at 2920 and 2850  $\text{cm}^{-1}$  decreased between the top and bottom layer which are attributed to methyl groups. Moreover, the band at 1720 to 1740  $\text{cm}^{-1}$ , which describe several compounds, i.e. aldehydes, ketones, carboxylic acids and esters, were already reduced in the top layer. They disappear at a very early stage of degradation. C=O and C=C vibration detected at wavenumber 1640  $\text{cm}^{-1}$  decreased from the top to the bottom layer, which suggests reduction of several compounds, such as amide I, carboxylates, aromatic ring modes and alkenes. Absorbance of N-H in plane at wavenumber 1546  $\text{cm}^{-1}$  that is characteristic for amides II band, decreased as well from the top to the bottom layer. In contrast to the input material, the top and bottom layer show a peak at around 1510  $\text{cm}^{-1}$  which is attributed to aromatic compounds. This can indicate abundance of lignocellulosic materials, which were not abundant in the input material. Instead this was most likely a result of the use of coconut fibre in the vermibed that was distributed in the whole vermicompost. However, this band slightly decreased from the top to the bottom layer, but less pronounced than bands characteristic for more easily degradable compounds.

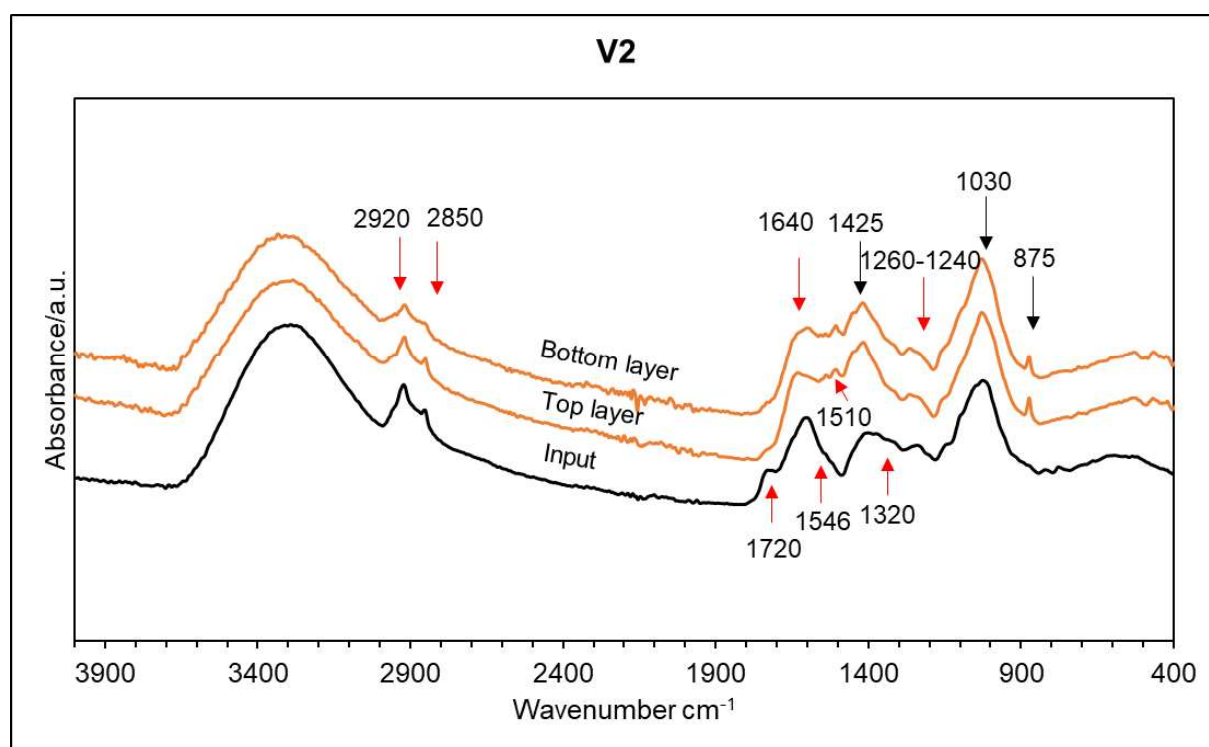


Figure 35: Infrared spectra showing the degradation process of V2- Vermicomposting with LD-PE foils from input material to the bottom layer

Furthermore, absorbance at 1320  $\text{cm}^{-1}$  which is assigned to aromatic primary and secondary amines declined marginally from the top to the bottom layer. The last indicator band to reduce was between 1260 and 1240  $\text{cm}^{-1}$ , which is assigned to C-N and C-O vibration and indicate carboxylic acids and amides (amide III band) that drop from the top to the bottom layer. Some absorbance bands developed in the vermicompost over time. Peaks at 1425 and 875  $\text{cm}^{-1}$  that are assigned to a C-O stretch and C-O out of plane respectively, proved an increase in carbonate compared to the input material. Due to degradation of organic matter, carbonates increased

relative to the biomass. As already described for composts, the bands that indicate clay minerals which are found at  $1030\text{ cm}^{-1}$ , also increased in the course of vermicomposting.

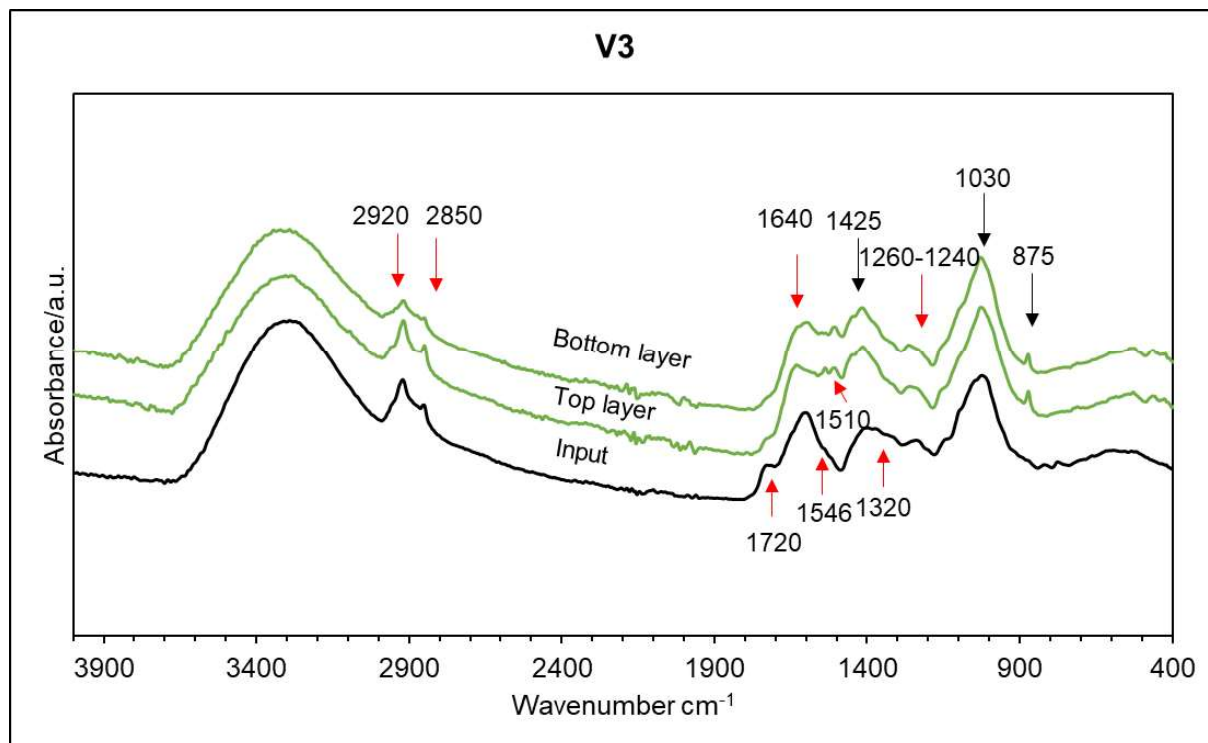


Figure 36: Infrared spectra showing the degradation process of V3-Vermicomposting with TPS-PBAT foils from input material to the bottom layer

Comparison of the infrared spectra of final vermicompost (bottom layer) and final compost, revealed differences, as seen in Figure 37 and highlighted by the black arrows. Absorbance at wavenumber  $1640\text{ cm}^{-1}$ , which is assigned to carboxylate, amide I, aromatic ring modes, and/or alkenes was higher in the vermicomposts compared to the compost samples. However, most likely this was a sign for more aromatic ring modes and alkenes which tend to increase in the final compost. Furthermore, carbonates as shown by the elevated absorbance at  $1425$  and  $875\text{ cm}^{-1}$  were more abundant in vermicompost most probably due to the addition of rock flour and lime. Apparently, also lignocellulosic materials, which are found at  $1510\text{ cm}^{-1}$ , were more abundant in vermicompost. Both, compost and vermicompost, show a decrease in  $1320\text{ cm}^{-1}$  in the final compost which is a sign for low microbial activity, and inefficiency in transformation rates to more resistant molecules (Smidt & Schwanninger, 2005).

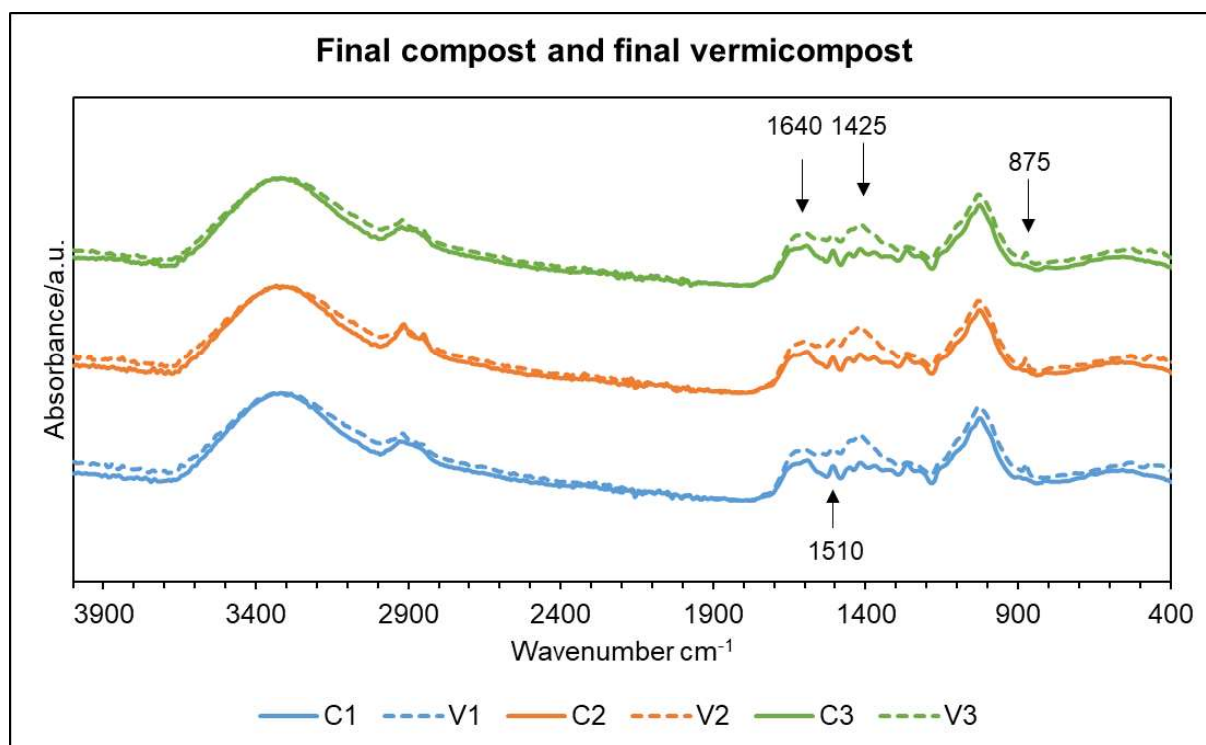


Figure 37: Comparison of the infrared spectra of the final compost (C1, C2 and C3) and vermicompost (V1, V2 and V3)

#### 4.4.3 Plastic particles

Plastic particles that were sorted out from the different fractions after wet sieving of compost and vermicompost, were counted and numbered. From these plastic particles, samples were collected and then analysed by ATR-FTIR spectroscopy and further screened by the spectral data base of the Institute to determine whether they were plastic and which kind. All spectra of LD-PE and TPS-PBAT particles were included into further analysis. Through the ATR-FTIR analysis, changes within the width and height of indicator bands can be detected. These were compared to the original LD-PE or TPS-PBAT bag. Indicator bands showed differences in their absorbance compared to the LD-PE or TPS-PBAT bags which could be attributed to a change in particles thickness. After composting and vermicomposting, it was difficult to separate LD-PE or TPS-PBAT particles from each other. Therefore, thickness might have influenced absorbance. Thus, data was normalised in respect to the highest absorption band.

##### 4.4.3.1 LD-PE particles

As already mentioned in chapter 4.3, many LD-PE particles were retrieved from the compost and vermicompost samples. In order to compare infrared spectra of the different plastic particles they were normalised to the highest peak, which was at  $2914\text{ cm}^{-1}$ , nevertheless, it was not the highest peak for all samples. In Figure 38 the infrared spectra of some LD-PE particles that were larger than  $6.3\text{ mm}$  in diameter are presented. The infrared spectra of the other LD-PE particles larger than  $6.3\text{ mm}$  and sized between  $6.3 - 2\text{ mm}$  can be found Figure 75, Figure 76, and Figure 77 in the appendix. No changes were found for the peaks at wavenumber  $2914$ ,  $2847$  and  $1468\text{ cm}^{-1}$  when compared to the original LD-PE bag. However,  $875$  and  $718\text{ cm}^{-1}$  had increased within all LD-PE particles. Furthermore,  $1464\text{ cm}^{-1}$  was more pronounced, and absorbance is even higher than at  $1468\text{ cm}^{-1}$ . Next to the typical peaks of the

original LD-PE bag, other bands had developed in some LD-PE particles. These bands are 1640, 1548, 1503, 1464, 1260, and 1030  $\text{cm}^{-1}$ .

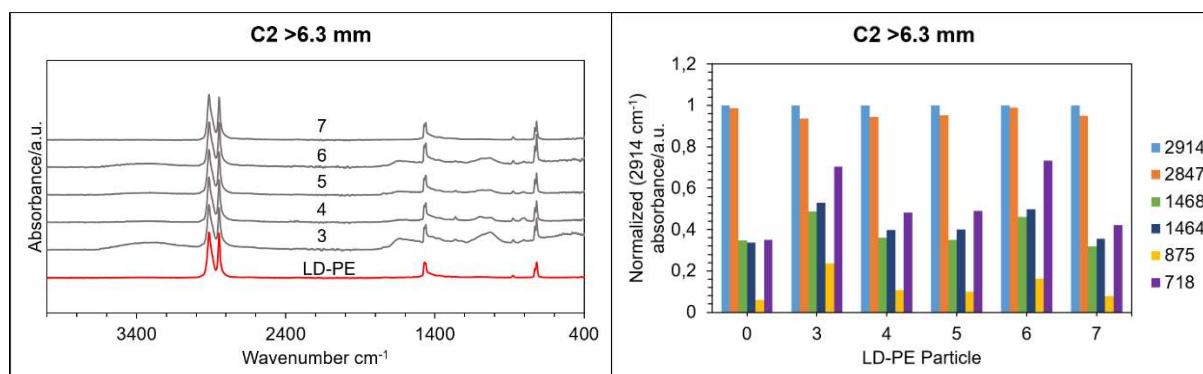


Figure 38: Infrared spectra (on the left) and characteristic wavenumbers selected from the infrared spectra normalized to 2914  $\text{cm}^{-1}$  (on the right) of manually sorted out LD-PE particles (Number 3, 4, 5, 6, 7) >6.3 mm in C2- Composting with LD-PE foils at the end of the experiment

Nevertheless, when comparing the spectra of LD-PE particles, which deviate the most from the original LD-PE bag, with the final compost as shown in Figure 39, it is clear that these peaks are a result of impurities from the compost that adhered to the particles.

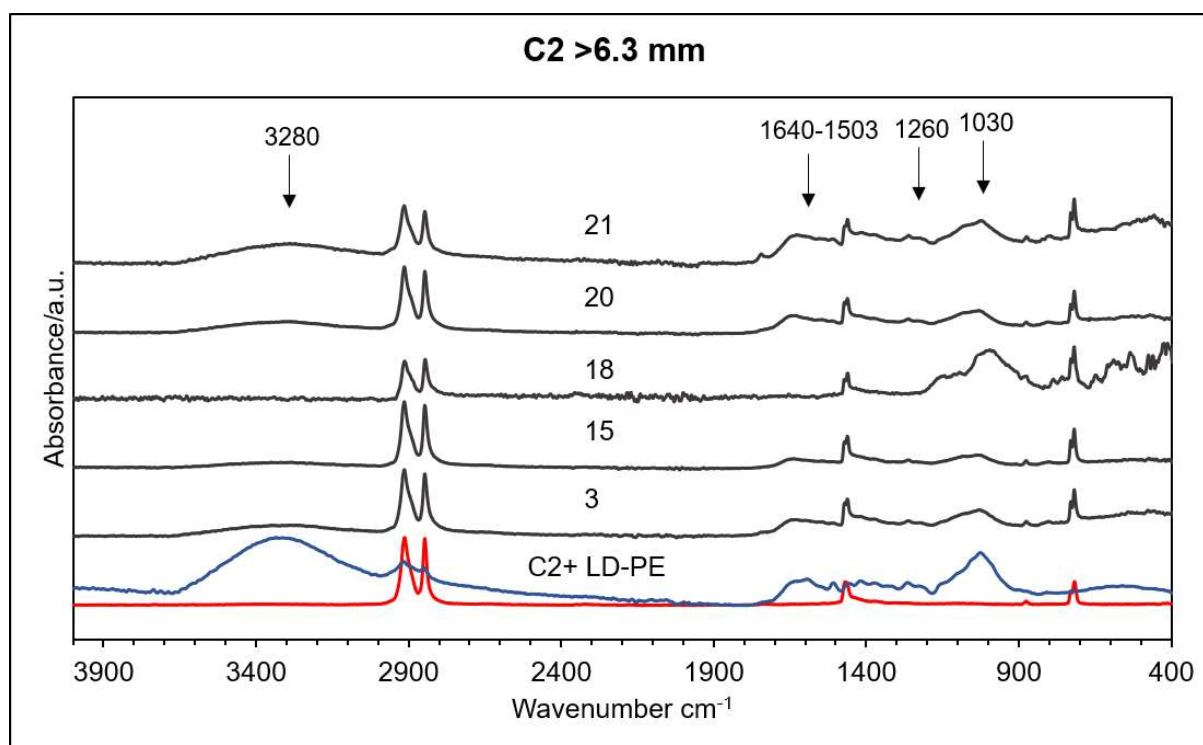


Figure 39: Comparison of the infrared spectra of manually sorted out LD-PE particles (Number 3, 15, 18, 20, 21) >6.3 mm which showed impurities and C2-Composting with LD-PE foils at the end of the experiment and the original LD-PE bag

Similar changes were also noted in the spectra of LD-PE particles sized 6.3 - 2 mm and 2 - 0.63 mm as shown in Figure 40 and Figure 41. Whereas absorbance at 2914 and 2874  $\text{cm}^{-1}$  did not change, absorbance at 1464  $\text{cm}^{-1}$  had become larger than 1468  $\text{cm}^{-1}$ . Furthermore, 875 and 718  $\text{cm}^{-1}$  are more pronounced in comparison to the original LD-PE bag. The infrared spectra show that less impurities could be found on these particles.

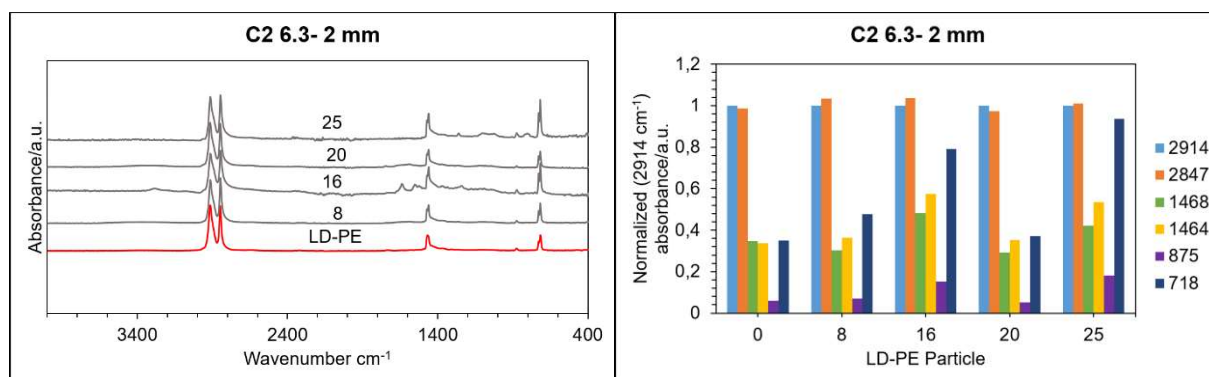


Figure 40: Infrared spectra (on the left) and characteristic wavenumbers selected from the infrared spectra normalized to 2914  $\text{cm}^{-1}$  (on the right) of manually sorted out LD-PE particles (Number 8, 16, 20, 25) sized 6.3 - 2 mm in C2- Composting with LD-PE foils at the end of the experiment

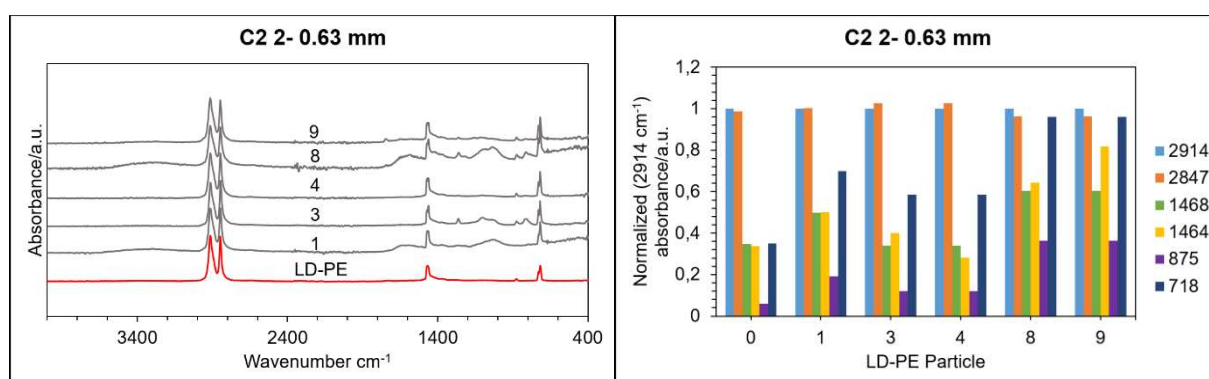


Figure 41: Infrared spectra (on the left) and characteristic wavenumbers selected from the infrared spectra normalized to 2914  $\text{cm}^{-1}$  (on the right) of manually sorted out LD-PE particles (Number 1, 3, 4, 8, 9) sized 2 - 0.63 mm in C2- Composting with LD-PE foils at the end of the experiment

Infrared spectra of LD-PE particles that were retrieved from V2 that were sized 6.3 - 2 mm and 2 - 0.63 mm are presented in Figure 42 and Figure 43. The infrared spectra of the other LD-PE particles sized 6.3 - 2 mm can be found in Figure 78 in the appendix. The changes in absorbance bands were comparable to the LD-PE particles found in C2. While peaks at 2914 and 2847  $\text{cm}^{-1}$  did not change. Absorbance at 1464  $\text{cm}^{-1}$  was more profound than at 1468  $\text{cm}^{-1}$ . Absorbance at 875  $\text{cm}^{-1}$  had increased significantly.

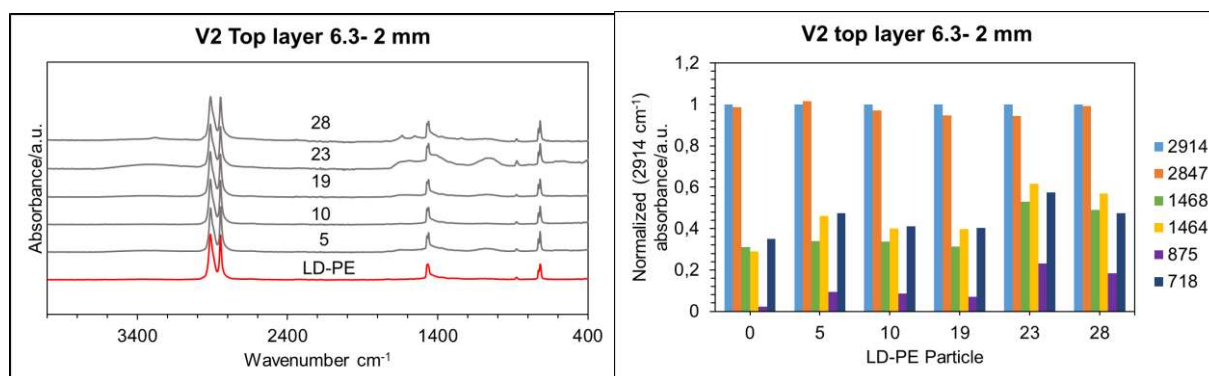


Figure 42: Infrared spectra (on the left) and characteristic wavenumbers selected from the infrared spectra normalized to 2914  $\text{cm}^{-1}$  (on the right) of manually sorted out LD-PE particles (Number 5, 10, 19, 23, 28) sized 6.3 - 2 mm in V2 top layer- Vermicomposting with LD-PE foils at the end of the experiment

In contrast LD-PE particles sized 2 - 0.63 mm did not show a significant increase at 875  $\text{cm}^{-1}$ .



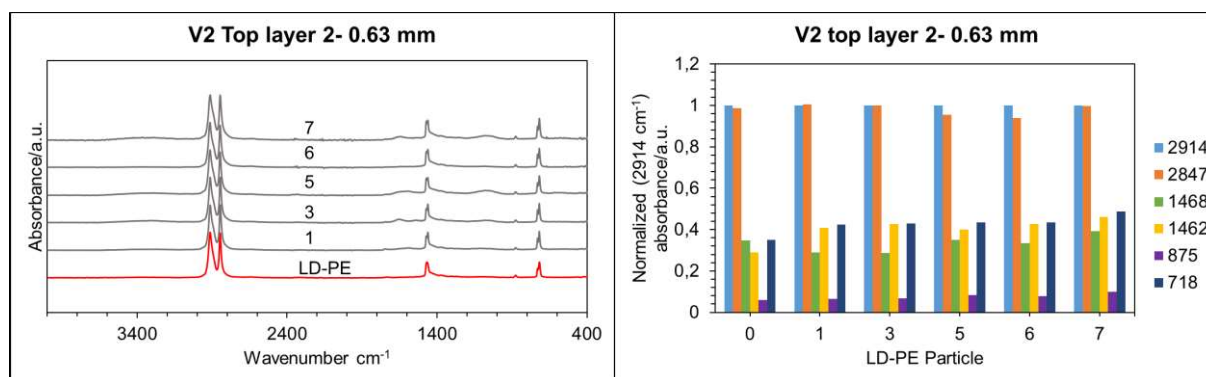


Figure 43: Infrared spectra (on the left) and characteristic wavenumbers selected from the infrared spectra normalized to 2914  $\text{cm}^{-1}$  (on the right) of manually sorted out LD-PE particles (Number 1, 3, 5, 6, 7) sized 2 - 0.63 mm in V2 top layer- Vermicomposting with LD-PE foils at the end of the experiment

Nevertheless, height of absorbance bands 1468, 875 and 718  $\text{cm}^{-1}$  seem to depend on the amount of impurities that had adhered to the particles. They were present in both compost and vermicompost. Therefore, the increase in absorbance might have been caused by an overlap of absorption bands belonging to both LD-PE particles and compost or vermicompost. Only the peak at 2847  $\text{cm}^{-1}$  did not change significantly. Thus, it was taken as reference to evaluate the degradation degree of particles. Since, no changes were evident in absorbance of 2847  $\text{cm}^{-1}$ , it is concluded that LD-PE foils did not degrade during the compost and vermicompost experiment. These results are in line with Rajandas et al. (2012) who stated that LD-PE takes decades to decompose.

#### 4.4.3.2 TPS-PBAT particles

TPS-PBAT particles were found in C3 and V3. Infrared spectra were normalised by referencing to the highest absorption band, i.e. 1711  $\text{cm}^{-1}$ , but it was not the highest absorption band for all particles.

Only two TPS-PBAT particles were retrieved from C3 and were further analysed with ATR-FTIR. Their spectra were similar to the original TPS-PBAT bag. However, some changes were visible as can be seen in Figure 44. Particle number 1 showed a decrease in the broad adsorption band between 3700 and 3300  $\text{cm}^{-1}$  which is attributed to the breakdown of long-chain starch molecules. Furthermore, the peaks at 1079 and 1018  $\text{cm}^{-1}$ , which are assigned to the C-O stretch as part of a glucose ring, were reduced. Starch can be degraded fast by microorganisms and, hence, it is a first sign for degradation. In contrast, bands attributed to PBAT, such as C-H bending at 1500 to 1250  $\text{cm}^{-1}$  and esters found at 1269  $\text{cm}^{-1}$  and 1184  $\text{cm}^{-1}$ , increased. However, since absorbance bands attributed to TPS decreased in almost all samples in comparison to the original TPS-PBAT bag, it must be assumed that absorbance of typical bands assigned to PBAT increased relatively.

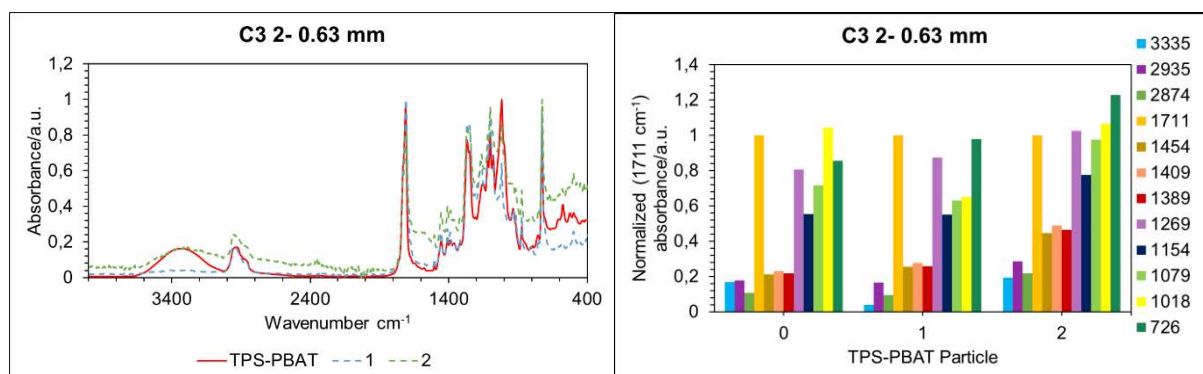


Figure 44: Infrared spectra (on the left) and characteristic wavenumbers selected from the infrared spectra normalized to 1711  $\text{cm}^{-1}$  (on the right) of manually sorted out TPS-PBAT particles (Number 1, 2) sized 2 - 0.63 mm in C3- Composting with TPS-PBAT foils at the end of the experiment

In Figure 45 TPS-PBAT particles that were retrieved from the top layer of V3 at a mesh width of 6.3 mm are compared to the original TPS-PBAT bag. Data was normalised in reference to the peak at 1711  $\text{cm}^{-1}$ , but the highest peak was found at 1018  $\text{cm}^{-1}$  in several spectra. Infrared spectra of the remaining particles are shown in Figure 79, Figure 80 and Figure 81 in the appendix. All TPS-PBAT particles except for number 33 declined in absorbance between 3700 and 3300  $\text{cm}^{-1}$ . Alongside the decrease at 3700 to 3300  $\text{cm}^{-1}$ , a decline at wavenumber 1018  $\text{cm}^{-1}$  was observed. Only particle number 5, 9 and 15 showed a decrease at 1079  $\text{cm}^{-1}$ . Additionally, particle 5 showed a decrease in absorbance of C-O at 1269  $\text{cm}^{-1}$ , which is attributed to the carbonyl group in ester. Particle number 52, 61, 2\_15 and 2\_25 that are shown in the appendix, present similar changes as particle number 5. The C=O bond at 1154  $\text{cm}^{-1}$  that is assigned to carbonyl groups in esters did not decrease at the same time. The double bond between the carbon and oxygen compound is harder for microorganisms to break down, whereas single bonds are more susceptible to microbial degradation. Other indicator bands attributed to PBAT increased relatively while bands characteristic for TPS declined.

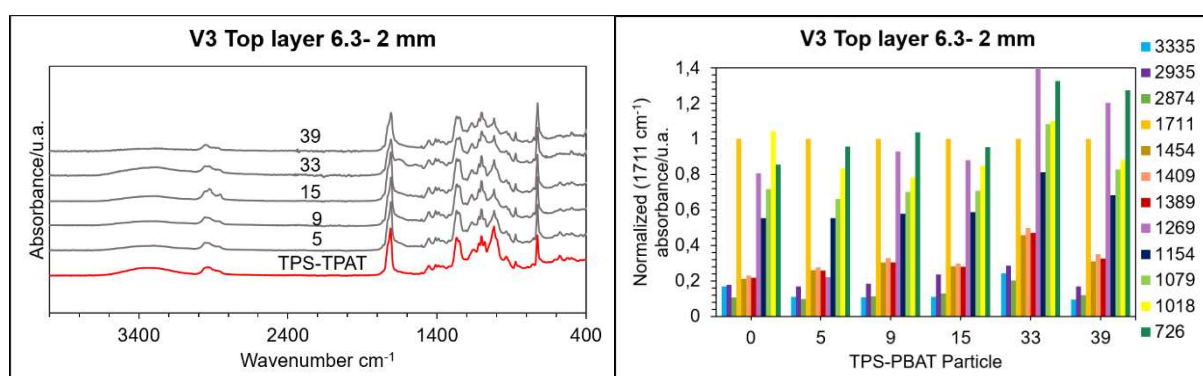


Figure 45: Infrared spectra (on the left) and characteristic wavenumbers selected from the infrared spectra normalized to 1711  $\text{cm}^{-1}$  (on the right) of manually sorted out TPS-PBAT particles (Number 5, 9, 15, 33, 39) sized 6.3 - 2 mm in V3 top layer- Vermicomposting with TPS-PBAT foils at the end of the experiment

Figure 46 presents the spectra of TPS-PBAT particles sized 2 - 0.63 mm in comparison to the original TPS-PBAT bag. The broad band between 3700 and 3300  $\text{cm}^{-1}$  declined in all particles except for particle number 48. The spectra of the same particles presented as well a decrease in 1018  $\text{cm}^{-1}$ .

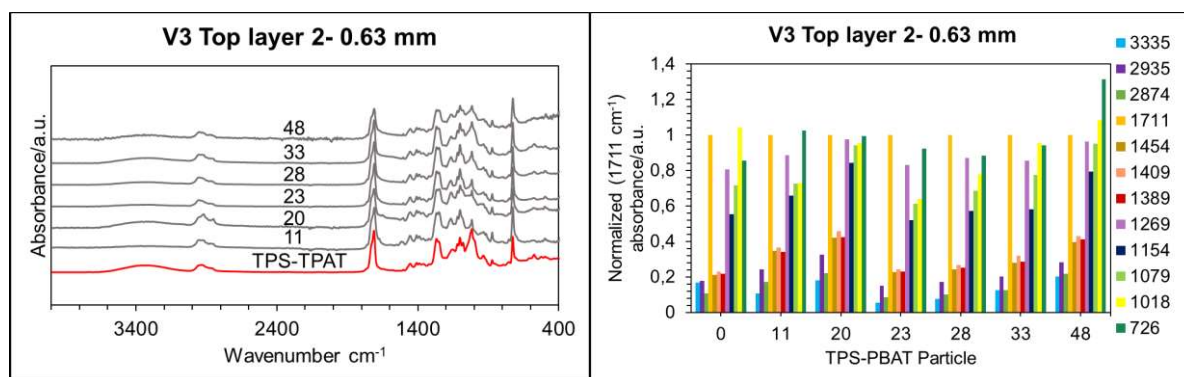


Figure 46: Infrared spectra (on the left) and characteristic wavenumbers selected from the infrared spectra normalized to 1711  $\text{cm}^{-1}$  (on the right) of manually sorted out TPS-PBAT particles (Number 11, 20, 23, 28, 33, 48) sized 2 - 0.63 mm in V3 top layer- Vermicomposting with TPS-PBAT foils at the end of the experiment

However, absorbance had not declined to the same degree among all particles. Particle number 20 had a less pronounced decline at 1018  $\text{cm}^{-1}$ , and no decrease at wavenumbers 3700 to 3300  $\text{cm}^{-1}$  at the same time. 23, 28, and 33 showed a more pronounced decrease at wavenumbers 3700 to 3300  $\text{cm}^{-1}$  compared to 1018  $\text{cm}^{-1}$ . Interestingly, all particles that showed a reduction in wavenumbers 3700 to 3300  $\text{cm}^{-1}$  also had a decrease in 1018  $\text{cm}^{-1}$ . Similar patterns were also seen in particles sized 6.3 - 2 mm in the top layer and particles sized 2 - 0.63 mm in the bottom layer of vermicompost. Therefore, it is assumed that a decrease in the C-O stretch at wavenumber 1018  $\text{cm}^{-1}$  is the first sign of the biodegradation process.

Fewer particles were found in the bottom layer of V3. Figure 47 shows the comparison between the infrared spectra of the original TPS-PBAT bag and 5 TPS-PBAT particles sized 2 - 0.63 mm. Data was normalised to the highest absorption band, namely 1711  $\text{cm}^{-1}$ , which was not the highest for all particles. The infrared spectra were baseline corrected, and TPS-PBAT particles isolated from vermicompost are presented in grey and the original TPS-PBAT bag in red to highlight the pronounced decrease in the two bands.

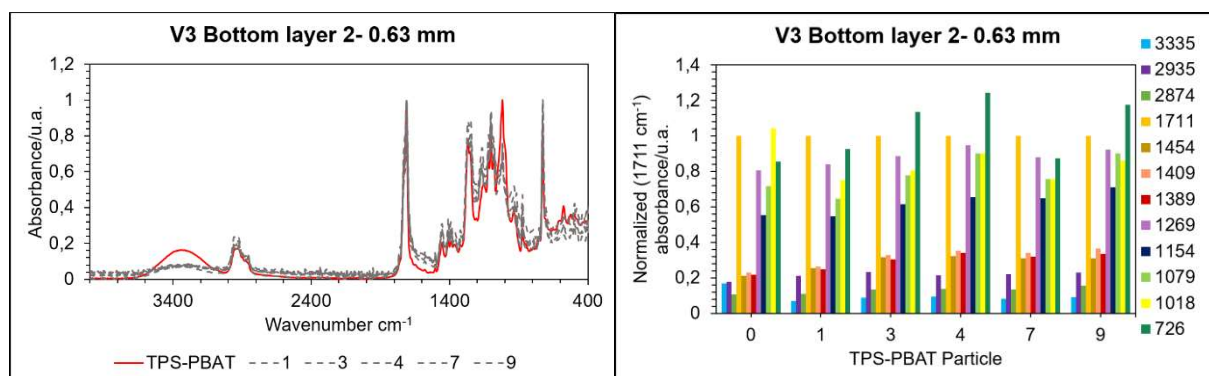


Figure 47: Infrared spectra (on the left) and characteristic wavenumbers selected from the infrared spectra normalized to 1711  $\text{cm}^{-1}$  (on the right) of manually sorted out TPS-PBAT particles (Number 1, 3, 4, 7, 9) sized 2 - 0.63 mm in V3 bottom layer- Vermicomposting with TPS-PBAT foils at the end of the experiment

All particles showed a decline in absorbance between 3700 and 3300  $\text{cm}^{-1}$  and at 1018  $\text{cm}^{-1}$ . In contrast to the particles that were collected from the top layer the degradation of both bands is evident for all particles of the bottom layer. Hence, the degradation degree of particles was apparently higher in the bottom layer. This phenomenon could be explained by the advanced degradation degree of



vermicompost in the bottom layer. Earthworms are found in the top layer where they feed on fresh organic matter. After processing the organic material, microorganisms take over in further degrading the remaining organic compounds and are active in the stabilization and maturation of vermicompost in the bottom layer. Other than that, particle number 1 showed a decrease in absorbance at  $1079\text{ cm}^{-1}$  that is attributed to glucose.

In summary, all TPS-PBAT particles saw first a decrease in wavenumber  $1018\text{ cm}^{-1}$ , followed by a decrease in wavenumbers  $3700$  to  $3300\text{ cm}^{-1}$ . Moreover, a reduction in absorbance of the C-O stretch at  $1079\text{ cm}^{-1}$  was an indication of further degradation of TPS. On the one hand, the C-O ester bond at  $1269\text{ cm}^{-1}$  was rarely degraded by microorganisms which is a first indication for enzymatic degradation of the PBAT part. On the other hand, some indicator bands assigned to PBAT increased relatively to the decrease in TPS. These findings are in line with Barragán et al. (2016) who stated that starch compounds degraded in Mater-Bi® after soil burial. However, the C=O bond that is assigned to an ester compound in PBAT was not reduced in the TPS-PBAT particles after composting or vermicomposting. Whereas, the C-O bond in the ester compound did decrease.

## 4.5 Earthworm biomass

At the beginning of the vermicomposting experiment earthworms were evenly distributed among the 3 experimental vermicomposting groups. 564.6 g of earthworms were placed in V1, 564.1 g in V2 and 563.6 g in V3. If every earthworm weighs approximately 0.4 g, 1,412 earthworm were in C1, 1,410 in C2, and 1,409 in C3 (Wormsystems GmbH, n.d.-b). On the 4<sup>th</sup> day approximately 30 dead and dry earthworms were found encircling the three vermicomposters which makes up for 12 g of earthworm biomass. Apparently, some earthworms had escaped during the weekend due to unfavourable conditions in the vermicomposters. Temperatures in the vermicomposters had reached between  $29 - 30\text{ °C}$  on the 4<sup>th</sup> day. Furthermore, fungi developed in V1 and V2 which is a sign of overloading. The earthworms might have faced an elevated microbial activity in the vermicomposters and were competing for oxygen. Therefore, several escaped the vermicomposters. Unfortunately, it was not clear how many had escaped and from which vermicomposter. Therefore, it was concluded that the earthworm biomass had probably decreased in all three vermicomposters. In order to prevent this incident, the vermicomposters were subsequently stored in a climatic chamber with a stable temperature of  $22 - 23\text{ °C}$ , or places with moderate temperatures like the basement of the Institute. Additionally, input material was supplied in smaller portions to avoid the formation of fungi. Initially, input material was added daily during the workweek (five days a week), but after 41 days it was added only twice a week.

At the end of the experiment earthworms were isolated from the vermicompost and the final earthworm biomass was assessed. In V1 775.4 g, in V2 371 g, and in V3 452.6 g of earthworms were recovered which makes up for 1,939 earthworms in V1, 928 in V2 and 1,132 in V3. Earthworm biomass had increased by 37.3 % in V1, whereas it had declined by 34.2 % in V2 and by 19.7 % in V3. Although some earthworms had escaped the vermicomposters after 4 days, it is assumed that earthworm biomass had not changed significantly, and these results are representative. In Figure 48 earthworm biomass for each experimental group is exhibited.

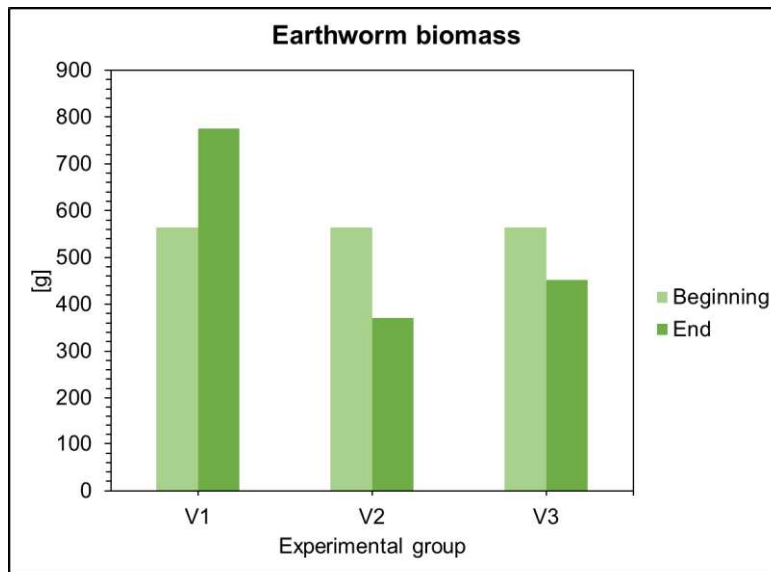


Figure 48: Earthworm biomass at the end of the experiment in V1- Vermicomposting without foils, V2- Vermicomposting with LD-PE foils and V3- Vermicomposting with TPS-PBAT foils

Studies about the effects of different input materials on earthworm health and survival are scarce. Even fewer studies investigated the effects of microplastics on earthworms. Huerta Lwanga et al. (2016) and Cao et al. (2017) proved that certain concentrations of microplastics caused mortality and a growth rate inhibition in the earthworm population. However, in these studies microplastics were added and not macro particles of plastics like in this thesis. Furthermore, different concentrations of microplastics were tested and resulted in a growth rate inhibition and mortality rate that directly correlated with the concentration of microplastics.

Moreover, earthworms that seemed to be halved and missed their back parts were found in V3. Rodriguez-Sejo et al. (2017) found that PE microplastic concentrations between 62.5 and 1,000 mg/kg soil on a dry matter basis caused histopathological damage to *Eisenia Andrei*. They ranged from gut damage to atrophy or detachment of the epithelium. Due to time and resource limitations no further examinations on the earthworms themselves were conducted, however, the observation of earthworm injury suggests that TPS-PBAT may cause similar histopathological damages as PE. This is the first study examining the degradation degree of both, biodegradable and non-biodegradable plastics during vermicomposting. Until now only non-biodegradable plastics were tested in previous studies. Thus, further research on this subject is required to assess the impacts of different plastic types on earthworms, including the investigation of the mechanisms causing mortality and growth rate inhibition among earthworms.

In conclusion, the significant difference in earthworm biomass between V1 and the two plastic containing vermicomposters indicates that both biodegradable and non-biodegradable plastics had a negative impact on the earthworm population. Increased mortality and inhibition of the growth rate are likely to have contributed to the decrease in earthworms. Although earthworm biomass in V2 and V3 has decreased significantly throughout the vermicomposting experiment, the mass reduction was like V1. It is known that earthworms aerate, fragment, and condition the organic material. However, the actual degradation process is conducted by microorganisms. Microorganisms might have compensated the reduced activity of earthworms, thereby achieving a similar reduction in mass.

#### 4.5.1 Heavy metal content of earthworms

A heavy metal analysis was conducted on the earthworms before they were placed in the vermicomposters and at the end of the experiment. The results are presented in Table 14. They show that Cr, Ni and Pb levels approximately stayed the same throughout the experiment. Cd increased in all vermicomposters except for V2. Like Liu et al. (2012) pointed out earthworms can accumulate heavy metals in their tissue and xenobiotic heavy metals are excreted very slowly or not at all. However, Hg decreased in all three groups at the end of the experiment. It was excreted by the earthworms in the course of the experiment, and up to a decrease of 79 % of Hg was detected in V2.

Cu concentrations were unchanged. In contrast, Zn concentrations decreased throughout the vermicomposting experiment although, earthworms possess physiological control over uptake and secretion of essential metals. The earthworms were most probably exposed to a higher concentration of Zn and Hg before being placed in the vermicomposters and then egested Hg and Zn in the course of the experiment. Yet, no samples of the vermibed before starting the experiment and of the final vermicompost were tested for heavy metals.

Table 14: Heavy metal content of earthworms at the start and at the end of the experiment in the three vermicomposters (V1, V2 and V3)

Sample	Heavy metal content [mg/kg dm] in earthworms						
	Cd	Cr	Cu	Ni	Pb	Zn	Hg
Earthworms	1.8	80.6	45.9	56.5	9.2	183.1	2.7
V1	2	80.8	46.3	56.5	9.3	156.8	1.5
V2	1.8	81	45.6	54.7	9.1	115.9	0.6
V3	2.3	78.8	47.8	54.1	9	135.6	1.4

## 4.6 Compost quality

### 4.6.1 Compost

Samples were withdrawn at the start of the experiment and on day 1, 8, 22, 48, 90, and 124 during the composting experiment. These were analysed for different parameters. Parameters of the individual compost reactors which belong to C1, C2, and C3 were averaged and plotted.

In Figure 49 water contents of the three groups are presented. It approximately stayed at the same level throughout the experiment. Compost reactors were supplied with water if necessary, therefore, the water content was always in the optimal range. A low water content can inhibit microbial activity and disrupt the rotting process. C1's water content ranged between maximum 79 and minimum 73 % dm, C2's water content was between maximum 75 and minimum 70 % dm, and C3's ranged between maximum 80 and minimum 72 % dm. Initial water content declined on day 7 for C1 and on day 21 for C2. Water content was slightly lower in C2 in comparison to C1 and C3 from the 21<sup>st</sup> day onwards. LD-PE particles are hydrophobic, hence, their ability to take up water

is limited (Oliveira Gama et al., 2018). In the case of C2, the hydrophobic LD-PE particles might have caused a lower water content in ratio to the dry matter.

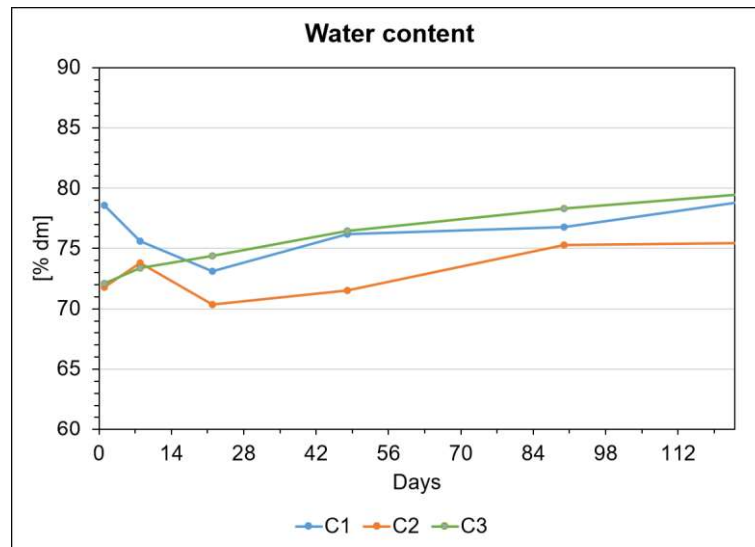


Figure 49: Water content for C1- Composting without foils, C2- Composting with LD-PE foils and C3- Composting with TPS-PBAT foils

Initial pH was around 5 and then changed to a more neutral pH. The biogenic waste had a pH of 5.2 and during the rotting process pH turned alkaline in all three groups as shown in Figure 50. After the first 8 days a neutral pH of 7 was already reached. This development has also been described by Bertoldi et al. (1983). LD-PE and TPS-PBAT particles do not seem to have any effect on the resulting pH. However, C1 turned slightly more alkaline than C2 and C3. The final values for pH were 8.1 for C1, 7.9 for C2, and 7.7 for C3.

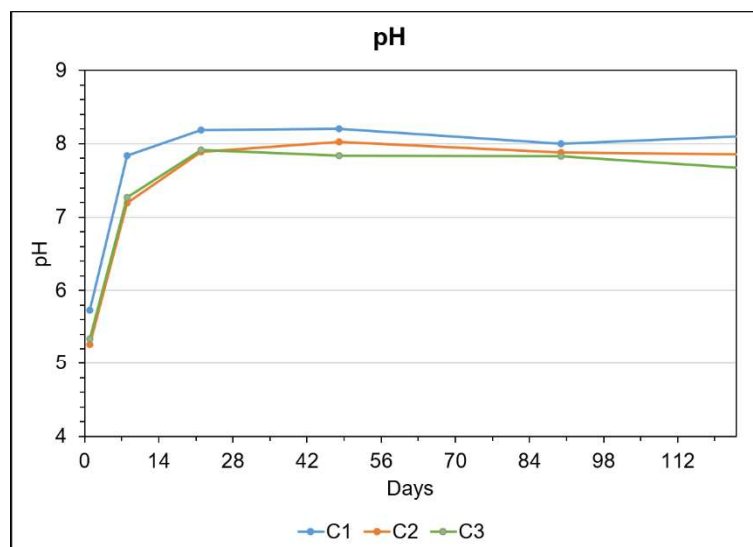


Figure 50: pH for C1- Composting without foils, C2- Composting with LD-PE foils and C3- Composting with TPS-PBAT foils

In Figure 51 electric conductivity is depicted in a diagram. Initial EC was 2.7 for C1, 2.1 for C2, and 2.5 for C3 and decreased to 2, 1.8, and 1.9 respectively.

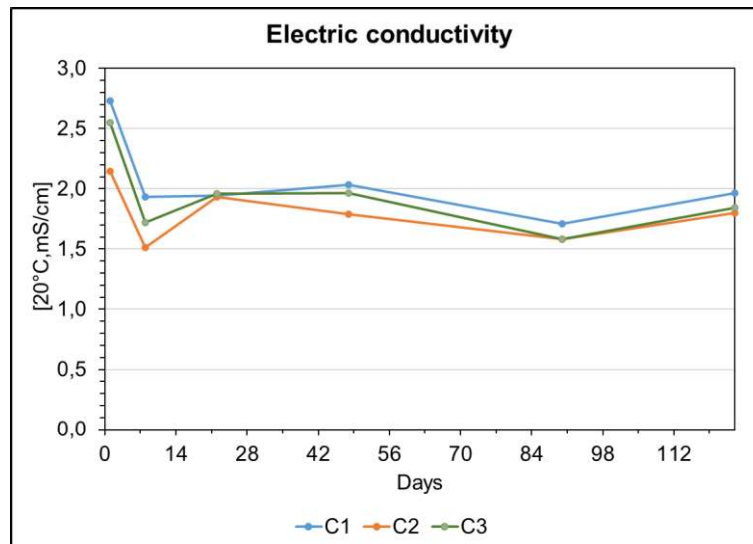


Figure 51: Electric conductivity for C1- Composting without foils, C2- Composting with LD-PE foils and C3- Composting with TPS-PBAT foils

After 8 days EC declined within all compost reactors and augmented after 22 days for C2 and C3. After 90 days EC decreased again for all compost reactors and marginally increased towards the end of the experiment. In total EC had declined 0.8 mS/cm in C1, 0.3 mS/cm in C2, and 0.7 mS/cm in C3. A decline in EC is not typical for the experiment since the concentration of salts should increase since biomass decreases and salts are left. The only way salts can be eliminated is through leaching. LLeó et al. also found a higher EC in leachate resulting from compost than in the compost. Leachate only evolved after 8 days during the experiment and it was added to the compost reactors again. However, salts might have adhered to the glass walls of the leachate tank while leachate evaporated. In line with this hypothesis, EC decreased significantly when leachate evolved. EC was highest in C1, second highest in C3 and lowest in C2.

At the beginning of the experiment loss on ignition (LOI) was 91.8 % dm for C1, 93.7 % dm for C2, and 92.9 % dm for C3. The slightly higher LOI for C2 and C3 can be explained by the addition of LD-PE and TPS-PBAT particles, which are mainly composed of carbon and, hence, increase the level of LOI. LOI declined steadily with C3 and varied for C1 and C2. More information is given in Figure 52. After 90 days a slight increase was noted in C1 and then a slight decrease towards the end. C2 decreased constantly, with an inconsiderable increase after 90 days. In total LOI has declined by 6.8 % dm for C1, 7.3 % dm for C2, and 9 % dm for C3.

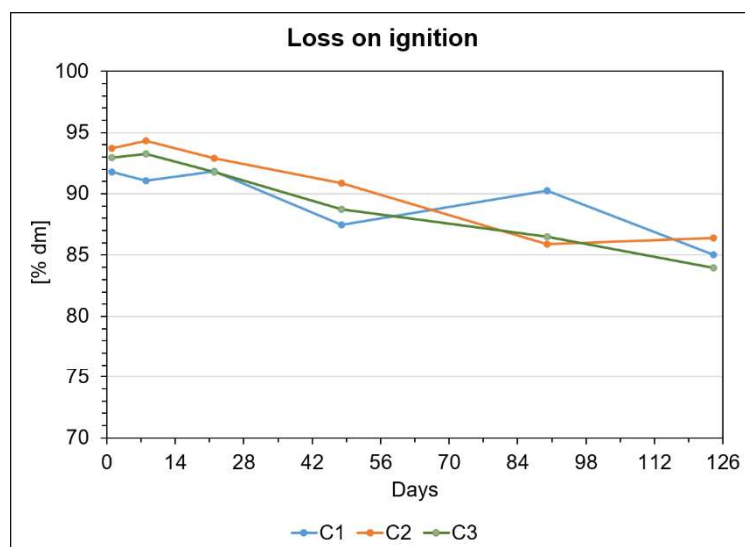


Figure 52: Loss on ignition for C1- Composting without foils, C2- Composting with LD-PE foils and C3- Composting with TPS-PBAT foils

Total organic carbon (TOC) marginally decreased throughout the composting process. At first it accounted for 47.4 % dm in C1, 47.5 % dm in C2, and 46.8 % dm in C3. In C1 TOC declined by 4.4 % dm, in C2 by 3.9 % dm, and in C3 by 3.6 % dm. However, data for C1 varied the most. It increased marginally after 22 days and then decreased until the 48<sup>th</sup> day. After that it enhanced slightly and dropped again at the end of the experiment as illustrated in Figure 53. During the rotting process TOC should decline since organic compounds are mineralized to CO<sub>2</sub>. Since the ratio between TOC and LOI stayed the same throughout the experiment, inhomogeneity of the samples might have attributed to the sudden increases in LOI and TOC. As already mentioned before, LD-PE and TPS-PBAT particles might not be adequately represented in the samples due to sample preparation. Therefore, C2 showed moderately higher values for TOC after 8 and 22 days. Also bulking agents might be inadequately represented in the samples since they could not be grinded thoroughly with the vibrating disc mill. However, a general decline in TOC and LOI is evident which proves that the input material was mineralized.

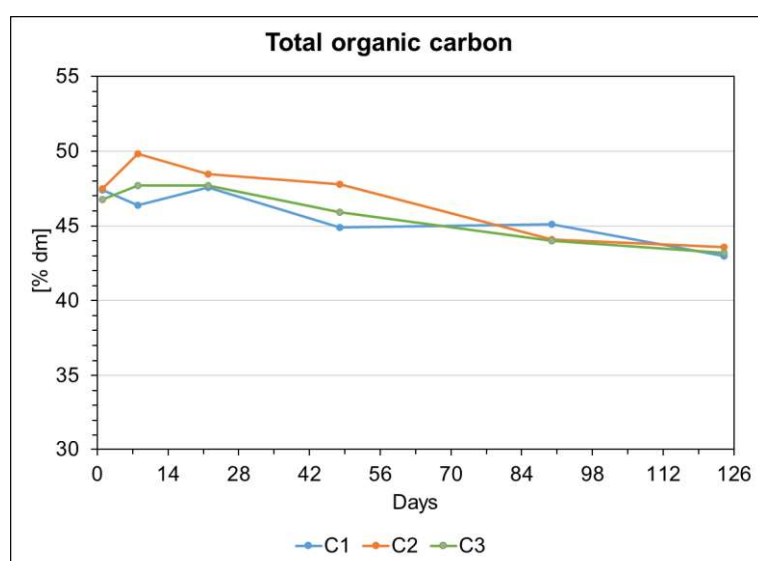


Figure 53: Total organic carbon for C1- Composting without foils, C2- Composting with LD-PE foils and C3- Composting with TPS-PBAT foils

In all three groups total nitrogen rose throughout the experiment, with a decline after 8 days as shown in Figure 54. This decline in TN might have occurred due to the change in pH from acidic to alkaline within the first 8 days, and due to the narrow C/N ratio of the biogenic waste. Biogenic waste that was added to the input material had an initial C/N ratio of 10.9 because of excessive nitrogen. Although total C/N ratio of the input material was higher than of the biogenic waste itself, microorganisms might have preferred the biogenic waste over the bulking agents. Bulking agents were composed mainly of wood chips made of lignin, which is not easily degradable. The biogenic waste was mostly made up of fruits and vegetables, which are more readily degradable. At the end of the experiment no signs of the biogenic waste were noticeable, but bulking agents were still visible. In consequence, microorganisms might have degraded biogenic waste at a faster pace than the bulking agents.

Furthermore, pH changed from acidic to alkaline which favours the conversion of  $\text{NH}_4$  to  $\text{NH}_3$ . A narrow C/N ratio can cause loss of nitrogen through volatilization. In summary, nitrogen might have been lost after 8 days due to denitrification and favourable environmental factors. At turning events a strong odour of  $\text{NH}_3$  was noticeable. After the first 8 days most easily degradable compounds were degraded, and microorganisms started seeking additional carbon sources such as bulking agents. Hence, excessive nitrogen was compensated by additional carbon. The difference between the initial value and final value is +0.66 % dm for C1, +0.59 % dm for C2 and +0.6 % dm for C3. The rise in TN is attributed to the loss in mass. C1 achieved the highest TN with 1.45 % dm, followed by C3 with 1.39 % dm, and lastly C2 with 1.24 % dm.

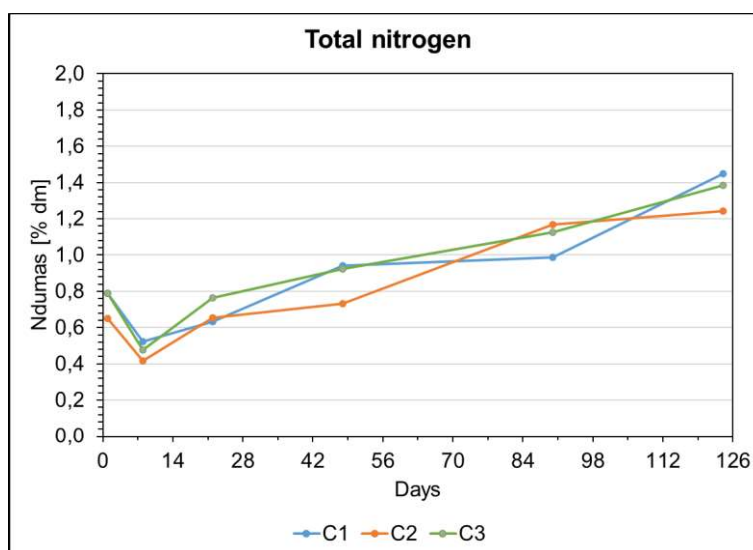


Figure 54: Total nitrogen for C1- Composting without foils, C2- Composting with LD-PE foils and C3- Composting with TPS-PBAT foils

Carbon to nitrogen ratio generally declined throughout the rotting process as can be seen in Figure 55. Initial C/N ratio was highest for C2 at 72.9, and similar for C1 at 60 and for C3 at 59.2. They are not in line with the optimal range of C/N, namely 25:1 to 35:1 as described by Amlinger et al. (2005). Although all three groups have similar TOC, C2 had a higher C/N ratio due to its low TN level. The rise in C/N ratio after the first 8 days can be explained by the slight increase in TOC and at the same time a decline in TN. After that the C/N ratio fell within all groups and accounted for 29.7 for C1, 35 for C2 and 31.1 for C3 at the end of the experiment. The steepest decline in C/N was recorded between the 8<sup>th</sup> and 22<sup>nd</sup> days in C2 and C3 and between the 22<sup>nd</sup>



and 48<sup>th</sup> day for C1. In total C/N ratio had declined 51 % in C1, 52 % in C2, and 47 % in C3.

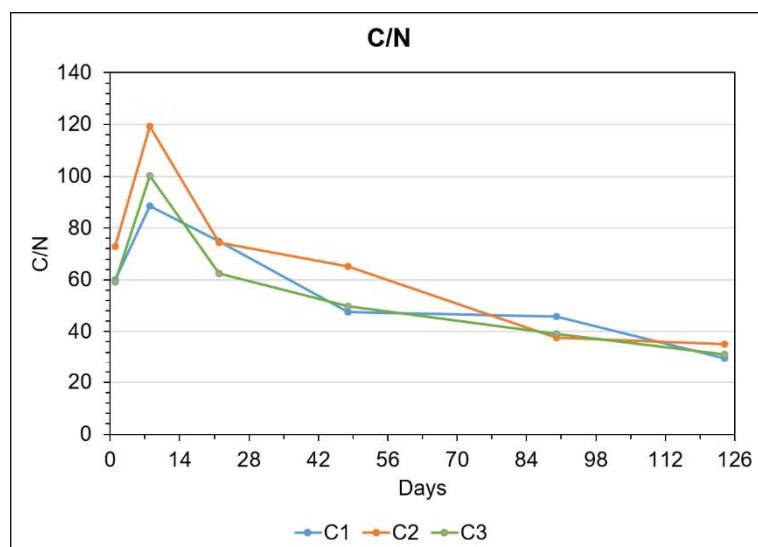


Figure 55: C to N ratio for C1- Composting without foils, C2- Composting with LD-PE foils and C3- Composting with TPS-PBAT foils

Humic acids (HA) were measured from the 22<sup>nd</sup> day onwards as depicted in Figure 56. Initial values for HA were 153 optical density/g odm for C1, 150 optical density/g odm for C2, and 145 optical density/g odm for C3.

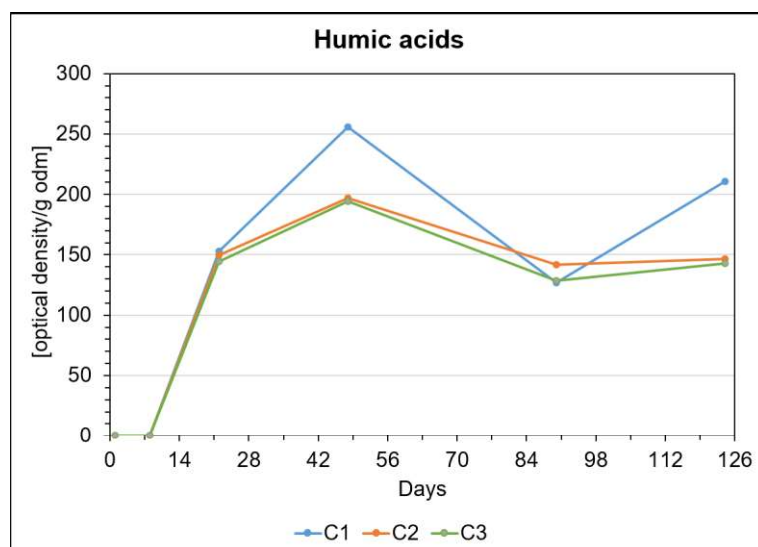


Figure 56: Humic acids for C1- Composting without foils, C2- Composting with LD-PE foils and C3- Composting with TPS-PBAT foils

They then rose after 48 days and dropped after 90 days. However, they increased again at the end of the experiment after 120 days. Overall, HA changed significantly for C1 from 153 optical density/g odm to 211 optical density/g odm. Whereas, they did not change significantly for C2 and C3. An increase of 38 % of HA was detected in C1 and C2's and C3's HA decreased by 2 % and 1 % respectively. The final value for C2 was 147 optical density/g odm and for C3 143 optical density/g odm. Initial values for HA were similar, but HA only slightly increased in C1.

In contrast to HA, fulvic acids (FA) did not differ significantly among the different groups as shown in Figure 57. Initial FA content was 29 optical density/g odm for C1, 32 optical density/g odm for C2, and 36 optical density/g odm for C3.



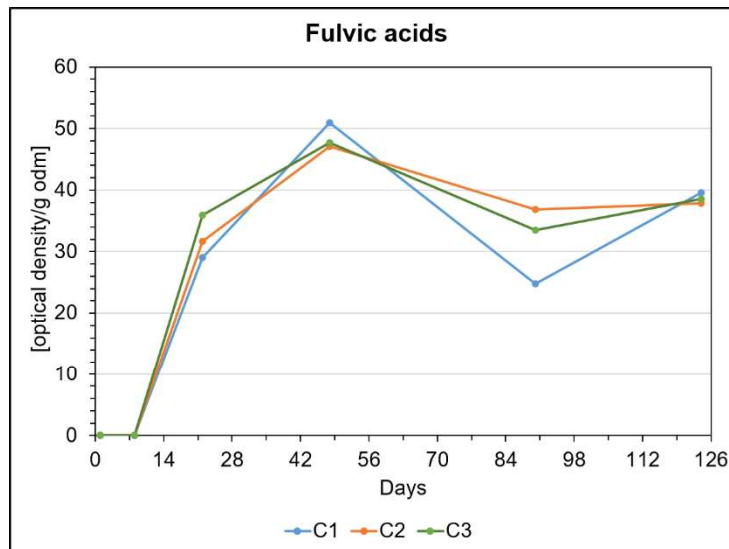


Figure 57: Fulvic acids for C1- Composting without foils, C2- Composting with LD-PE foils and C3- Composting with TPS-PBAT foils

Maximum values were 51 optical density/g odm for C1, 47 optical density/g odm for C2, and 48 optical density/g odm for C3 after 48 days. However, they slightly dropped, and the end values were 40 optical density/g odm for C1, 38 optical density/g odm for C2, and 39 optical density/g odm for C3.

#### 4.6.2 Vermicompost

In the course of the vermicomposting experiment leachate was collected in the collection tank. The first leachate (leachate 1) and last leachate (leachate 2) that was collected were measured for TKN, total phosphor (TP),  $\text{NH}_4\text{-N}$ , and  $\text{NO}_3\text{-N}$ . Total potassium (K) was only measured for leachate 1 and pH and EC were assed for leachate 2. Table 15 shows the values for these parameters. Surprisingly, the values differ strongly between leachate 1 and 2. Total nitrogen is similar, nevertheless total phosphor is a 100 % higher in leachate 1 than in leachate 2,  $\text{NH}_4\text{-N}$  concentration is 93 % higher in leachate 2 and  $\text{NO}_3\text{-N}$  is 88 % higher in leachate 1. Leachate evolved at all time during vermicomposting and probably varies in its composition due to many different factors. Firstly, the input material plays a major role as it contains all nutrients that might dissolve in leachate. Secondly, the activity of the microorganisms and earthworms determines if these nutrients are either bound in biomass of organisms or in the biomass of the vermicompost.

Table 15: Parameters assessed for leachate 1 and 2

	TKN [mg/l]	TP [mg/l]	K [mg/l]	$\text{NH}_4\text{-N}$ [mg/l]	$\text{NO}_3\text{-N}$ [mg/l]	pH	EC [mS/cm]
Leachate 1	115	19.3	2	2.8	26.4		
Leachate 2	80	0.09		37.1	3.1	8.8	9.7

Samples from the vermicompost were only withdrawn once at the end of the experiment. In the following section, data from the composting experiment (C) and vermicomposting experiment (V) are, therefore, compared based on the final values. Furthermore, vermicompost was divided into two halves, one top (T) and one bottom (B) layer. Final values of the compost reactors are compared to the bottom layer of the

vermicomposters since it represents the mature vermicompost. Values for the input material of the vermicomposting experiment (Input) were calculated by forming a mean value of the input materials that was added from day 1 - 28 and 29 - 120. The mean value was calculated by the ratio of mass that was added from each input material. In Figure 58 water content of the compost reactors, vermicomposters and of the input material for vermicomposters are shown. There are subdivided into group 1 where no foils were added, 2 where LD-PE foils were added, and 3 where TPS-PBAT foils were added.

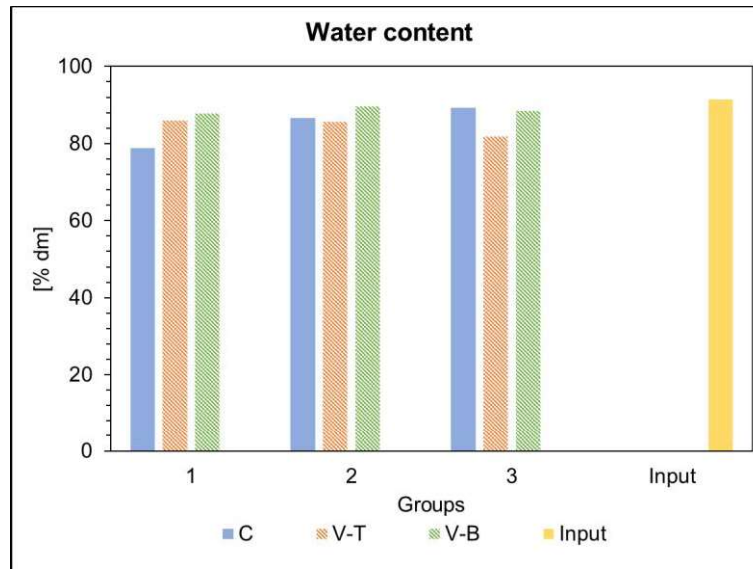


Figure 58: Water content for compost reactors, vermicomposters (T+B) and input material for vermicomposters

The input material had an initial water content of 91 % dm. Water content was slightly higher in the bottom layer than in top layer which is surprising since the organic matter was always placed on the top layer. Deviation between top and bottom layer were 1.9 % dm for V1, 4.1 % dm for V2, and 6.6 % dm for V3. These differences are not significantly high, yet, a trend is noticeable. During the experiment temperatures did not reach over 25 °C. In consequence, water did most likely not evaporate excessively. However, leachate was collected in a collecting tank at the bottom of the vermicomposter. When water exceeded water holding capacity of the vermicompost, it probably leaked downwards and was collected as leachate in the collecting tank. If the collecting tank was filled to its maximum capacity, waterlogging might have occurred. Another explanation could be that water holding capacity of the top and bottom layer differ significantly, since the degradation process was not fully completed in the top layer compared to bottom layer. Water content was 88 % dm in the bottom layer of V1, 90 % dm in the bottom layer of V2, and 88 % dm in the bottom layer of V3. According to Domínguez and Edwards (2011a) the optimum water content lies between 80 - 85 % dm. Hence, water content was slightly higher during this vermicomposting experiment. Compost reactors had a lower water content than vermicomposters due to evaporation of water during the rotting process. Temperatures are higher during composting than during vermicomposting. LLeó et al. (2013) reported as well that water content is higher with vermicomposting.

As illustrated in Figure 59 pH did not differ significantly between the top and bottom layer. Both values were above 8 and alkaline. Yet, the bottom layer was slightly more alkaline with a difference of 2 % for V1, 2 % for V2, 1 % for V3 compared to the top layer. Further, leachate 2 had a pH of 8.8 which is similar to the final values of the

bottom layers which were 8.8 for V1, 8.7 for V2, and 8.5 for V3. V3's bottom layer exhibited the lowest among the three experimental groups. Also, C3 proved the lowest pH among the three compost reactors. TPS-PBAT particles might have some buffering characteristics or its degradation evokes acidic bioproducts. Input material presented an acidic pH of 4.8 and was marginally too acidic for vermicomposting. Nevertheless, vermicompost turned from acidic to alkaline. Majlessi et al. (2012) also reported a turn from acidic to alkaline. The monthly amendment of rock flour and lime might have attributed to the alkaline values since it elevates the pH. Also, earthworms can excrete lime in order to control pH.

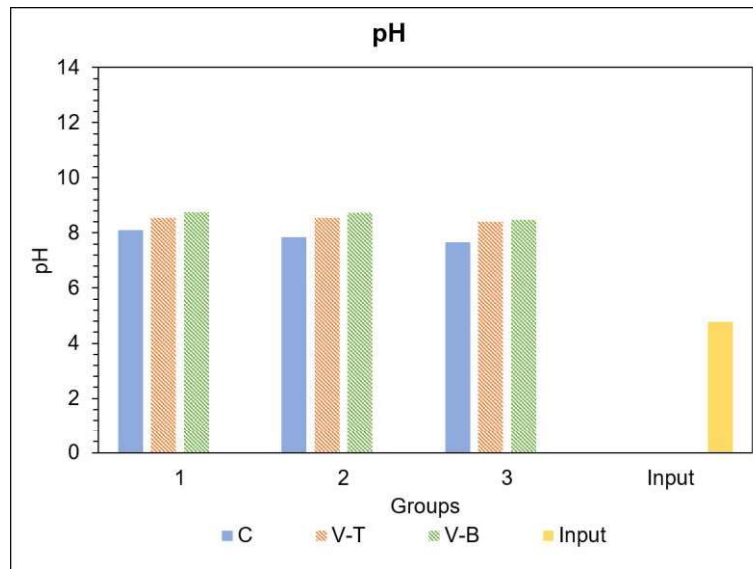


Figure 59: pH for compost reactors, vermicomposters (T+B) and input material for vermicomposters

Electric conductivity decreased within all three vermicomposters as shown in Figure 60. Input material had an initial EC of 8.4 mS/cm. After more than 120 days of vermicomposting final value for V1 was 3 mS/cm, for V2 3.1 mS/cm, and for V3 3.8 mS/cm. EC was slightly lower in the top layer compared to the bottom layer. This phenomenon can be explained by looking at leachate 2 which had an EC of 9.7 mS/cm. Lazcano et al. (2008) also reported that EC declines due to precipitation. Within the vermicomposters water is supplied by the organic matter that is added. If water exceeds the maximum water holding capacity of the vermicompost, it runs downwards into the collecting tank. With the water also soluble compounds, such as salts, pass through the vermicomposters. Therefore, the concentration might be higher in the bottom layer. The highest difference between top and bottom layer was found within V3 with an increase of 60 %. In this case many salts must have precipitated in the leachate. Comparing the composting experiment with the vermicomposting experiment EC was slightly higher in the final vermicompost than in the final compost.

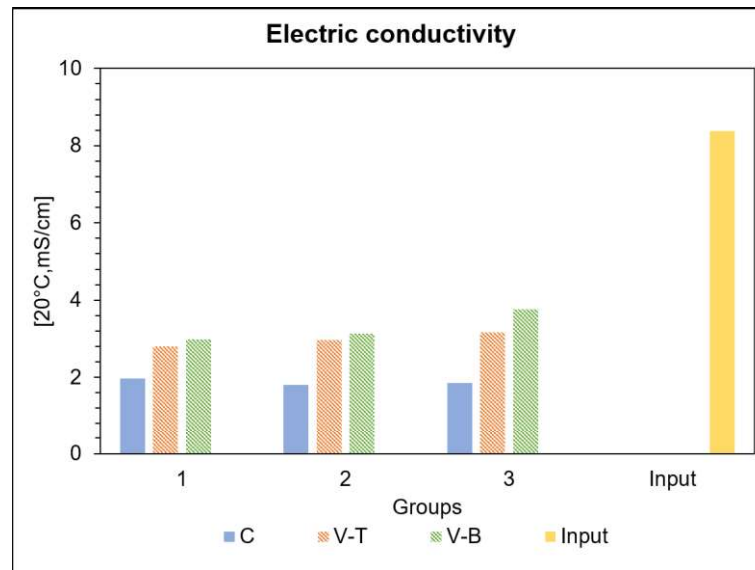


Figure 60: EC for compost reactors, vermicomposters (T+B) and input material for vermicomposters

In Figure 61 loss on ignition (LOI) is presented. During vermicomposting LOI of the input material decreased which accounted for 84.9 % dm. LOI was higher in the top layer than in the bottom layer. It was 55.7 % dm for V1, 57.16 % dm for V2, 55.81 % dm for V3 and reduced to 50.5 % dm, 55.2 % dm, and 54.2 % dm respectively. Thus, a greater change in LOI occurred in V1 compared to the other experimental groups. The reduction in LOI between the top and the bottom can be explained by the mineralization process of organic matter. The organic matter of the top layer was not yet fully degraded and mineralized. Hence, the difference between the two layers.

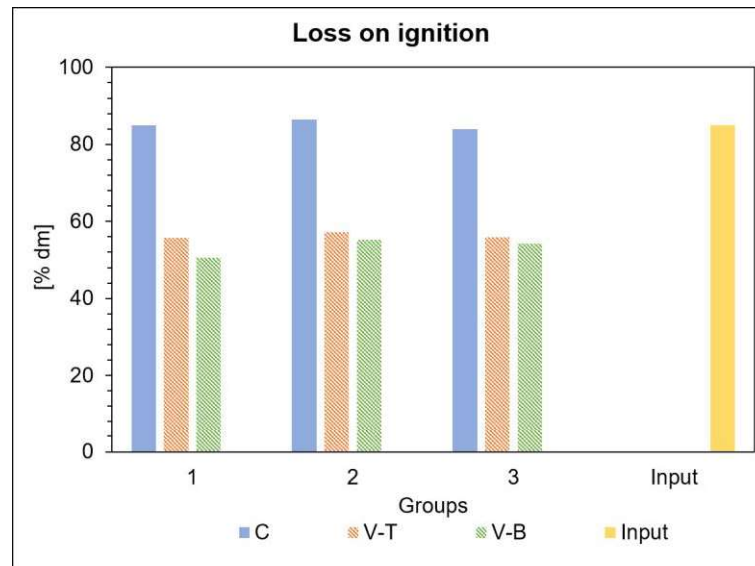


Figure 61: Loss on ignition for compost reactors, vermicomposters (T+B) and input material for vermicomposters

In line with these findings, TOC also decreased throughout the degradation process as illustrated in Figure 62. Initial TOC was 42.8 % dm in the input material. It decreased to 27.8 % dm for V1, 27.7 % dm for V2, and 25.9 % dm for V3. In comparison to LOI, TOC stayed relatively the same throughout the top and bottom layer of V1 and V2. Other organic compounds, such as organic nitrogen, were most likely more abundant in the top layer of the vermicomposters. Nevertheless, a discrepancy between the top and bottom layer of V3 is noticeable. It accounts for an increase of 2.3 % dm in the top

layer which might result from the addition of TPS-PBAT particles to the input material. These particles were mainly located in the top layer of the vermicompost.

TOC and LOI of the compost were higher than of vermicompost. These findings are in line with the results of LLeó et al. (2013) and Suthar and Gairola (2014). Carbon is used either as energy source for microorganisms and other organisms, turned into biomass or is mineralized. TOC declined between 15 and 16.9 % dm during vermicomposting whereas it only declined between 3.6 and 4.4 % dm during composting. Thus, more carbon must have been lost by mineralization to CO<sub>2</sub> or accumulation in earthworm biomass during vermicomposting. However, no CO<sub>2</sub> measurements could be taken from the vermicomposters since the vermicompost was too moist. Nevertheless, input material of the compost reactors was additionally composed of wood chips which are decomposed at a slower rate. In practise, bulking agents would be sorted out from the compost, but in this thesis, they were not extracted from the compost. Hence, TOC and LOI are not comparable between compost reactors and vermicomposters.

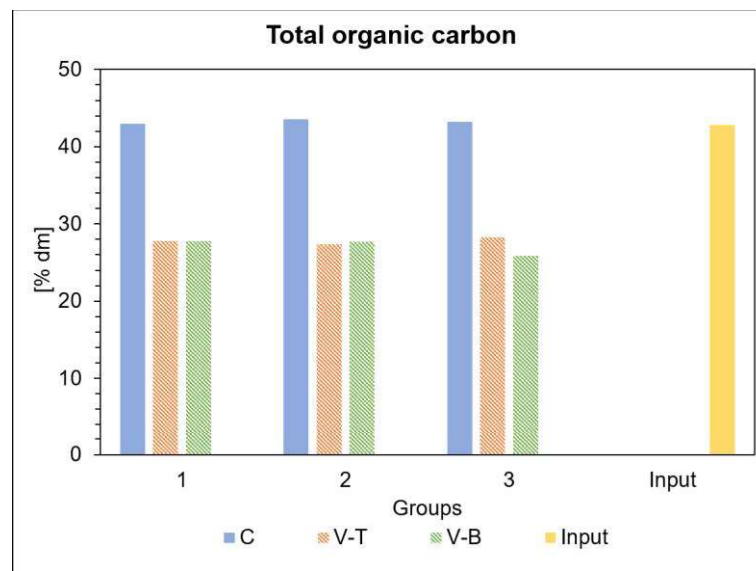


Figure 62: Total organic carbon for compost reactors, vermicomposters (T+B) and input material for vermicomposters

Figure 63 presents total nitrogen (TN). In the course of the experiment total nitrogen has decreased. The value for the input material was 3.2 % dm. Total nitrogen in the bottom layer was 1.4 % dm for V1, 1.3 % dm for V2, and 1.3 % dm for V3. A loss in nitrogen might suggest the volatilization of nitrogen or loss through leachate. The latter is more plausible since high concentration of TKN were found in leachate 2. It accounted for 81 mg/l. TN is probably higher in the top layers than in the bottom layers since biogenic waste has not been fully degraded. In the composting experiment TN increased throughout the experiment due to loss in biomass. Nevertheless, TN as a percentage of dry matter was lower in the input material of the compost reactors than of the vermicomposters as they included bulking agents. When comparing the value of the biogenic waste with the final values of the composting experiment, it appears that TN decreased as well. TN of the compost reactors and vermicomposters were similar and were almost identical at the end of the experiments.

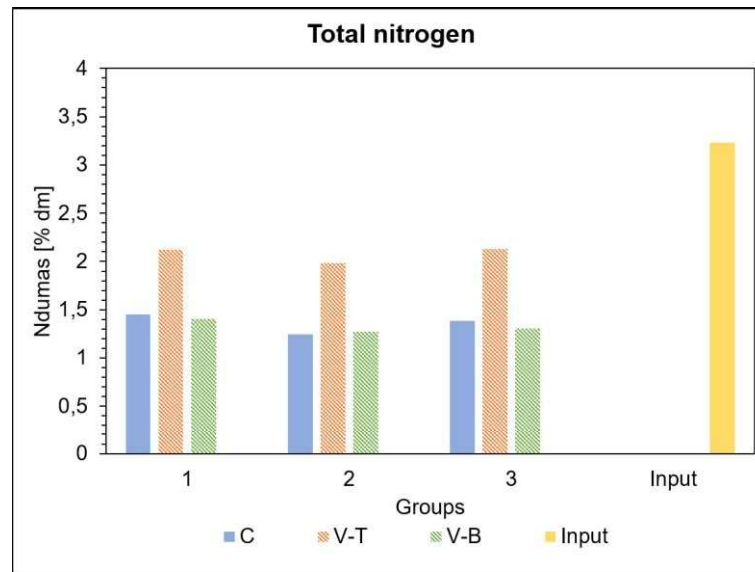


Figure 63: Total nitrogen for compost reactors, vermicomposters (T+B) and input material for vermicomposters

C to N ratio (C/N) increased among the top layers during vermicomposting since TN decreased as exhibited in Figure 64. It increased by 51 % for V1, 57 % for V2, and 50 % for V3 in the bottom layer, and the final values were 20, 22 and 20 respectively. Initial C/N ratio was 13 for the input material which does not lie in the optimal range of 25:1 to 30:1 as reported by Domínguez and Edwards (2011b). Compared to the experimental groups in composting, the final value is 33 % lower for V1, 38 % lower for V2, and 36 % lower for V3. Vermicomposters might have required a more carbon rich input material to outweigh the nitrogen load. TN is similar for composting and vermicomposting. However, TOC is higher within the final compost samples. Thus, C/N is narrower for the vermicomposting experiment.

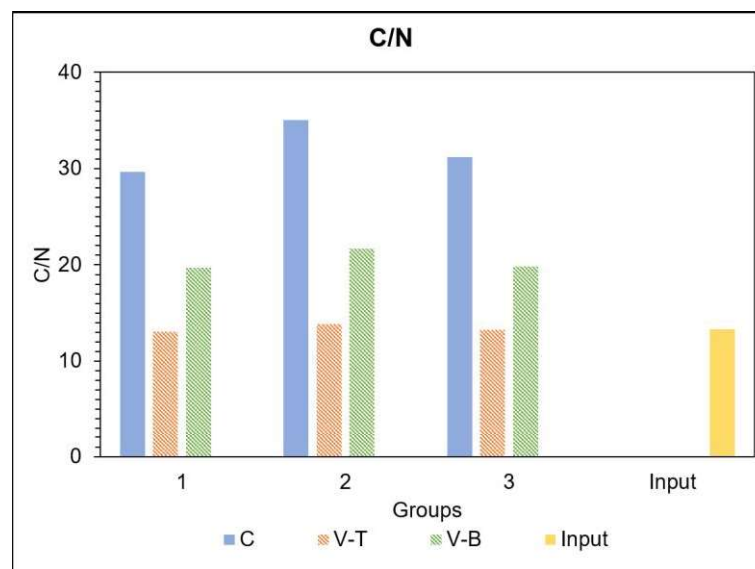


Figure 64: C to N ratio for compost reactors, vermicomposters (T+B) and input material for vermicomposters

The formation of humic and fulvic acids differed between the two layers in vermicompost, as can be seen in Figure 65 and in Figure 66. While humic acids were higher in the top layer compared to the bottom layer, fulvic acids were higher in the bottom layer compared to the top layer. This means that the ratio between humic and



fulvic acids might have changed in the course of the degradation process. As already stated, the top layer has not undergone the full degradation process like the bottom layer. Consequently, humic acids might have dissolved in the leachate due to the high pH during vermicomposting. The ratio between humic and fulvic acids is 2.5:1 in the top layer and changed to 1.7:1 in the bottom layer for V1, 2.6:1 and 1.7:1 for V2, and 3:1 to 1.9:1 for V3 respectively. In all three cases fulvic acids increased about 10 % in comparison to humic acids. Final values for HA were 188 optical density/g odm for V1, 179 optical density/g odm for V2, and 171 optical density/g odm for V3. In conclusion, final values did not vary significantly between the different experimental groups.

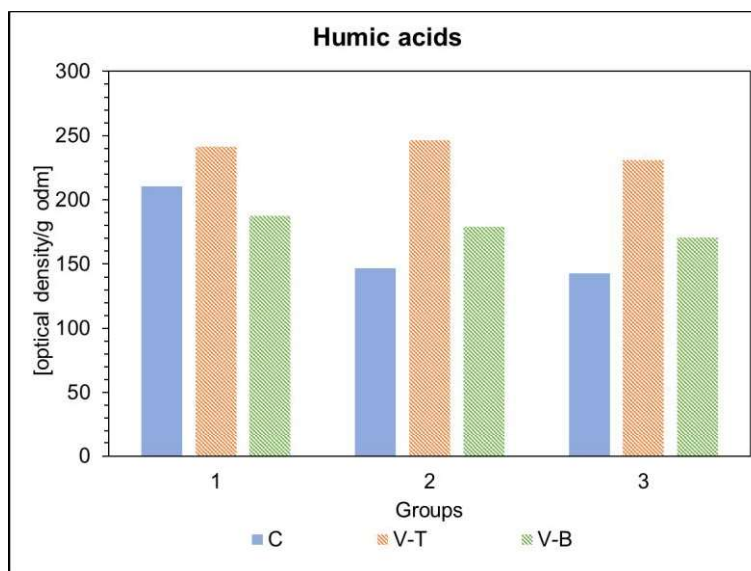


Figure 65: Humic acids for compost reactors, vermicomposters (T+B) and input material for vermicomposters

The difference between the composting and vermicomposting experiment concerning humic acids was very moderate. In group 1 humic acids were 11 % higher in the final compost than in the final vermicompost. For group 2 and group 3 it was the other way around, it was 22 % and 20 % higher in V2 and V3 respectively. FA were higher in vermicompost compared to the compost. An increase of 185 % in V1, 180 % in V2, and 138 % in V3 was observed. Final values were 113 optical density/g odm, 106 optical density/g odm, and 92 optical density/g odm respectively. No significant discrepancy can be noted between the three vermicomposting groups. In summary, FA build-up occurred at a higher rate during vermicomposting compared to composting which can probably be attributed to the microbial population prevailing in vermicompost.

Nevertheless, values for humic acids were moderate in comparison to other samples analysed at the Institute of Waste Management which generally lie between 800 – 3900 optical density/g odm. Rotting parameters were optimal in both experiments. Yet, the input material was mostly composed of fruits and vegetables and less of composites containing lignin or hemicelluloses. Hence, humic acids formation was rather low.

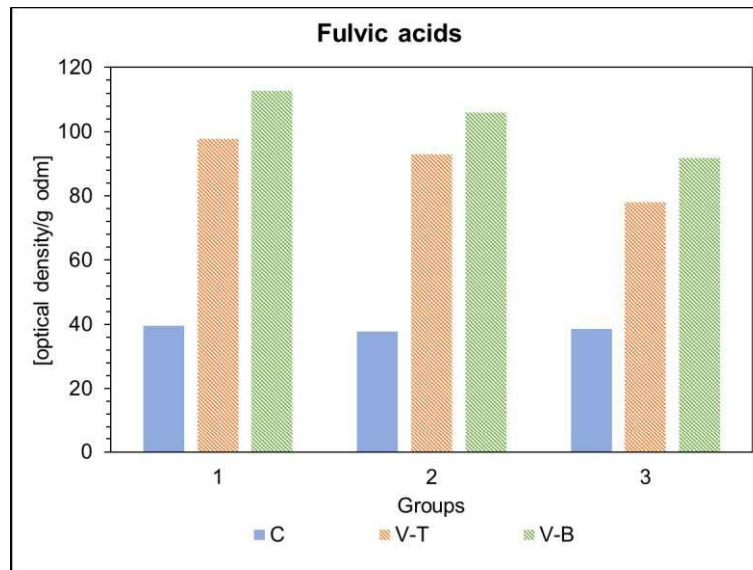


Figure 66: Fulvic acids for compost reactors, vermicomposters (T+B) and input material for vermicomposters

$\text{NO}_3\text{-N}$  concentration decreased during vermicomposting and composting compared to the input material, whereas  $\text{NH}_4\text{-N}$  concentration increased in some cases. Input material had a  $\text{NH}_4\text{-N}$  and  $\text{NO}_3\text{-N}$  concentration of 8 mg/kg dm and 25 mg/kg dm respectively.  $\text{NH}_4\text{-N}$  values in the compost were comparable between groups and accounted for 0.8 mg/kg dm for C1, 1 mg/kg dm for C2 and 0.8 mg/kg dm for C3. In contrast,  $\text{NH}_4\text{-N}$  values in the vermicompost varied between groups as illustrated in Figure 67.

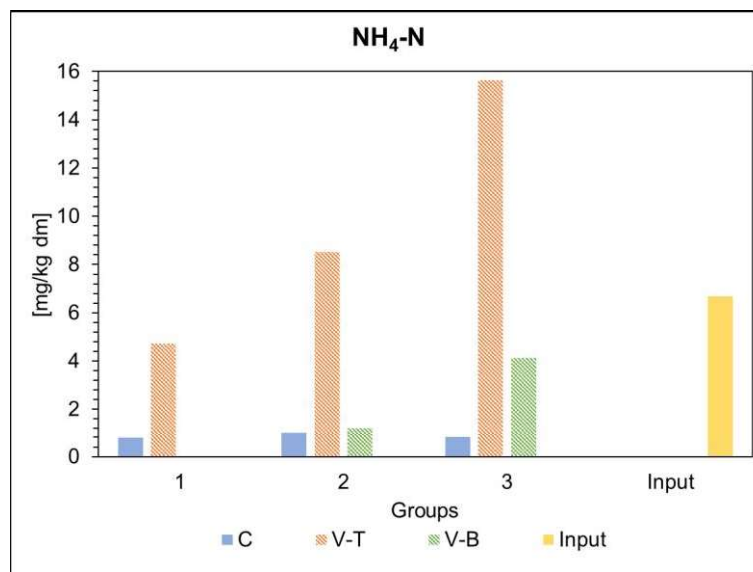


Figure 67:  $\text{NH}_4\text{-N}$  for compost reactors, vermicomposters (T+B) and input material for vermicomposters

The highest  $\text{NH}_4\text{-N}$  concentration was found with V3 at 15.7 mg/kg dm which was even higher than the value of the input material. The second highest concentration was measured for V2 with 8.5 mg/kg dm, and the lowest value was found in V1 with 4.7 mg/kg dm. These concentrations decreased during the degradation process as the bottom layer exhibited a lower concentration of  $\text{NH}_4\text{-N}$ . It was reduced in V1 to 100 %, in V2 to 86 %, and in V3 to 74 %.  $\text{NH}_4\text{-N}$  concentrations were probably higher in the top layer of the vermicomposters as the input material was placed on top of it. Through leaching, nitrification and denitrification processes the  $\text{NH}_4\text{-N}$  concentration may have



been reduced in the bottom layer. Leachate 2 exhibited a  $\text{NH}_4\text{-N}$  concentration of 37.1 mg/l, thus,  $\text{NH}_4\text{-N}$  has most probably precipitated. In contrast,  $\text{NO}_3\text{-N}$  concentration was only 3.1 mg/l.

Concentrations for  $\text{NO}_3\text{-N}$  were comparable in the composts, with C1 containing 3.8 mg/kg dm, C2 4.4 mg/kg dm, and C3 7.3 mg/kg dm. In vermicompost  $\text{NO}_3\text{-N}$  was not detectable in V3 and the top layer of V2. Highest concentrations were found in V1 with 8.8 mg/kg dm in the top layer and 0.6 mg/l in the bottom layer. 2.3 mg/kg dm were found in the bottom layer of V2 as shown in Figure 68. Aira and Domínguez (2009) reported the loss of ammonium through nitrification processes in the earthworm cast and denitrification processes in the anaerobic earthworm gut. This might explain why less ammonium and more nitrate was found in V1's top layer compared to the other experimental groups. V1 experienced a growth in the earthworm population during the experiment. Therefore, earthworms processed more organic matter and excreted more cast. This phenomenon might have enhanced nitrification processes which led to a higher  $\text{NO}_3\text{-N}$  concentration in the top layer. In line with these results, the earthworm population in V3 and V2 were lower and, hence, nitrification might have been reduced in the top layer compared to V1.

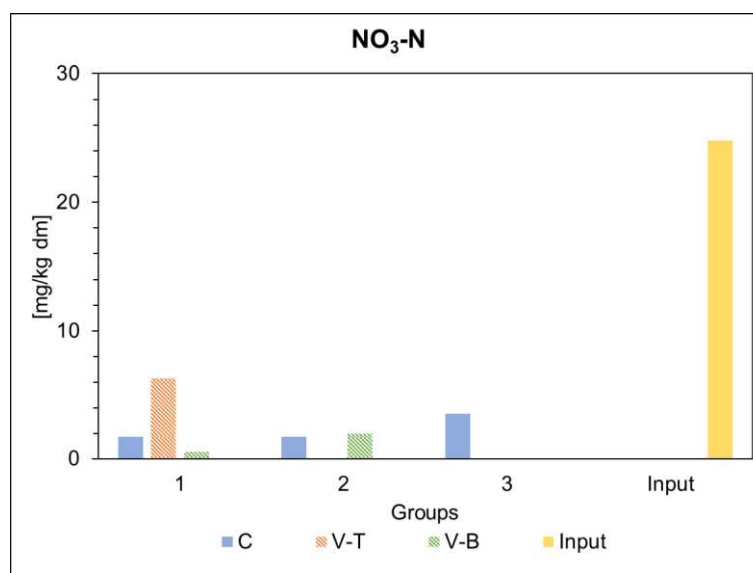


Figure 68:  $\text{NO}_3\text{-N}$  for compost reactors, vermicomposters (T+B) and input material for vermicomposters

The initial input material that was added to every compost reactor presented a  $\text{RA}_4$  of 114.3 mg  $\text{O}_2/\text{g dm}$  as can be seen in Figure 69. This suggests a high  $\text{O}_2$  consumption and, hence, a low stability and high reactivity of the material.

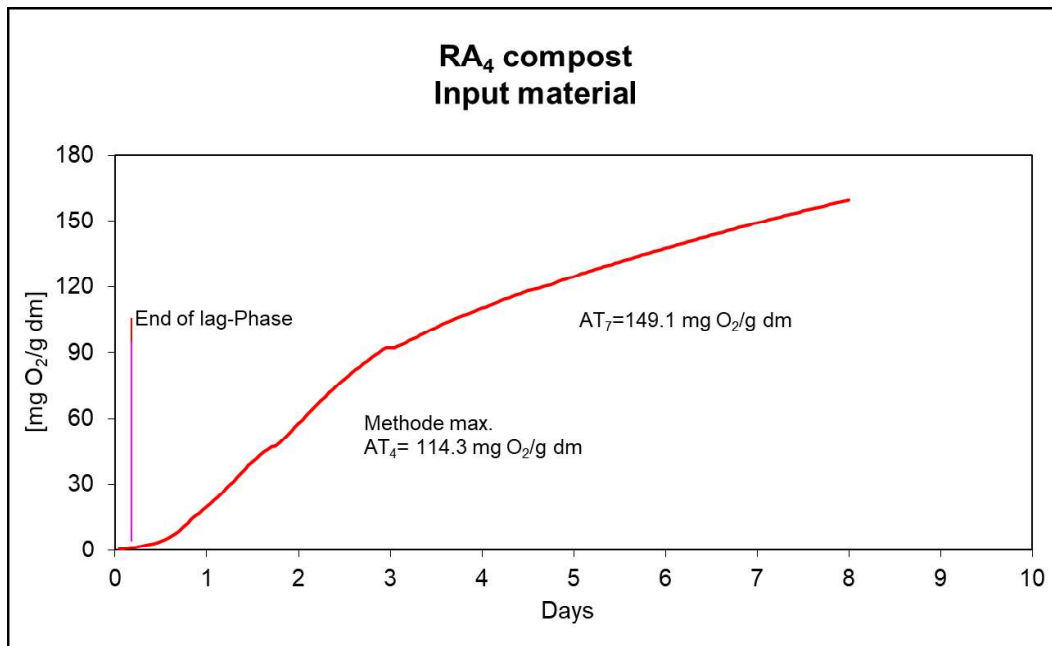


Figure 69: RA<sub>4</sub> for the input material of the composting experiment

In contrast to the input material, C1, C2, and C3 had a relatively low RA<sub>4</sub> as shown in Figure 70. It accounted for 5.3 mg O<sub>2</sub>/g dm, 4.4 mg O<sub>2</sub>/g dm, and 4.6 mg O<sub>2</sub>/g dm respectively. The results clearly show that the compost was stable and mature. RA<sub>4</sub> was slightly lower in C2 and C3 compared to C1, which shows that the plastic particles do not have an impact on maturity and stabilisation of the compost

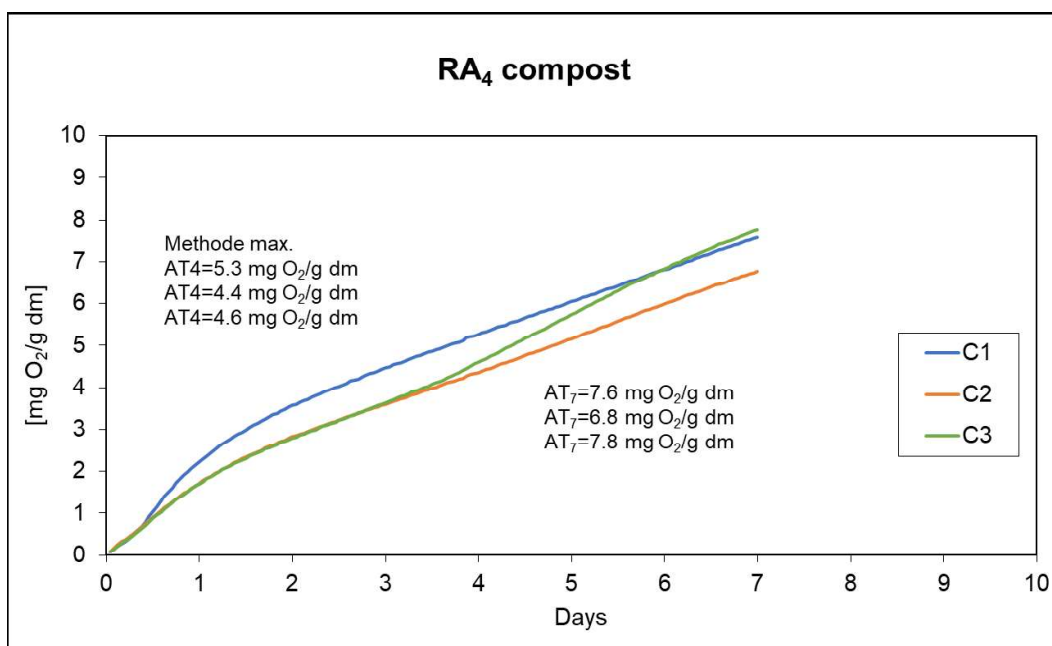


Figure 70: RA<sub>4</sub> for C1- Composting without foils, C2- Composting with LD-PE foils and C3- Composting with TPS-PBAT foils at the end of the experiment

With vermicomposting RA<sub>4</sub> was higher in the top layer compared to the bottom layer as seen in Figure 71 and Figure 72. It was 31.8 mg O<sub>2</sub>/g dm for V1, 50.7 mg O<sub>2</sub>/g dm for V2, and 38.7 mg O<sub>2</sub>/g dm for V3 in the top layers. As expected, the vermicompost of the top layer was still more reactive than of the bottom layer since the input material was always put on top of it. Of note, V2 presented the highest RA<sub>4</sub> as it was supplied with input material only three days before the ending of the experiment.

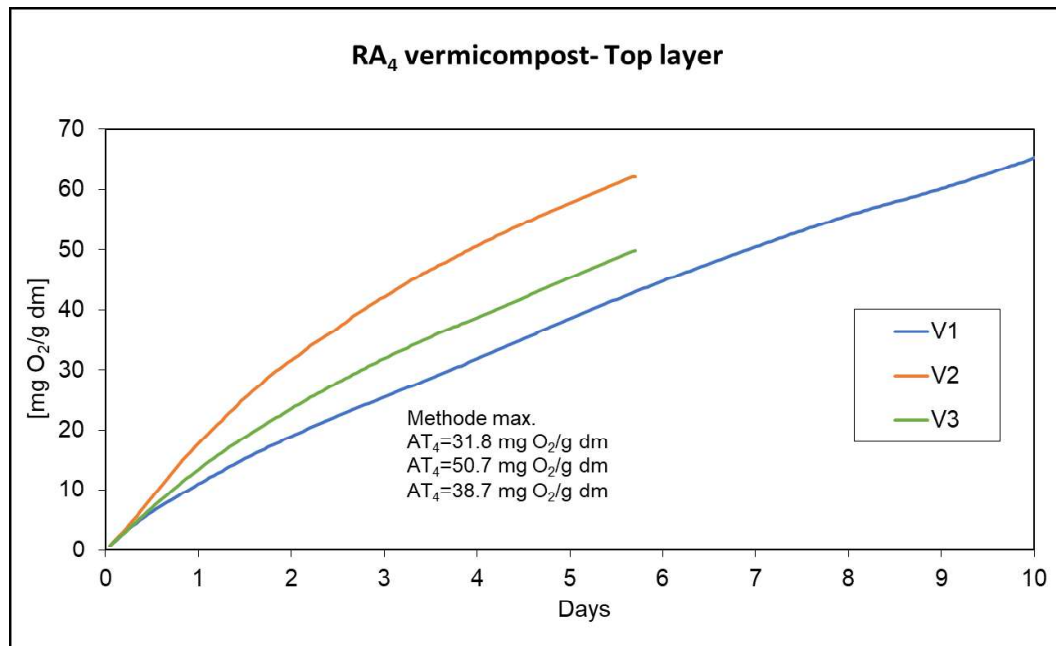


Figure 71: RA<sub>4</sub> for the top layer of V1- Vermicomposting without foils, V2- Vermicomposting with LD-PE foils and V3- Vermicomposting with TPS-PBAT foils at the end of the experiment

At the end of the experiment RA<sub>4</sub> was 13.8 mg O<sub>2</sub>/g dm for V1, 20.5 mg O<sub>2</sub>/g dm for V2, and 11.8 mg O<sub>2</sub>/g dm for V3. These values are higher than the values of the composting experiment. This is due to the fact that input material was supplied periodically, and leachate evolved. Thus, the vermicompost in the bottom layer were slightly more reactive.

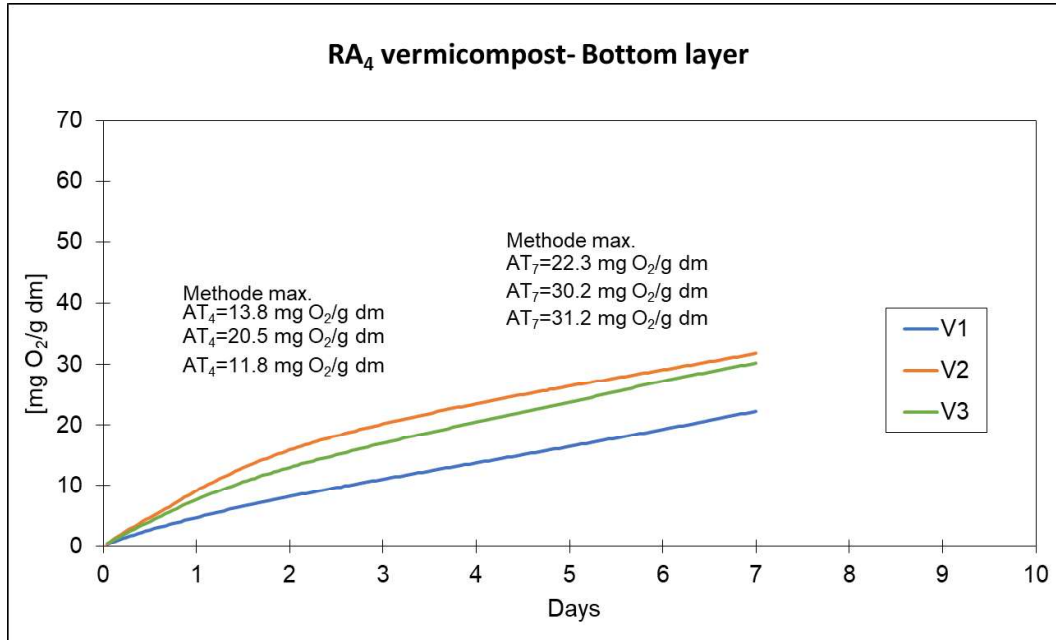


Figure 72: RA<sub>4</sub> for the bottom layer of V1- Vermicomposting without foils, V2- Vermicomposting with LD-PE foils and V3- Vermicomposting with TPS-PBAT foils at the end of the experiment

## 5 Conclusion and outlook

As expected, the LD-PE bags did not degrade during composting or vermicomposting. Many LD-PE particles were retrieved from the compost and vermicompost samples after wet sieving and their ratio to dry mass even increased since the mass of compost and vermicompost decreased at the same time. Most LD-PE particles in C3 were larger than 6.3 mm. In the top layer of V3 they were mostly sized 6.3 - 2 mm, and none were found in the bottom layer. Most probably LD-PE will not degrade, even not after more than 4 months. However, compost and vermicompost need four months to mature and to be applicable to horticulture and agriculture. Thus, LD-PE bags need to be removed from the biogenic waste stream before composting, as already practised by the municipal waste management company MA48 in Vienna.

On the other hand, the TPS-PBAT bags, which are commercially available under the name Mater-Bi®, disintegrated to 99.93 % during composting within 124 days as only 21 particles/kg dm sized 2 - 0.63 mm were found. This complies with the regulations of EN 13432. TPS-PBAT did not disintegrate during vermicomposting, despite partial biodegradation shown by ATR-FTIR analysis. The starch parts were most susceptible to microbial degradation. First, TPS was degraded as it is easily available for microorganisms. Characteristic indicator bands assigned to PBAT rarely decreased, although some particles saw a decrease in ester compounds. Furthermore, TPS- PBAT particles found in the top layer were mostly 6.3 - 2 mm, whereas they were 2 - 0.63 mm in the bottom layer of V3. The vermicompost of the bottom layer proved an advanced degradation of organic matter and, hence, TPS-PBAT particles in the bottom layer of V3 showed a more pronounced decrease in TPS compared to the top layer of V3. Also, the smallest plastic particle fraction can adhere to the earthworm body and can be transported to deeper layers.

These results prove that TPS-PBAT undergoes partial biodegradation during vermicomposting, but to a lesser extent than during (technical) composting within more than 124 days. Heat, and the composition of the microbial community are likely to play a major role in the degradation of TPS-PBAT. Hence, in practise TPS-PBAT bags should only be used to support pre-collection of biogenic waste for technical composting. However, it is difficult to separate it from non-biodegradable bags, such as LD-PE, in the sorting process of a composting plant. As a consequence, waste management systems should urge their customers – if they do not want to use multi-use-systems- to collect biogenic waste in biodegradable plastic bags.

In the case of vermicomposting, it is not recommended to add TPS-PBAT bags, since they require more than 120 days for their degradation. Furthermore, both TPS-PBAT and LD-PE content correlated with a decrease in earthworm biomass. Addition of plastics might have caused growth inhibition or may be lethal to earthworms. Although some scientists have already conducted studies on the impact of microplastics on earthworms, literature is scarce, particularly on the influence of biodegradable plastics. More studies need to focus on the influence of microplastics on earthworms. These studies are not only relevant to vermicomposting, but also to soil ecosystems in general.

The earthworm population might have had a direct influence on  $\text{NH}_4\text{-N}$  and  $\text{NO}_3\text{-N}$  concentrations in vermicompost since they most probably enhance the nitrification cycle by reinforcing nitrifying microorganisms in their cast and by aerating the vermibed.  $\text{NH}_4\text{-N}$  decreased most in V1's and least in V3's top layer, whereas  $\text{NO}_3\text{-N}$

was highest in V1 and least in V3. This trend might be attributed to the number of earthworms that were found at the end of the experiment. Earthworm population declined in V2 and V3, whereas it increased in V1. Therefore, the enhancement of the nitrification cycle by earthworms was less pronounced in V3 than in V1. This example shows the crucial role of earthworms in the degradation process.

Also, the compost reactors saw a loss in total nitrogen. It most probably did not decline due to leachate, as the leachate was added again to the compost. This was rather an effect of nitrogen volatilization since a scent of ammonia was noticeable at turning events. Conditions were favourable for loss of nitrogen as C/N ratio of the biogenic waste was narrow and pH turned alkaline from the first 8 days onwards.

Earthworms can accumulate heavy metals in their tissue and xenobiotic metals are excreted slowly or not at all. Furthermore, they possess physiological control over uptake and secretion of essential metals. However, heavy metal analysis revealed that earthworms must have excreted Zn and Hg in this vermicomposting experiment. They were most likely exposed to higher levels of Hg and Zn before they were placed in the vermicomposters and then egested Hg and Zn over the course of the experiment. Nevertheless, no samples of the vermibed, where they were stored before, nor of the final vermicompost were tested for heavy metals.

Comparing the rotting and compost quality parameters between composting and vermicomposting, some differences are evident. Rotting parameters were optimal in both experiments which ensured that the results of this thesis are eligible. Water content stayed approximately the same during composting, as water was supplied whenever necessary, whereas water content decreased between 10 and 11 % from the top to the bottom layer during vermicomposting. Water could leak from the vermicomposters when water holding capacity was exceeded. This water was then collected as leachate and it probably caused the precipitation of several soluble salts and nitrogen, inter alia in form of  $\text{NH}_4\text{-N}$ . Therefore, leachate of the vermicompost contained many plant nutrients, but also salts. Also, phosphor and potassium were found to be high. However, it should only be applied in dilution as it is too concentrated for direct application. The composting experiment did not produce as much leachate as the vermicomposting experiment probably due to higher prevailing temperatures.

TPS-PBAT particles had different influences on the hydrologic balance in compost and vermicompost. They incorporated water due to their hydrophilic characteristics. Hence, less leachate evolved in V3 compared to V1, yet, water content was not negatively impacted. Moreover, in C3 water content was highest and more condensate evolved in comparison to the other experimental groups due to the higher water holding capacity of TPS-PBAT. Furthermore, both C3 and V3 showed the lowest pH among the experimental groups.

EC was higher in all three experimental groups of the vermicomposting experiment compared to the composting experiment which can cause damage to plants. Total nitrogen was almost the same for both experiments, in contrast TOC and LOI were lower in the vermicomposts than in the composts because of the addition of structure rich material to the feedstock mixture for composting. In contrast, the amount of FA was significantly higher in vermicompost compared to compost. The present microbial composition or gut associated processes in earthworms must have generated a higher rate of FA during vermicomposting.  $\text{RA}_4$  was higher in the bottom layer of vermicompost and was more reactive than compost. Vermicomposters were periodically supplied with fresh input material and, therefore, showed a higher

reactiveness. The ATR-FTIR analysis further exhibited that vermicompost contained more aromatic compounds and alkenes, carbonates and lignocellulosic materials. The carbonates most likely originated from the addition of rock flour and lime to the vermicomposters.

In summary, plastic particles extensively impacted vermicomposting as they caused a decline in the earthworm population, which is an essential driver for vermicomposting. Nevertheless, rotting parameters and compost quality did not seem to have been negatively influenced by this development, except for  $\text{NO}_3\text{-N}$  and  $\text{NH}_4\text{-N}$  levels. The microbial community most likely compensated for the lack in earthworms. A tipping point, where earthworms are not able to control or suppress microbial composition was not reached, since temperatures did not rise above 25 °C like during composting. Nevertheless, this scenario seems to be plausible in case of microplastic addition.

## Bibliography

- Abbadie, L. (2003). *The priming effect of organic matter: a question of microbial competition ?* 35, 837–843. [https://doi.org/10.1016/S0038-0717\(03\)00123-8](https://doi.org/10.1016/S0038-0717(03)00123-8)
- Adeosun, S. O., Usman, M. A., Akpan, E., & Dibia, W. I. (2014). Characterization of LDPE Reinforced with Calcium Carbonate—Fly Ash Hybrid Filler. *Journal of Minerals and Materials Characterization and Engineering*, 2, 334–345. <https://doi.org/10.4236/jmmce.2014.24038>
- Aira, M., & Domínguez, J. (2009). *Microbial and nutrient stabilization of two animal manures after the transit through the gut of the earthworm Eisenia fetida ( Savigny , 1826 )*. 161, 1234–1238. <https://doi.org/10.1016/j.jhazmat.2008.04.073>
- Aira, M., Monroy, F., & Domínguez, J. (2009). *Changes in bacterial numbers and microbial activity of pig slurry during gut transit of epigeic and anecic earthworms*. 162, 1404–1407. <https://doi.org/10.1016/j.jhazmat.2008.06.031>
- Ali, U., Sajid, N., Khalid, A., Riaz, L., & Rabbani, M. (2015). A Review on Vermicomposting of Organic Wastes. *Environmental Progress & Sustainable Energy*, 34(4), 1050–1062. <https://doi.org/10.1002/ep12100>
- Amlinger, F., Peyr, S., Hildebrandt, U., Cuhls, C., & Clemens, J. (2005). *Stand der Technik der Kompostierung; Richtlinie des Bundesministeriums für Land- und Forstwirtschaft, Umwelt und Wasserwirtschaft*.
- Anastasi, A., Varese, G. C., & Filipello Marchisio, V. (2005). Isolation and identification of fungal communities in compost and vermicompost . In *Mycologia* (Vol. 97, Issue 1, pp. 33–44). Taylor & Francis . <https://doi.org/10.1080/15572536.2006.11832836>
- Arancon, N. Q., Edwards, C. A., Webster, K. A., & Buckerfield, J. C. (2011). The potential of vermicomposts as plant growth media for greenhouse crop production. In C. A. Edwards, N. Q. Arancon, & R. Sherman (Eds.), *Vermiculture technology: earthworms, organic wastes, and environmental management* (pp. 103–128). CRC Press.
- Arancon, N. Q., Galvis, P. A., & Edwards, C. A. (2005). Suppression of insect pest populations and damage to plants by vermicomposts . In *Bioresource Technology* (Vol. 96, Issue 10, pp. 1137–1142). Elsevier Ltd . <https://doi.org/10.1016/j.biortech.2004.10.004>
- Aspray, T. J., Dimambro, M. E., Wallace, P., Howell, G., & Frederickson, J. (2015). Static, dynamic and inoculum augmented respiration based test assessment for determining in-vessel compost stability. *Waste Management*, 42, 3–9. <https://doi.org/10.1016/j.wasman.2015.04.027>
- Barragán, H., M Pelacho, A., & Martín-Closas, L. (2016). Degradation of agricultural biodegradable plastics in the soil under laboratory conditions. *Soil Research*, 54. <https://doi.org/10.1071/SR15034>
- Barrena, R., Font, X., Gabarrell, X., & Sánchez, A. (2014). Home composting versus industrial composting: Influence of composting system on compost quality with focus on compost stability . In *Waste Management* (Vol. 34, Issue 7, pp. 1109–1116). Elsevier Ltd . <https://doi.org/10.1016/j.wasman.2014.02.008>
- Beck-Friis, B., Smårs, S., Jönsson, H., & Kirchmann, H. (2001). Gaseous emissions of

- carbon dioxide, ammonia and nitrous oxide from organic household waste in a compost reactor under different temperature regimes . In *Journal of Agricultural and Engineering Research* (Vol. 78, Issue 4, pp. 423–430). ACADEMIC PRESS LTD . <https://doi.org/10.1006/jaer.2000.0662>
- Binner, E., Smidt, E., Tintner, J., Böhm, K., & Lechner, P. (2011). How to enhance humification during composting of separately collected biowaste: impact of feedstock and processing. *Waste Management & Research*, 29(11), 1153–1163.
- Blouin, M., Barrere, J., Meyer, N., Lartigue, S., Barot, S., & Mathieu, J. (2019). Vermicompost significantly affects plant growth. A meta-analysis . In *Agronomy for Sustainable Development* (Vol. 39, Issue 4, pp. 1–15). Springer Paris . <https://doi.org/10.1007/s13593-019-0579-x>
- Böhm, R. (2007). Pathogenic agents. In Luis F Diaz (Ed.), *Compost science and technology* (1., Vol. 8, pp. 177–200). Elsevier.
- Bouché, M. B. (1977). Strategies lombriciennes. *Ecological Bulletins*, 25, 122–132.
- Brandelero, R. P. H., Grossmann, M. V. E., & Yamashita, F. (2011). Effect of the method of production of the blends on mechanical and structural properties of biodegradable starch films produced by blown extrusion . In *Carbohydrate Polymers* (Vol. 86, Issue 3, pp. 1344–1350). Elsevier Ltd . <https://doi.org/10.1016/j.carbpol.2011.06.045>
- Brandsch, J., & Piringer, O. (2008). Characteristics of plastic packaging. In O. G. Piringer & A. L. Baner (Eds.), *Plastic packaging: interactions with food and pharmaceuticals* (2., compl., pp. 15–60). Wiley-VCH Verl.
- Brown, K., Ghoshdastidar, A. J., Hanmore, J., Frazee, J., & Tong, A. Z. (2013). Membrane bioreactor technology: A novel approach to the treatment of compost leachate . In *Waste Management* (Vol. 33, Issue 11, pp. 2188–2194). Elsevier Ltd . <https://doi.org/10.1016/j.wasman.2013.04.006>
- Butt, K. R., & Lowe, C. N. (2010). Controlled Cultivation of Endogeic and Anecic Earthworms. In *Biology of earthworms* (pp. 107–121). [https://doi.org/10.1007/978-3-642-14636-7\\_10](https://doi.org/10.1007/978-3-642-14636-7_10)
- Cai, L., Gong, X., Id, X. S., Li, S., & Yu, X. (2018). *Comparison of chemical and microbiological changes during the aerobic composting and vermicomposting of green waste*. 1–17. <https://doi.org/10.1371/journal.pone.0207494>
- Cao, D., Wang, X., Luo, X., Liu, G., & Zheng, H. (2017). Effects of polystyrene microplastics on the fitness of earthworms in an agricultural soil. *IOP Conference Series: Earth and Environmental Science*, 61(1), 6–10. <https://doi.org/10.1088/1755-1315/61/1/012148>
- Castillo, J. M., Romero, E., & Nogales, R. (2013). Dynamics of microbial communities related to biochemical parameters during vermicomposting and maturation of agroindustrial lignocellulose wastes. *Bioresource Technology*, 146, 345–354. <https://doi.org/10.1016/j.biortech.2013.07.093>
- Chinaglia, S., Tosin, M., & Degli-innocenti, F. (2018). Biodegradation rate of biodegradable plastics at molecular level. *Polymer Degradation and Stability*, 147(December 2017), 237–244. <https://doi.org/10.1016/j.polymdegradstab.2017.12.011>
- Ciavatta, C., Govi, M., Simoni, A., & Sequi, P. (1993). Evaluation of heavy metals



- during stabilization of organic matter in compost produced with municipal solid wastes . In *Bioresource Technology* (Vol. 43, Issue 2, pp. 147–153). Elsevier Ltd . [https://doi.org/10.1016/0960-8524\(93\)90174-A](https://doi.org/10.1016/0960-8524(93)90174-A)
- Colthup, N. B., Daly, L. H., & Wiberley, S. E. (1975). *Introduction to infrared and raman spectroscopy* (2.). Acad. Press .
- Cosin, D. J. D., Novo, M., & Fernández, R. (2010). Reproduction of Earthworms: Sexual Selection and Parthenogenesis. In *Biology of Earthworms* (pp. 69–86). [https://doi.org/10.1007/978-3-642-14636-7\\_5](https://doi.org/10.1007/978-3-642-14636-7_5)
- Curry, J. P., & Schmidt, O. (2007). The feeding ecology of earthworms - A review. *Pedobiologia*, 50(6), 463–477. <https://doi.org/10.1016/j.pedobi.2006.09.001>
- De Bertoldi, M., Vallini, G., & Pera, A. (1983). The biology of composting: A review. *Waste Management & Research*, 1, 157–176. [https://doi.org/10.1016/0734-242X\(83\)90055-1](https://doi.org/10.1016/0734-242X(83)90055-1)
- Diaz, L.F. (2007). Introduction. In L.F Diaz, M. De Bertoldi, W. Bidlingmaier, & E. Stentiford (Eds.), *Compost Science and Technology: Waste management series* (1st ed., pp. 1–5). Elsevier Science.
- Domínguez, J. (2011). The microbiology of vermicomposting. In C. A. Edwards, N. Q. Arancon, & R. Sherman (Eds.), *Vermiculture technology: earthworms, organic wastes, and environmental management* (pp. 53–66). CRC Press.
- Dominguez, J., Aira, M., Kolbe, A. R., Gomez-Brandon, M., & Perez-Losadaz, M. (2019). Changes in the composition and function of bacterial communities during vermicomposting may explain beneficial properties of vermicompost . In *SCIENTIFIC REPORTS* (Vol. 9, Issue 1, pp. 9611–9657). NATURE PUBLISHING GROUP . <https://doi.org/10.1038/s41598-019-46018-w>
- Domínguez, J., & Edwards, C. A. (2011a). Biology and ecology of earthworm species used for vermicomposting. In C. A. Edwards, N. Q. Arancon, & R. Sherman (Eds.), *Vermiculture technology: earthworms, organic wastes, and environmental management* (pp. 27–40). CRC Press.
- Domínguez, J., & Edwards, C. A. (2011b). Relationships between Composting and Vermicomposting. In C. A. Edwards, N. Q. Arancon, & R. Sherman (Eds.), *Vermiculture technology: earthworms, organic wastes, and environmental management* (pp. 11–25). CRC Press. <https://doi.org/10.1201/b10453-3>
- Egle, L., Rolland, C., & Broukal, S. (2017). *Strategische Umweltprüfung zum Wiener Abfallwirtschaftsplan (Wr. AWP) 2019-2024 und zum Wiener Abfallvermeidungsprogramm (Wr. AVP) 2019-2024*.
- Elfehri Borchani, K., Carrot, C., & Jaziri, M. (2015). Biocomposites of Alfa fibers dispersed in the Mater-Bi® type bioplastic: Morphology, mechanical and thermal properties. *Composites Part A: Applied Science and Manufacturing*, 78, 371–379. <https://doi.org/10.1016/J.COMPOSITESA.2015.08.023>
- Endres, H.-J., & Siebert-Raths, A. (2009). *Technische Biopolymere Rahmenbedingungen, Marktsituation, Herstellung, Aufbau und Eigenschaften* (A. Siebert-Raths (ed.)). Hanser.
- European Parliament and Council Directive 94/62/EC of 20 December 1994 on packaging and packaging waste, Directive 94/62/EC (1994).*

- Evans, G. M., & Furlong, J. C. (2003). *Environmental biotechnology: theory and application*. Wiley.
- Garg, V. K., Suthar, S., & Yadav, A. (2012). Management of food industry waste employing vermicomposting technology. *Bioresource Technology*, 126, 437–443. <https://doi.org/10.1016/j.biortech.2011.11.116>
- Gerzabek, M. H., Danneberg, O., & Kandeler, E. (1993). Bestimmung des Humifizierungsgrades. In F. Schinner, R. Öhlinger, E. Kandeler, & R. Margesin (Eds.), *Bodenbiologische Arbeitsmethoden* (pp. 107–109). Springer.
- Gould, J. M., Gordon, G. H., Dexter, L. B., & Swanson, C. L. (1990). Biodegradation of starch-containing plastic. In J. E. Glass & G. Swift (Eds.), *Agricultural and synthetic polymers biodegradability and utilization* (pp. 66–75). American Chemical Society.
- Gu, W., Lu, Y., Tan, Z., Xu, P., Xie, K., Li, X., & Sun, L. (2017). Fungi diversity from different depths and times in chicken manure waste static aerobic composting. In *Bioresource Technology* (Vol. 239, pp. 447–453). Elsevier Ltd. <https://doi.org/10.1016/j.biortech.2017.04.047>
- Guerrero-Pérez, M. O., & Patience, G. S. (2020). Experimental methods in chemical engineering: Fourier transform infrared spectroscopy—FTIR. In *The Canadian Journal of Chemical Engineering* (Vol. 98, Issue 1, pp. 25–33). John Wiley & Sons, Inc. <https://doi.org/10.1002/cjce.23664>
- Gunadi, B., & Edwards, C. A. (2003). *The effects of multiple applications of different organic wastes on the growth, fecundity and survival of Eisenia fetida (Savigny) (Lumbricidae)*. 321–329.
- Hait, S., & Tare, V. (2011). Vermistabilization of primary sewage sludge. *Bioresource Technology*, 102(3), 2812–2820. <https://doi.org/10.1016/j.biortech.2010.10.031>
- Helmberger, M. S., Tiemann, L. K., Grieshop, M. J., & Morriën, E. (2020). Towards an ecology of soil microplastics. In *Functional Ecology* (Vol. 34, Issue 3, pp. 550–560). <https://doi.org/10.1111/1365-2435.13495>
- Hoshino, A., Sawada, H., Yokota, M., Tsuji, M., & Kimura, M. (2001). Influence of weather conditions and soil properties on degradation of biodegradable plastics in soil. *Soil Science and Plant Nutrition*, 47(1), 35–43. <https://doi.org/10.1080/00380768.2001.10408366>
- Huang, K., Li, F., Wei, Y., Chen, X., & Fu, X. (2013). Changes of bacterial and fungal community compositions during vermicomposting of vegetable wastes by *Eisenia foetida*. In *Bioresource Technology* (Vol. 150, pp. 235–241). Elsevier Ltd. <https://doi.org/10.1016/j.biortech.2013.10.006>
- Huerta Lwanga, E., Gertsen, H., Gooren, H., Peters, P., Salánki, T., Van Der Ploeg, M., Besseling, E., Koelmans, A. A., & Geissen, V. (2016). Microplastics in the Terrestrial Ecosystem: Implications for *Lumbricus terrestris* (Oligochaeta, Lumbricidae). *Environmental Science and Technology*, 50(5), 2685–2691. <https://doi.org/10.1021/acs.est.5b05478>
- Huerta Lwanga, E., Thapa, B., Yang, X., Gertsen, H., Salánki, T., Geissen, V., & Garbeva, P. (2018). Decay of low-density polyethylene by bacteria extracted from earthworm's guts: A potential for soil restoration. *Science of the Total Environment*, 624, 753–757. <https://doi.org/10.1016/j.scitotenv.2017.12.144>
- Insam, H., & De Beroldi, M. (2007). Compost science and technology. In L.F Diaz, M.

- De Bertoldi, W. Bidlingmaier, & E. Stentiford (Eds.), *Compost Science and Technology: Waste management* (1., Vol. 8, pp. 25–48). Elsevier.
- Insam, H., Franke-Whittle, I., & Goberna, M. (2010). Microbes in aerobic and anaerobic waste treatment. In H. Insam, F.-W. Ingrid, & M. Goberna (Eds.), *Microbes at work: from wastes to resources* (pp. 1–34). Springer.
- Iwata, T. (2015). *Biodegradable and Bio-Based Polymers : Future Prospects of Eco-Friendly Plastics*. 150, 3210–3215. <https://doi.org/10.1002/anie.201410770>
- Jurado, M., López, M. J., Suárez-Estrella, F., Vargas-García, M. C., López-González, J. A., & Moreno, J. (2014). Exploiting composting biodiversity: Study of the persistent and biotechnologically relevant microorganisms from lignocellulose-based composting . In *Bioresource Technology* (Vol. 162, pp. 283–293). Elsevier Ltd . <https://doi.org/10.1016/j.biortech.2014.03.145>
- Karamanlioglu, M., & Robson, G. D. (2013). The influence of biotic and abiotic factors on the rate of degradation of poly ( lactic ) acid ( PLA ) coupons buried in compost and soil. *Polymer Degradation and Stability*, 98(10), 2063–2071. <https://doi.org/10.1016/j.polymdegradstab.2013.07.004>
- Kaushik, P., & Garg, V. K. (2004). Dynamics of biological and chemical parameters during vermicomposting of solid textile mill sludge mixed with cow dung and agricultural residues. *Bioresource Technology*, 94(2), 203–209. <https://doi.org/10.1016/j.biortech.2003.10.033>
- Khater, E. S. G. (2015). Some Physical and Chemical Properties of Compost . In *International Journal of Waste Resources* (Vol. 5, Issue 1). <https://doi.org/10.4172/2252-5211.1000172>
- Kijchavengkul, T., Auras, R., & Rubino, M. (2008). Measuring gel content of aromatic polyesters using FTIR spectrophotometry and DSC . In *Polymer Testing* (Vol. 27, Issue 1, pp. 55–60). Elsevier Ltd . <https://doi.org/10.1016/j.polymertesting.2007.08.007>
- Kjeldahl, J. (1883). Neue Methode zur Bestimmung des Stickstoffs in organischen Körpern". *Zeitschrift Für Analytische Chemie*, 22(1), 366–383. <https://doi.org/10.1017/CBO9781107415324.004>
- Larsen, K. L., & McCartney, D. M. (2000). Effect of C:N Ratio on Microbial Activity and N Retention: Bench-scale Study Using Pulp and Paper Biosolids . In *Compost Science & Utilization* (Vol. 8, Issue 2, pp. 147–159). Taylor & Francis . <https://doi.org/10.1080/1065657X.2000.10701760>
- Lazcano, C., Gómez-brandón, M., & Domínguez, J. (2008). Comparison of the effectiveness of composting and vermicomposting for the biological stabilization of cattle manure. *Chemosphere*, 72, 1013–1019. <https://doi.org/10.1016/j.chemosphere.2008.04.016>
- Li, L., Wu, J., Tian, G., & Xu, Z. (2009). *Effect of the transit through the gut of earthworm ( Eisenia fetida ) on fractionation of Cu and Zn in pig manure*. 167, 634–640. <https://doi.org/10.1016/j.jhazmat.2009.01.013>
- Liu, F., Zhu, P., & Xue, J. (2012). Comparative Study on Physical and Chemical Characteristics of Sludge Vermicomposted by Eisenia Fetida . In *Procedia Environmental Sciences* (Vol. 16, pp. 418–423). Elsevier B.V . <https://doi.org/10.1016/j.proenv.2012.10.058>

- Lleó, T., Albacete, E., Barrena, R., Font, X., Artola, A., & Sánchez, A. (2013). Home and vermicomposting as sustainable options for biowaste management. *Journal of Cleaner Production*, 47, 70–76. <https://doi.org/10.1016/j.jclepro.2012.08.011>
- Magistratsabteilung 48. (2019). *Sammlung von biogenem Abfall*. <https://www.wien.gv.at/umwelt/ma48/beratung/muelltrennung/biogener-abfall/sammlung.html>
- Maji, D., Misra, P., Singh, S., & Kalra, A. (2017). Humic acid rich vermicompost promotes plant growth by improving microbial community structure of soil as well as root nodulation and mycorrhizal colonization in the roots of *Pisum sativum*. *Applied Soil Ecology*, 110, 97–108. <https://doi.org/10.1016/j.apsoil.2016.10.008>
- Majlessi, M., Eslami, A., Najafi Saleh, H., Mirshafieean, S., & Babaii, S. (2012). Vermicomposting of food waste: Assessing the stability and maturity . In *Iranian Journal of Environmental Health Science and Engineering* (Vol. 9, Issue 25, pp. 1–6). BMC . <https://doi.org/10.1186/1735-2746-9-25>
- Makan, A., Assobhei, O., & Mountadar, M. (2013). Effect of initial moisture content on the in-vessel composting under air pressure of organic fraction of municipal solid waste in Morocco . In *Iranian Journal of Environmental Health Science and Engineering* (Vol. 10, Issue 3, p. 3). BIOMED CENTRAL LTD . <https://doi.org/10.1186/1735-2746-10-3>
- Mc Carthy, G., Lawlor, P. G., Coffey, L., Nolan, T., Gutierrez, M., & Gardiner, G. E. (2011). An assessment of pathogen removal during composting of the separated solid fraction of pig manure . In *Bioresource Technology* (Vol. 102, Issue 19, pp. 9059–9067). Elsevier Ltd . <https://doi.org/10.1016/j.biortech.2011.07.021>
- Millner, P., Ingram, D., Mulbry, W., & Arikan, O. A. (2014). Pathogen reduction in minimally managed composting of bovine manure . In *Waste Management* (Vol. 34, Issue 11, pp. 1992–1999). Elsevier Ltd . <https://doi.org/10.1016/j.wasman.2014.07.021>
- Monroy, F., Aira, M., & Domínguez, J. (2009). Reduction of total coliform numbers during vermicomposting is caused by short-term direct effects of earthworms on microorganisms and depends on the dose of application of pig slurry. *Science of the Total Environment*, 407(20), 5411–5416. <https://doi.org/10.1016/j.scitotenv.2009.06.048>
- Morgan, J. E., & Morgan, A. J. (1999). *The accumulation of metals ( Cd , Cu , Pb , Zn and Ca ) by two ecologically contrasting earthworm species ( Lumbricus rubellus and Aporrectodea caliginosa ) : implications for ecotoxicological testing*. 13.
- Mu, J., Li, H., Li, X., Jiao, J., Ji, G., Wu, J., & Hu, F. (2017). Biocontrol potential of vermicompost through antifungal volatiles produced by indigenous bacteria . In *Biological Control* (Vol. 112, pp. 49–54). Elsevier Inc . <https://doi.org/10.1016/j.biocontrol.2017.05.013>
- Ndegwa, P. M., & Thompson, S. A. (2001). Integrating composting and vermicomposting in the treatment and bioconversion of biosolids. *Bioresource Technology*. [https://doi.org/10.1016/S0960-8524\(00\)00104-8](https://doi.org/10.1016/S0960-8524(00)00104-8)
- Negi, R., & Suthar, S. (2013). Vermistabilization of paper mill wastewater sludge using *Eisenia fetida*. *BIORESOURCETECHNOLOGY*, 128, 193–198. <https://doi.org/10.1016/j.biortech.2012.10.022>

- Niyazi, R., & Chaurasia, S. (2014). *Vermiremoval of heavy metals from fly ash by employing earthworm Eisenia foetida*. 6(1), 1–8.
- Novamont S.p.A. (2015). *Biodegradability and compostability*. [http://materbi.com/en/about/biodegradability-and-compostability/?noredirect=en\\_US](http://materbi.com/en/about/biodegradability-and-compostability/?noredirect=en_US)
- Oliveira Gama, R., Bretas, R. E. S., & Oréface, R. L. (2018). Control of the Hydrophilic/Hydrophobic Behavior of Biodegradable Natural Polymers by Decorating Surfaces with Nano- and Micro-Components . In *Advances in Polymer Technology* (Vol. 37, Issue 3, pp. 654–661). Wiley Subscription Services, Inc . <https://doi.org/10.1002/adv.21706>
- ÖNORM EN 13432. (2008). *Packaging-Requirements for packaging recoverable through composting and biodegradation – Test scheme and evaluation criteria for the final acceptance of packaging* (ÖNORM EN 13432: 2008 02 01).
- ÖNORM EN ISO 11885. (2009). *Wasserbeschaffenheit - Bestimmung von ausgewählten Elementen durch induktiv gekoppelte Plasma-Atom-Emissionsspektrometrie (ICP-OES)* (ÖNORM EN ISO 11885:2009 11 01).
- ÖNORM S 2027-4. (2012). *Beurteilung von Abfällen aus der mechanisch-biologischen Behandlung-Teil 4: Stabilitätsparameter- Atmungsaktivität (AT4)* (ÖNORM S 2027-1:2002-07).
- Palaniyandi, S. A., Yang, S. H., Zhang, L., & Suh, J.-W. (2013). Effects of actinobacteria on plant disease suppression and growth promotion . In *Applied Microbiology and Biotechnology* (Vol. 97, Issue 22, pp. 9621–9636). Springer Berlin Heidelberg . <https://doi.org/10.1007/s00253-013-5206-1>
- Pirsaheb, M., Khosravi, T., & Sharafi, K. (2013). *Domestic scale vermicomposting for solid waste management*. 1–5.
- Raaijmakers, J. M., & Mazzola, M. (2012). Diversity and Natural Functions of Antibiotics Produced by Beneficial and Plant Pathogenic Bacteria. *Annu. Rev. Phytopathol.*, 50, 424. <https://doi.org/10.1146/annurev-phyto-081211-172908>
- Rajandas, H., Parimannan, S., Sathasivam, K., Ravichandran, M., & Su Yin, L. (2012). A novel FTIR-ATR spectroscopy based technique for the estimation of low-density polyethylene biodegradation . In *Polymer Testing* (Vol. 31, Issue 8, pp. 1094–1099). Elsevier Ltd . <https://doi.org/10.1016/j.polymertesting.2012.07.015>
- Rillig, M. C., Ziersch, L., & Hempel, S. (2017). Microplastic transport in soil by earthworms . In *Scientific Reports* (Vol. 7, Issue 1, pp. 1362–1366). NATURE PUBLISHING GROUP . <https://doi.org/10.1038/s41598-017-01594-7>
- Rodríguez-Seijo, A., da Costa, J. P., Rocha-Santos, T., Duarte, A. C., & Pereira, R. (2018). Oxidative stress, energy metabolism and molecular responses of earthworms (*Eisenia fetida*) exposed to low-density polyethylene microplastics. *Environmental Science and Pollution Research*, 25(33), 33599–33610. <https://doi.org/10.1007/s11356-018-3317-z>
- Rodríguez-Seijo, A., Lourenço, J., Rocha-Santos, T. A. P., da Costa, J., Duarte, A. C., Vala, H., & Pereira, R. (2017). Histopathological and molecular effects of microplastics in *Eisenia andrei* Bouché. *Environmental Pollution*, 220, 495–503. <https://doi.org/10.1016/j.envpol.2016.09.092>
- Romero, C., Ramos, P., Costa, C., & Márquez, M. C. (2013). Raw and digested

- municipal waste compost leachate as potential fertilizer: comparison with a commercial fertilizer . In *Journal of Cleaner Production* (Vol. 59, pp. 73–78). Elsevier Ltd . <https://doi.org/10.1016/j.jclepro.2013.06.044>
- Rudnik, E. (2008). *Compostable polymer materials* (1.). Elsevier .
- Salter, C. E., & Edwards, C. A. (2011). The production of vermicompost aqueous solutions or teas. In C. A. Edwards, N. Q. Arancon, & R. Sherman (Eds.), *Vermiculture technology: earthworms, organic wastes, and environmental management* (pp. 153–164). CRC Press.
- Shah, A. A., Hasan, F., Hameed, A., & Ahmed, S. (2008). *Biological degradation of plastics : A comprehensive review*. 26, 246–265. <https://doi.org/10.1016/j.biotechadv.2007.12.005>
- Sharabi, N. E. D., & Bartha, R. (1993). Testing of some assumptions about biodegradability in soil as measured by carbon dioxide evolution. *Applied and Environmental Microbiology*, 59(4), 1201–1205.
- Shirai, M., Olivato, J., Garcia, P., Müller, C., Grossmann, M., & Yamashita, F. (2013). Thermoplastic starch/polyester films: Effects of extrusion process and poly (lactic acid) addition. *Materials Science & Engineering. C, Materials for Biological Applications*, 33, 4112–4117. <https://doi.org/10.1016/j.msec.2013.05.054>
- Singh, A., Singh, D. P., Tiwari, R., Kumar, K., Vir, R., Singh, S., Prasanna, R., Saxena, A. K., & Nain, L. (2015). Taxonomic and functional annotation of gut bacterial communities of *Eisenia foetida* and *Perionyx excavatus*. *Microbiological Research*, 175, 48–56. <https://doi.org/10.1016/j.micres.2015.03.003>
- Singh, R. P., Singh, P., Araujo, A. S. F., Ibrahim, M. H., & Sulaiman, O. (2011). Management of urban solid waste : Vermicomposting a sustainable option. 'Resources, Conservation & Recycling', 55(7), 719–729. <https://doi.org/10.1016/j.resconrec.2011.02.005>
- Sinha, R. K. (2011). *Earthworms - the waste managers : : their role in sustainable waste management converting waste into resource while reducing greenhouse gases*. Nova Science Publishers, Inc.,.
- Sinha, R. K., Herat, S., Bharambe, G., & Brahmabhatt, A. (2010). *Vermistabilization of sewage sludge ( biosolids ) by earthworms : converting a potential biohazard destined for landfill disposal into a pathogen-free , nutritive and safe biofertilizer for farms*. March 2009, 872–881. <https://doi.org/10.1177/0734242X09342147>
- Sintim, H. Y., Bary, A. I., Hayes, D. G., English, M. E., Schaeffer, S. M., Miles, C. A., Zelenyuk, A., Suski, K., & Flury, M. (2019). Release of micro- and nanoparticles from biodegradable plastic during in situ composting . In *Science of the Total Environment* (Vol. 675, pp. 686–693). Elsevier B.V . <https://doi.org/10.1016/j.scitotenv.2019.04.179>
- Smidt, E., & Schwanninger, M. (2005). Characterization of waste materials using FTIR spectroscopy: Process monitoring and quality assessment. *Spectroscopy Letters*, 38(3), 247–270. <https://doi.org/10.1081/SL-200042310>
- Sundberg, C., & Jönsson, H. (2008). Higher pH and faster decomposition in biowaste composting by increased aeration . In *Waste Management* (Vol. 28, Issue 3, pp. 518–526). Elsevier Ltd . <https://doi.org/10.1016/j.wasman.2007.01.011>
- Suthar, S., & Gairola, S. (2014). Nutrient recovery from urban forest leaf litter waste

- solids using *Eisenia fetida*. *Ecological Engineering*, 71, 660–666. <https://doi.org/10.1016/j.ecoleng.2014.08.010>
- Swati, A., & Hait, S. (2017a). A Comprehensive Review of the Fate of Pathogens during Vermicomposting of Organic Wastes. *Journal of Environment Quality*, 47(1), 16. <https://doi.org/10.2134/jeq2017.07.0265>
- Swati, A., & Hait, S. (2017b). Fate and bioavailability of heavy metals during vermicomposting of various organic wastes — A review. *Process Safety and Environmental Protection*, 109, 30–45. <https://doi.org/10.1016/j.psep.2017.03.031>
- Tang, J.-C., Shibata, A., Zhou, Q., & Katayama, A. (2007). Effect of temperature on reaction rate and microbial community in composting of cattle manure with rice straw . In *Journal of Bioscience and Bioengineering* (Vol. 104, Issue 4, pp. 321–328). Elsevier B.V . <https://doi.org/10.1263/jbb.104.321>
- Tokiwa, Y., & Calabia, B. P. (2004). Degradation of microbial polyesters. *Biotechnology Letters*, 26(15), 1181–1189. <https://doi.org/10.1023/B:BILE.0000036599.15302.e5>
- Tripetchkul, S., Pundee, K., Koonsrisuk, S., & Akeprathumchai, S. (2012). Co-composting of coir pith and cow manure: initial C/N ratio vs physico-chemical changes . In *International Journal of Recycling of Organic Waste in Agriculture* (Vol. 1, Issue 1, pp. 1–8). Springer-Verlag . <https://doi.org/10.1186/2251-7715-1-15>
- TÜV AUSTRIA HOLDING AG. (2020). *Certifications*. <http://www.tuv-at.be/green-marks/certifications/ok-compost-seedling/?amp=>
- Vargas-García, M. C., Suárez-Estrella, F., López, M. J., & Moreno, J. (2010). Microbial population dynamics and enzyme activities in composting processes with different starting materials . In *Waste Management* (Vol. 30, Issue 5, pp. 771–778). Elsevier Ltd . <https://doi.org/10.1016/j.wasman.2009.12.019>
- Verordnung des Bundesministers für Land- und Forstwirtschaft, Umwelt und Wasserwirtschaft über Qualitätsanforderungen an Komposte aus Abfällen (Kompostverordnung)*, BGBl. II Nr. 292/2001 (2001).
- Weithmann, N., Möller, J. N., Löder, M. G. J., Piehl, S., Laforsch, C., & Freitag, R. (2018). Organic fertilizer as a vehicle for the entry of microplastic into the environment. *Science Advances*, 4(4). <https://doi.org/10.1126/sciadv.aap8060>
- Wichuk, K. M., Tewari, J. P., & McCartney, D. (2011). Plant Pathogen Eradication During Composting: A Literature Review . In *Compost Science & Utilization* (Vol. 19, Issue 4, pp. 244–266). Taylor & Francis . <https://doi.org/10.1080/1065657X.2011.10737008>
- Wormsystems GmbH. (n.d.-a). *BETRIEBSANLEITUNG – FUNKTIONSWEISE*. Retrieved 7 March 2020, from <https://wurmkiste.at/richtig-kompostieren/>
- Wormsystems GmbH. (n.d.-b). *Richtig kompostieren in Wohnräumen mit der Wurmbox*. Retrieved 30 January 2020, from <https://wurmkiste.at/richtig-kompostieren/>
- Wu, Y., Shaaban, M., Zhao, J., Hao, R., & Hu, R. (2015). Effect of the earthworm gut-stimulated denitrifiers on soil nitrous oxide emissions. *European Journal of Soil Biology*, 70, 104–110. <https://doi.org/10.1016/j.ejsobi.2015.08.001>

- Xiao, Z., Liu, M., Jiang, L., Chen, X., Griffiths, B. S., Li, H., & Hu, F. (2016). Vermicompost increases defense against root-knot nematode (*Meloidogyne incognita*) in tomato plants . In *Applied Soil Ecology* (Vol. 105, pp. 177–186). Elsevier B.V . <https://doi.org/10.1016/j.apsoil.2016.04.003>
- Yaacob, N. D., Ismail, H., & Ting, S. S. (2016). Soil burial of polylactic acid/paddy straw powder biocomposite. In *BioResources* (Vol. 11, Issue 1, pp. 1255–1269). NORTH CAROLINA STATE UNIV DEPT WOOD & PAPER SCI. <https://doi.org/10.15376/biores.11.1.1255-1269>
- Zee, M. Van Der. (2014). Methods for Evaluating the Biodegradability of Environmentally Degradable Polymers. *Handbook of Biodegradable Polymers*, 1–28.
- Ziechmann, W. (1996). *Huminstoffe und ihre Wirkungen* . Spektrum, Akad. Verl .



## Appendix

Appendix 1: Calibration Curves of NO <sub>3</sub> -N and NH <sub>4</sub> -N .....	100
Appendix 2: Supplementary figures to the ATR-FTIR spectroscopy of plastic particles .....	101
Appendix 3: Composting parameters of compost, vermicompost and input material .....	103
Appendix 4: Statistical R-Output .....	105

## Appendix 1: Calibration Curves of NO<sub>3</sub>-N and NH<sub>4</sub>-N

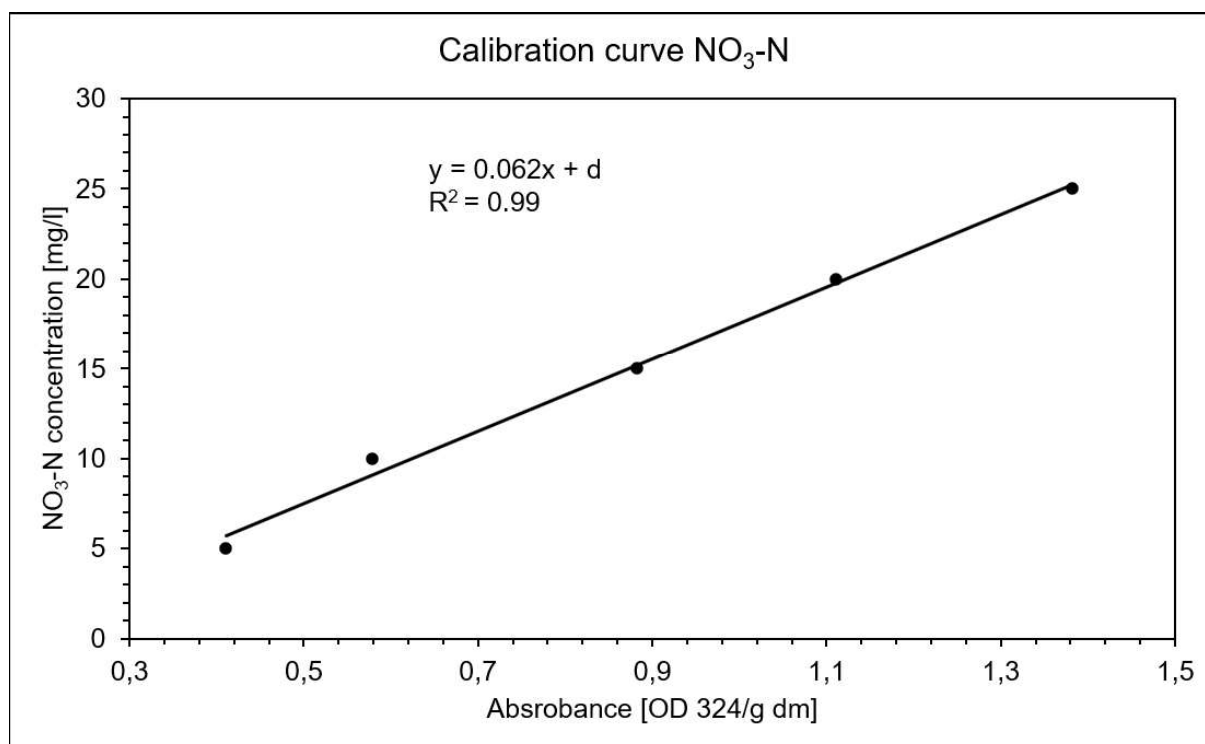


Figure 73: Calibration curve for photometrical absorbance of NO<sub>3</sub>-N

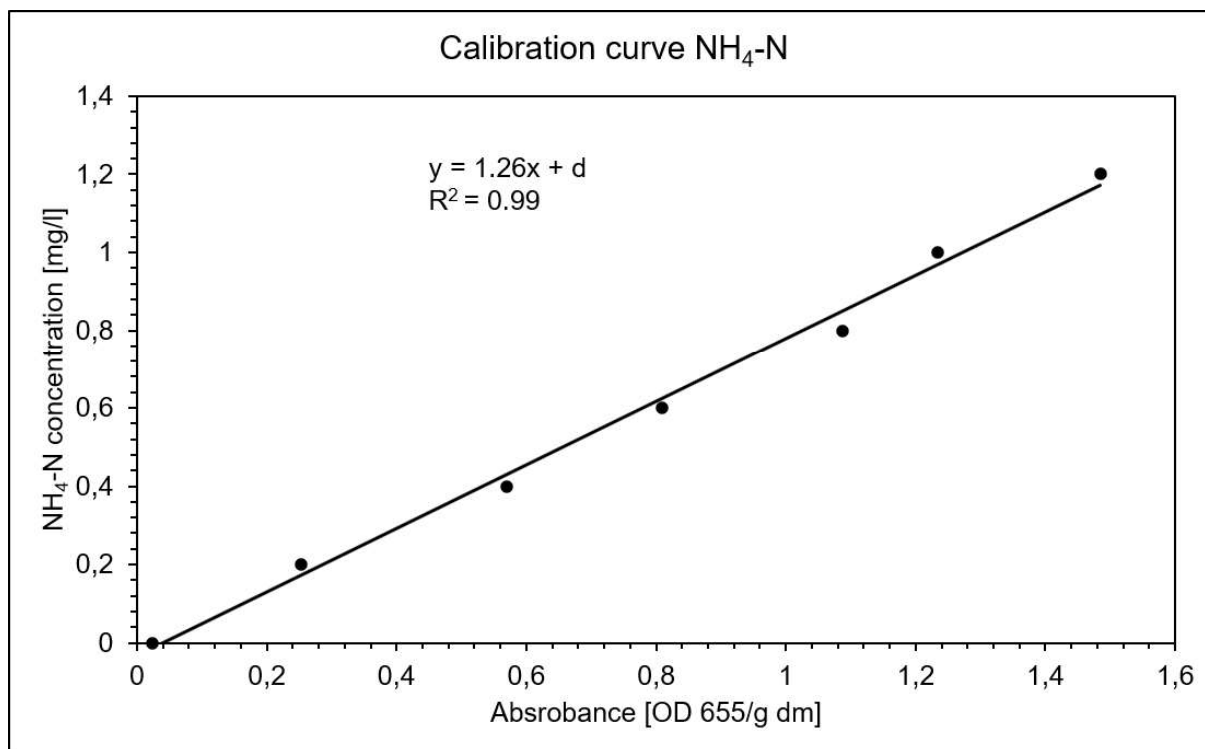


Figure 74: Calibration curve for photometrical absorbance of NH<sub>4</sub>-N

## Appendix 2: Supplementary figures to the ATR-FTIR spectroscopy of plastic particles

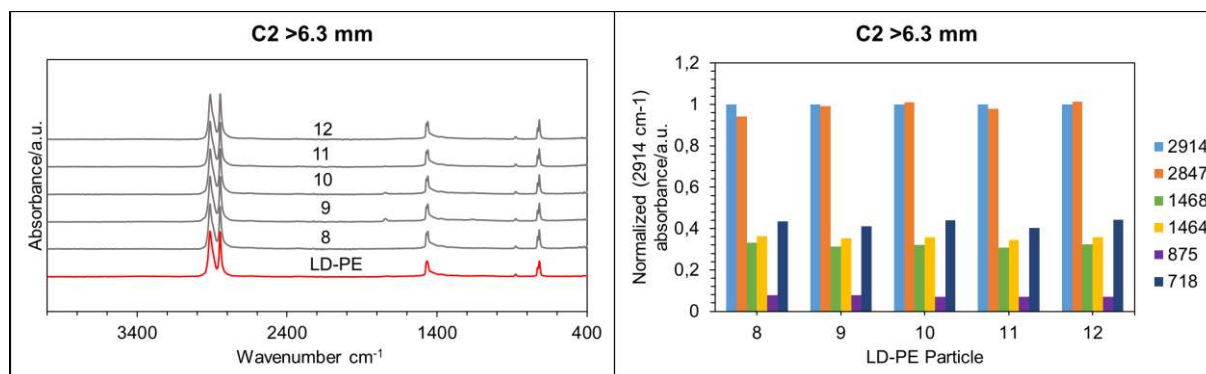


Figure 75: Infrared spectra (on the left) and characteristic wavenumbers selected from the infrared spectra normalized to 2914  $\text{cm}^{-1}$  (on the right) of manually sorted out LD-PE particles (Number 8, 9, 10, 11, 12) >6.3 mm in C2- Composting with LD-PE foils at the end of the experiment

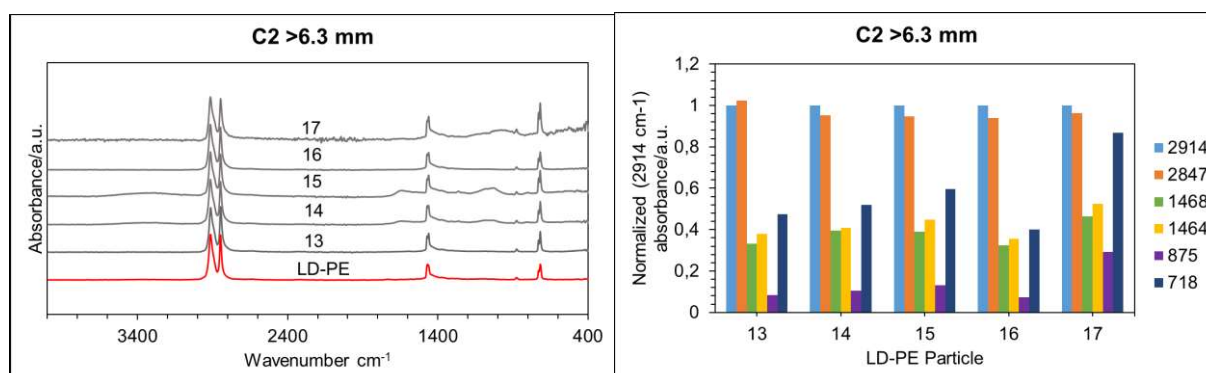


Figure 76: Infrared spectra (on the left) and characteristic wavenumbers selected from the infrared spectra normalized to 2914  $\text{cm}^{-1}$  (on the right) of manually sorted out LD-PE particles (Number 13, 14, 15, 16, 17) >6.3 mm in C2- Composting with LD-PE foils at the end of the experiment

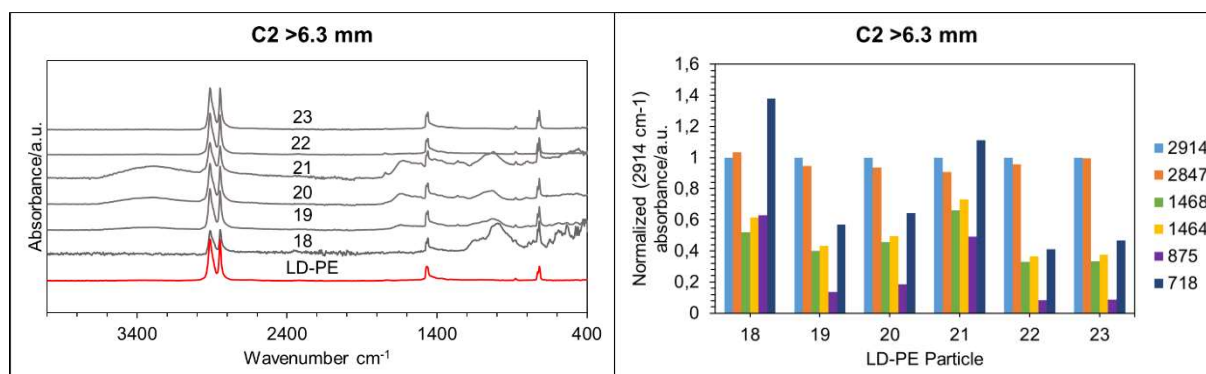


Figure 77: Infrared spectra (on the left) and characteristic wavenumbers selected from the infrared spectra normalized to 2914  $\text{cm}^{-1}$  (on the right) of manually sorted out LD-PE particles (Number 18, 19, 20, 21, 22, 23) >6.3 mm in C2- Composting with LD-PE foils at the end of the experiment

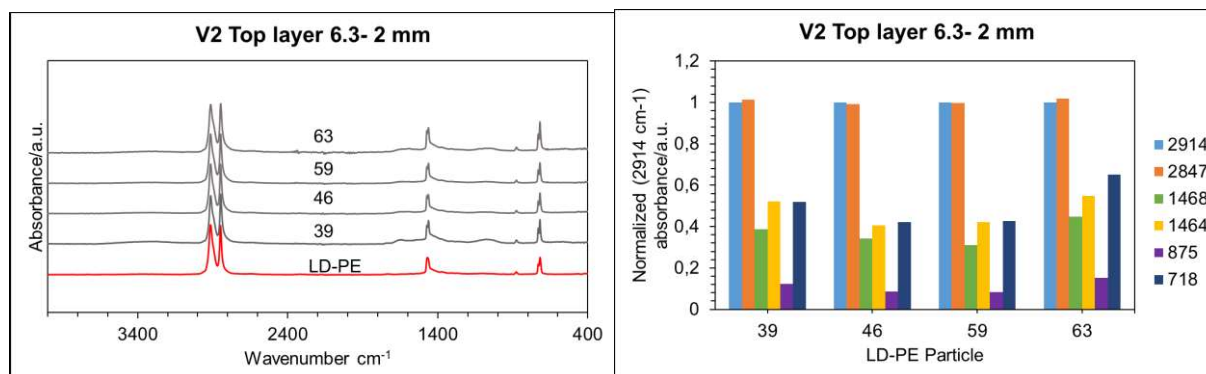


Figure 78: Infrared spectra (on the left) and characteristic wavenumbers selected from the infrared spectra normalized to 2914  $\text{cm}^{-1}$  (on the right) of manually sorted out LD-PE particles (Number 39, 46, 59, 63) sized 6.3 - 2 mm in V2 top layer- Vermicomposting with LD-PE foils at the end of the experiment

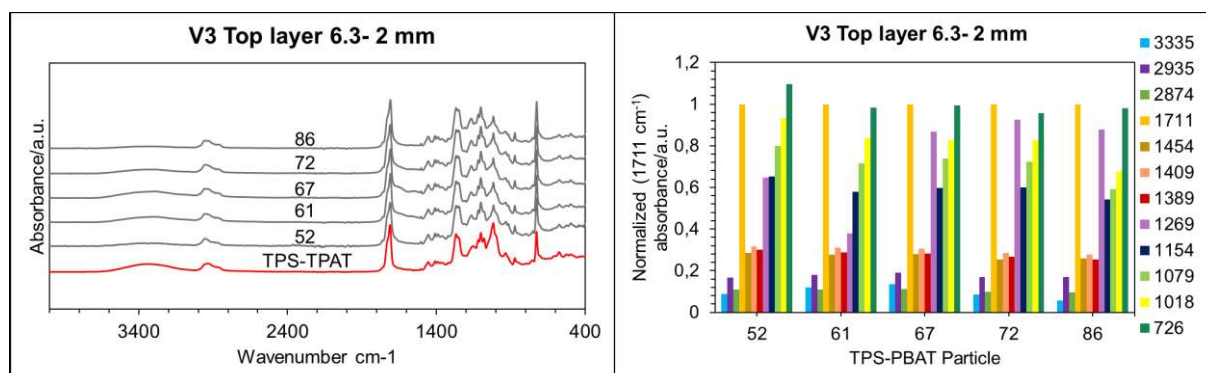


Figure 79: Infrared spectra (on the left) and characteristic wavenumbers selected from the infrared spectra normalized to 1711  $\text{cm}^{-1}$  (on the right) of manually sorted out TPS-PBAT particles (Number 52, 61, 67, 72, 86) sized 6.3 - 2 mm in V3 top layer- Vermicomposting with TPS-PBAT foils at the end of the experiment

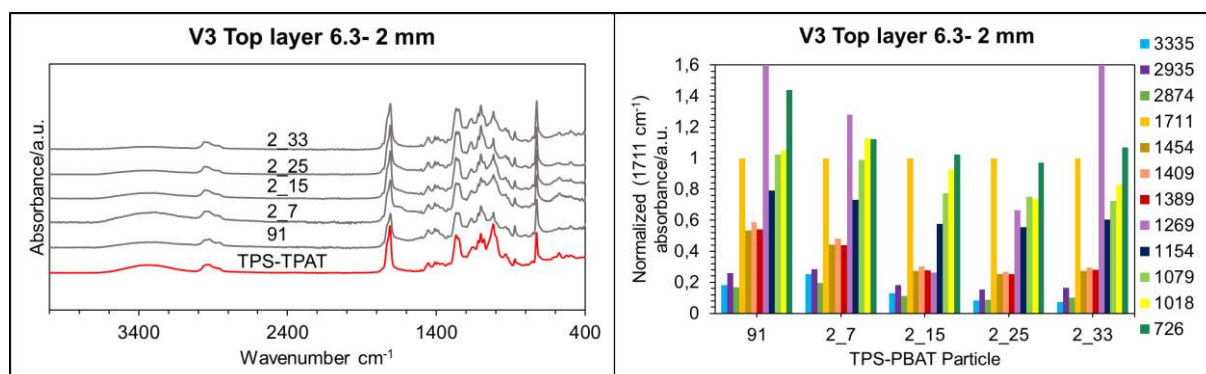


Figure 80: Infrared spectra (on the left) and characteristic wavenumbers selected from the infrared spectra normalized to 1711  $\text{cm}^{-1}$  (on the right) of manually sorted out TPS-PBAT particles (Number 91, 2\_7, 2\_15, 2\_25, 2\_33) sized 6.3 - 2 mm in V3 top layer- Vermicomposting with TPS-PBAT foils at the end of the experiment

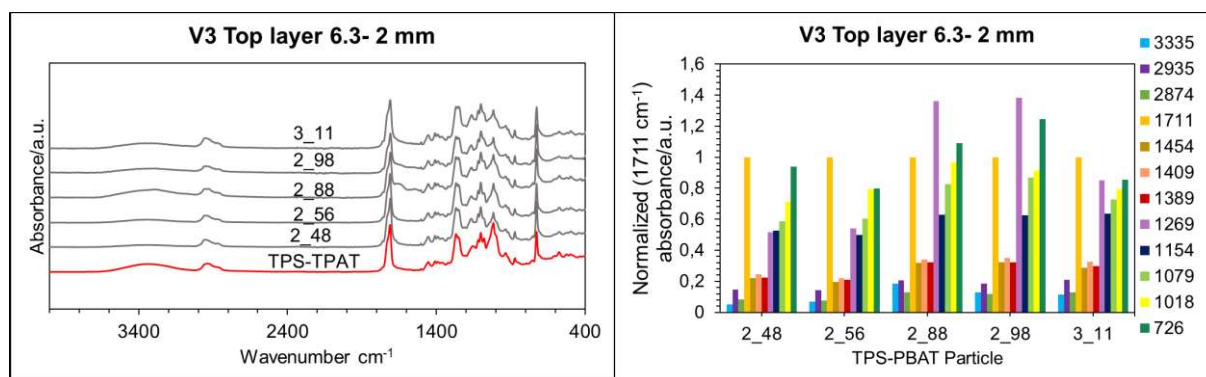


Figure 81: Infrared spectra (on the left) and characteristic wavenumbers selected from the infrared spectra normalized to 1711  $\text{cm}^{-1}$  (on the right) of manually sorted out TPS-PBAT particles (Number 2\_48, 2\_56, 2\_88, 2\_98, 3\_11) sized 6.3 - 2 mm in V3 top layer- Vermicomposting with TPS-PBAT foils at the end of the experiment

## Appendix 3:Composting parameters of compost, vermicompost and input material

Table 16: Compost parameters of C1- Composting without foils

	C1								
Day	LOI [% dm]	HA [optical density/g odm]	FA [optical density/g odm]	pH	EC [20°C,mS/cm]	TOC [% dm]	TN [% dm]	C/N	WC [% dm]
1	91,8	0	0	5,7	2,7	47,4	0,8	60,0	79
8	91,1	0	0	7,8	1,9	46,4	0,5	88,6	76
22	91,8	153	29	8,2	1,9	47,6	0,6	75,0	73
48	87,5	256	51	8,2	2,0	44,9	0,9	47,6	76
90	90,3	127	25	8,0	1,7	45,1	1,0	45,7	77
124	85,0	211	40	8,1	2,0	43,0	1,4	29,7	79

Table 17: Compost parameters of C2- Composting with LD-PE foils

	C2								
Day	LOI [% dm]	HA [optical density/g odm]	FA [optical density/g odm]	pH	EC [20°C,mS/cm]	TOC [% dm]	TN [% dm]	C/N	WC [% dm]
1	93,7	0	0	5,3	2,1	47,5	0,7	72,9	72

8	94,3	0	0	7,2	1,5	49,8	0,4	119,2	74
22	92,9	150	32	7,9	1,9	48,5	0,7	74,2	70
48	90,9	197	47	8,0	1,8	47,8	0,7	65,2	72
90	85,9	142	37	7,9	1,6	44,1	1,2	37,7	75
124	86,4	147	38	7,9	1,8	43,6	1,2	35,0	75

Table 18: Compost parameters of C3 Composting with TPS-PBAT foils

	<b>C3</b>								
<b>Day</b>	<b>LOI [% dm]</b>	<b>HA [optical density/g odm]</b>	<b>FA [optical density/g odm]</b>	<b>pH</b>	<b>EC [20°C,mS/cm]</b>	<b>TOC [% dm]</b>	<b>TN [% dm]</b>	<b>C/N</b>	<b>WC [% dm]</b>
1	92,9	0	0	5,3	2,6	46,8	0,8	59,2	72
8	93,3	0	0	7,3	1,7	47,7	0,5	100,2	73
22	91,8	145	36	7,9	2,0	47,7	0,8	62,4	74
48	88,7	194	48	7,8	2,0	45,9	0,9	49,7	76
90	86,5	129	33	7,8	1,6	44,0	1,1	39,1	78
124	84,0	143	39	7,7	1,8	43,2	1,4	31,2	79

Table 19: Compost parameters of compost and vermicompost (T+B) at the end of the experiment

	<b>1</b>			<b>2</b>			<b>3</b>		
<b>Parameters</b>	<b>C1</b>	<b>V1-T</b>	<b>V1-B</b>	<b>C2</b>	<b>V2-T</b>	<b>V2-B</b>	<b>C3</b>	<b>V3-T</b>	<b>V3-B</b>
<b>LOI [% dm]</b>	85,0	55,7	50,5	86,4	57,2	55,2	84,0	55,8	54,2
<b>HA [optical density/g odm]</b>	211	241	188	147	246	179	143	231	171
<b>FA [optical density/g odm]</b>	40	98	113	38	93	106	39	78	92
<b>pH</b>	8,1	8,6	8,8	7,9	8,5	8,7	7,7	8,4	8,5
<b>EC [mS/cm]</b>	2,0	2,8	3,0	1,8	3,0	3,1	1,8	3,2	3,8

<b>TOC [% dm]</b>	43,0	27,7	27,8	43,6	27,4	27,7	43,2	28,2	25,9
<b>TN [% dm]</b>	1,4	2,1	1,4	1,2	2,0	1,3	1,4	2,1	1,3
<b>C/N</b>	29,7	13,1	19,7	35,0	13,8	21,7	31,2	13,3	19,8
<b>WC [% dm]</b>	79	86	88	75	86	90	79	82	88
<b>NH4-N [mg/kg]</b>	0,8	4,7	0,0	1,0	8,5	1,2	0,8	15,6	4,1
<b>NO3-N [mg/kg]</b>	3,8	8,8	0,6	4,4	0,0	2,3	7,3	0,0	0,0

Table 20: Compost parameters of the Input material of compost (C) and vermicompost (V)

Parameters	Input C	Input V
<b>LOI [% dm]</b>	74,8	84,9
<b>pH</b>	5,2	4,8
<b>EC [mS/cm]</b>	8,8	8,4
<b>TOC [% dm]</b>	38,4	42,8
<b>TN [% dm]</b>	3,5	3,2
<b>C/N</b>	10,9	13,3
<b>MC [% dm]</b>	91	91
<b>NH4-N [mg/kg]</b>	11,4	7,7
<b>NO3-N [mg/kg]</b>	29,3	24,8

## Appendix 4: Statistical R-Output

Call:

```
lm(formula = CO2.Control ~ Temperature.Control, data = CO2_Temperature_Averaged)
```

Residuals:

```
      Min       1Q   Median       3Q      Max
-5.9703 -1.6710 -0.4131  1.2774  9.6419
```

Coefficients:

```
              Estimate Std. Error t value Pr(>|t|)
(Intercept)    -4.75688     1.23734   -3.844 0.000211 ***
Temperature.Control  0.29597     0.02832  10.450 < 2e-16 ***
Signif. codes:  0 '***' 0.001 '**' 0.01 '*' 0.05 '.' 0.1 ' ' 1
```

---

Residual standard error: 2.554 on 101 degrees of freedom

(1 observation deleted due to missingness)

Multiple R-squared: 0.5195, Adjusted R-squared: 0.5148

F-statistic: 109.2 on 1 and 101 DF, p-value: < 2.2e-16

Call:

```
lm(formula = CO2.LD.PE ~ Temperature.LD.PE, data = CO2_Temperature)
```

Residuals:

Min	1Q	Median	3Q	Max
-4.4079	-1.4327	-0.1832	0.9787	10.2697

Coefficients:

	Estimate	Std. Error	t value	Pr(> t )
(Intercept)	-6.04262	1.01131	-5.975	3.47e-08 ***
Temperature.LD.PE	0.32833	0.02324	14.129	< 2e-16 ***

---

Signif. codes: 0 '\*\*\*' 0.001 '\*\*' 0.01 '\*' 0.05 '.' 0.1 ' ' 1

Residual standard error: 2.053 on 101 degrees of freedom

(1 observation deleted due to missingness)

Multiple R-squared: 0.664, Adjusted R-squared: 0.6607

F-statistic: 199.6 on 1 and 101 DF, p-value: < 2.2e-16

Call:

```
lm(formula = CO2.TPS.PBAT ~ Temperature.TPS.PBAT, data = CO2_Temperature_Averaged)
```

Residuals:

Min	1Q	Median	3Q	Max
-4.6585	-1.5245	-0.1129	1.1244	9.5520

Coefficients:

	Estimate	Std. Error	t value	Pr(> t )
(Intercept)	-4.88131	1.03633	-4.71	7.91e-06 ***
Temperature.TPS.PBAT	0.29844	0.02373	12.58	< 2e-16 ***

---

Signif. codes: 0 '\*\*\*' 0.001 '\*\*' 0.01 '\*' 0.05 '.' 0.1 ' ' 1

Residual standard error: 2.131 on 101 degrees of freedom

(1 observation deleted due to missingness)

Multiple R-squared: 0.6104, Adjusted R-squared: 0.6065

F-statistic: 158.2 on 1 and 101 DF, p-value: < 2.2e-16

Call:

```
lm(formula = Absorbance ~ NO3.N.concentration..mg.l., data = Calibration_curve)
```

Residuals:

1	2	3	4	5	6
-0.06205	0.08284	-0.01628	0.02161	-0.01550	-0.01062



Coefficients:

	Estimate	Std. Error	t value	Pr(> t )
(Intercept)	0.062048	0.039305	1.579	0.19
NO3.N.concentration..mg.l.	0.053223	0.002596	20.499	3.34e-05 ***

---

Signif. codes: 0 '\*\*\*' 0.001 '\*\*' 0.01 '\*' 0.05 '.' 0.1 ' ' 1

Residual standard error: 0.05431 on 4 degrees of freedom

Multiple R-squared: 0.9906, Adjusted R-squared: 0.9882

F-statistic: 420.2 on 1 and 4 DF, p-value: 3.345e-05

Call:

```
lm(formula = Aborbance. ~ NH4.N.concentration..mg.l., data =
  Calibration_curve_ammonia)
```

Residuals:

1	2	3	4	5	6	7
-0.02161	-0.03679	0.03504	0.02886	0.06168	-0.03650	-0.03068

Coefficients:

	Estimate	Std. Error	t value	Pr(> t )
(Intercept)	0.04461	0.03041	1.467	0.202
NH4.N.concentration..mg.l.	1.22589	0.04217	29.071	9.03e-07 ***

---

Signif. codes: 0 '\*\*\*' 0.001 '\*\*' 0.01 '\*' 0.05 '.' 0.1 ' ' 1

Residual standard error: 0.04463 on 5 degrees of freedom

Multiple R-squared: 0.9941, Adjusted R-squared: 0.9929

F-statistic: 845.1 on 1 and 5 DF, p-value: 9.02